TECHNISCHE UNIVERSITÄT MÜNCHEN

Institut für Organische Chemie und Biochemie
Lehrstuhl für Biotechnologie

Regulation of SRF via Rac-Actin-MAL Signalling in Epithelial Cells

Stephan Busche

Vollständiger Abdruck der von der Fakultät für Chemie
der Technischen Universität München zur Erlangung des akademischen Grades eines
Doktors der Naturwissenschaften
genehmigten Dissertation.

Vorsitzender: Univ.-Prof. Dr. St. J. Glaser

Prüfer der Dissertation:

1. Priv.-Doz. Dr. N. Budisa
2. Univ.-Prof. Dr. J. Buchner

Die Dissertation wurde am 29.10.2008 bei der Technischen Universität München eingereicht und durch die Fakultät für Chemie am 03.12.2008 angenommen.

for my parents

Index

I. Summary

Compact layers of epithelial cells cover all external and internal surfaces throughout the body. These cells are interconnected via several specialised major adhesive contacts, some of which are in turn dynamically and functionally linked to the actin cytoskeleton. The actin remodelling-dependent regulation of contact formation and dissociation is an essential process for morphogenetic processes during the development of new tissues and the controlled growth and turnover of adult tissues. Contact-dissociation is a hallmark of Epithelial-Mesenchymal Transition (EMT), a highly conserved process indispensable during morphogenesis and implicated in promoting carcinoma invasion and metastasis.

Within this study I investigated whether epithelial cell-cell contact dissociation has an impact on MAL-dependent Serum Response Factor (SRF)-mediated gene expression. I show that the calcium dependent dissociation of epithelial contacts strictly correlates with SRF-mediated transcription, with a specific threshold of 0.05 mM. By constrast, normal and cancer cells lacking E-cadherin-dependent contacts fail to activate SRF. AGS cells, which are deficient for Adherens junctions (AJs) but still form Tight junctions (TJs), also fail to activate SRF; an introduction of E-cadherin reconstitutes SRF inducibility. This suggests that AJ rather than TJ components are essential for signal transmission. Along with contact dissociation Rac1 and RhoA are fast and transiently GTP-loaded. Constitutive active mutants identified both GTPases as sufficient for SRF activation. However, the utilization of clostridial toxins identified Rac, but not Rho, as required for SRF reporter activation and expression of the known endogenous MAL-dependent SRF targets *vinculin* and *smooth muscle α-actin*. Upon calcium withdrawal the actin cytoskeleton is remodelled and the cellular G-actin pool slightly depleted. An elevation of the G-actin level blocks SRF activation, whereas its depletion induces SRF. This demonstrates that changes in the actin treadmilling process, which reduce the cellular G-actin level, are sufficient and required for SRF activation. Rho/ROCK-signalling induced actomyosin contraction is not sufficient to activate SRF, yet a prerequisite. Furtermore, direct evidence for a MAL-dependency in signal transmission is provided: on the one hand calcium withdrawal induces the dissociation of the actin/MAL complex, and on the other hand dominant negative or constitutive active MAL constructs block or activate SRF, respectively. Overall, I conclude that E-cadherin dependent cell-cell contacts regulate SRF through the cellular G-actin pool. Furthermore, contact dissociation activates, presumably via Adherens junctions, a signalling cascade including Rac, G-actin and MAL to mediate SRF-induced target gene expression.

I. Zusammenfassung

Epitheliale Zellen kleiden alle äußeren und inneren Oberflächen des Körpers aus. Sie sind untereinander durch spezialisierte adhäsive Zellkontakte verbunden, von denen manche funktionell an das Aktin-Zytoskelett gekoppelt sind. Die Regulation der Ausbildung und Auflösung von epithelialen Zellkontakten ist abhängig von Umlagerungen des Aktin Zytoskeletts. Dies wiederum ist ein essentieller Prozess während der Entwicklung neuer Gewebe und kontrolliertem Wachstum sowie der Regeneration von bestehenden Geweben. Die Auflösung von Zellkontakten ist ein Kennzeichen der Epithelialen-Mesenchymalen Transition (EMT). EMT ist ein hochkonservierter Prozess, der unabdingbar während der Embryonalentwicklung ist, aber auch die Invasivität von Karzinomen und Metastasierung fördert.

In dieser Arbeit untersuche ich, ob die Auflösung epithelialer Zellkontakte einen Einfluss auf die MAL-abhängige SRF-vermittelte Genexpression hat. Ich zeige, dass die kalziumabhängige Auflösung epithelialer Kontakte exakt mit Serum Response Factor (SRF)-vermittelter Transkription korreliert, mit einem spezifischen Grenzwert von 0.05 mM. Normale Zellen oder Krebszellen, die keine E-Cadherin-abhängigen Zellkontakte ausbilden, zeigen im Gegensatz dazu keine SRF Aktivierung. AGS Zellen, die keine Adherens junctions (AJs), jedoch Tight junctions (TJs) ausbilden, aktivieren SRF ebenfalls nicht; eine Einbringung von E-Cadherin in die Zellen stellt die SRF Aktivierbarkeit her. Daher scheinen Komponenten der AJ essentiell für eine Signalweiterleitung zu sein. Einhergehend mit der Auflösung der Zellkontakte werden Rac1 und RhoA schnell und transient mit GTP beladen. Konstitutive aktive Mutanten beider GTPasen sind hinreichend für die SRF Aktivierung. Durch Verwendung von clostridialen Toxinen konnte Rac, nicht jedoch Rho, als notwendig für die Aktivierung des SRF Reporterkonstrukts und der Expression der bereits beschriebenen endogenen MAL-abhängigen SRF Zielgene *Vinculin* und *Smooth Muscle α-Actin* identifiziert werden. Nach Kalziumentzug wird das Aktin Zytoskelett umgelagert und der zelluläre G-Aktin Vorrat vermindert. Eine Erhöhung des G-Aktin Levels verhindert die SRF Aktivierung, während eine Verminderung SRF aktiviert. Dies beweist, dass Veränderungen der Aktin-Dynamik, welche den zellulären G-Aktin Level vermindern, hinreichend und notwendig für die SRF Aktivierung sind. Rho-ROCK vermittelte Aktomyosin Kontraktilität ist nicht hinreichend für die SRF Aktivierung, wohl aber eine Voraussetzung. Desweitern wurden direkte Beweise für die MAL-abhängige Signalweiterleitung erbracht: so bewirkt der Kalziumentzug die Trennung des Aktin/MAL Komplexes, und dominant negative oder konstitutiv aktive MAL-Konstrukte blockieren beziehungsweise aktivieren SRF. Unabhängig davon zeige ich, dass die E-Cadherin-vermittelte Ausbildung von epithelialen Kontakten zu einer SRF Aktivierung führt. Für eine Signalweiterleitung ist die Verminderung des zellulären G-Aktin Levels notwendig. Zusammenfassend schlussfolgere ich, dass E-Cadherin-bedingte Zellkontakte SRF über das zelluläre G-Aktin regulieren. Dabei aktiviert die Auflösung der Kontakte, wahrscheinlich der Adherens junctions, eine Signalkaskade über Rac, G-Aktin und MAL und vermittelt so die SRF Zielgenexpression.

II. Introduction

1. The Epithelium

The epithelium is a sheetlike layer of tissue covering an external surface or lining a cavity within the body. Several different types of epithelia are characterized dependent on morphology and function. Simple, single-layered epithelia often selectively transport small molecules and ions through the tissue layer whereas stratified, multi-layered epithelia commonly serve as protective surfaces and barriers. Multilayered transitional epithelia allow expansion and contraction. Simple and stratified epithelia are formed by either squamous, cuobidal or columnar shaped cells, transitional epithelia by a mixture of them. All epithelial cells appear polarized as they are sectioned by their membranes typically into discrete apical, lateral and basal surfaces (Figure 1). The apical membrane is the upper surface, the basal membrane usually contacts an underlying extracellular matrix (ECM). The basal and lateral surface is often similar in composition and therefore termed basolateral surface. Laterally, adjacent cells are connected by different major adhesive structures including desmosomes, Gap junctions and the apical junctional complex (AJC) comprised of Adherens and Tight junctions (Figure 1). Adherens junctions (AJs, also named zonulae adherens), Tight junctions (TJs, also zonulae occludens) and desmosomes were first identified by electron microscopy as a tripartite junctional complex bordering the apico-basolateral membrane in simple epithelia (Farquhar and Palade, 1963). Desmosomes form in connection with their attached intermediate filament network a supracellular scaffolding that distributes mechanical forces throughout the tissue. They are also involved in processes of differentiation and tissue morphogenesis. Desmogleins and desmocollins, both belonging to the cadherin family, cooperate to form the intercellular Ca^{2+}-dependent adhesive interface. Their

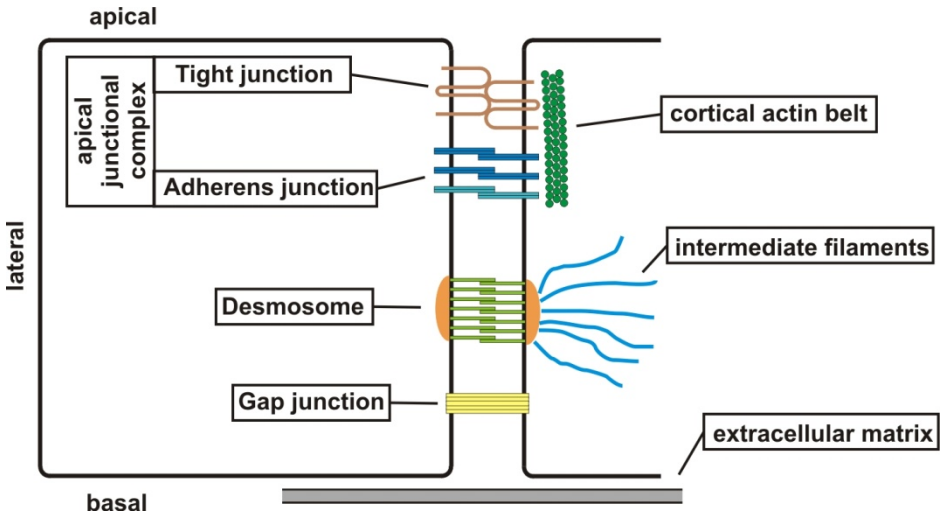

Figure 1: Major adhesive structures in polarized epithelial cells.

cytoplasmic tails bind to armadillo family member proteins which are, in turn, linked to the intermediate filaments via the plakin family member desmoplakin (Green and Simpson, 2007). Gap junctions were also first identified by electron microscopy (Robertson, 1963). They connect the cytoplasms of adjacent cells via protein-lined channels allowing ion and small molecule exchange.

2. Molecular composition of the apical junctional complex

Per definition the apical junctional complex is comprised of AJs and TJs (Figure 1).

2.1. Tight junctions

TJs are located most apical providing an ion- and size-specific barrier (Anderson *et al.*, 2004). They mark the border between the apical and basolateral membrane domains and impede in a "fence" like fashion the diffusion of their respective components (Miyoshi and Takai, 2008). Major tramsmembrane components of the TJ are the IgG-like family of junctional adhesion molecules (JAMs) and the four transmembrane spanning protein families of occludins and claudins (Schneeberger and Lynch, 2004). JAMs are not exclusively found on TJ containing cells and forced expression in fibroblasts does not induce the formation of TJs (Ebnet *et al.*, 2004). Occludin deficient TJs are fully functional, leaving the physiological role of occludins unclear (Saitou *et al.*, 2000). The claudin family consists of at least 24 organ and tissue specific members, which induce Ca^{2+}-independent cell-cell adhesion upon expression in fibroblasts. They are responsible for strength, size and ion specificity of TJ barriers (Furuse and Tsukita, 2006). JAMs, occludin and claudins are locally clustered in tight junction strands by interaction with cytoplasmic scaffolding partners, most importantly the zonula occludens proteins ZO-1, ZO-2 and ZO-3, which belong to the guanylate kinase-like homologs family (Schneeberger and Lynch, 2004). Epithelial cells depleted for ZO-1 and ZO-2 are well polarized including functional AJs, but completely lack TJs. In this system ZO-1 and ZO-2, but not ZO-3, were shown to be essential for claudin clustering, TJ strand formation and barrier function (Umeda *et al.*, 2006). The ZO-proteins directly interact with claudins and occludin via their N-terminal PDZ domain, whereas their C-terminus can associate with actin, providing a direct link to the cytoskeleton (Schneeberger and Lynch, 2004).

2.2. Adherens junctions

AJs are located immediately below the TJs (Figure 1). They perform multiple functions including the initiation and stabilization of cell-cell adhesion, regulation of the actin cytoskeleton and intracellular signalling (Gumbiner, 2005). The core of the AJ is formed by classical cadherin superfamily glycoproteins, such as E-, P-, N- and R-cadherin (Gooding *et al.*, 2004), and catenin family members

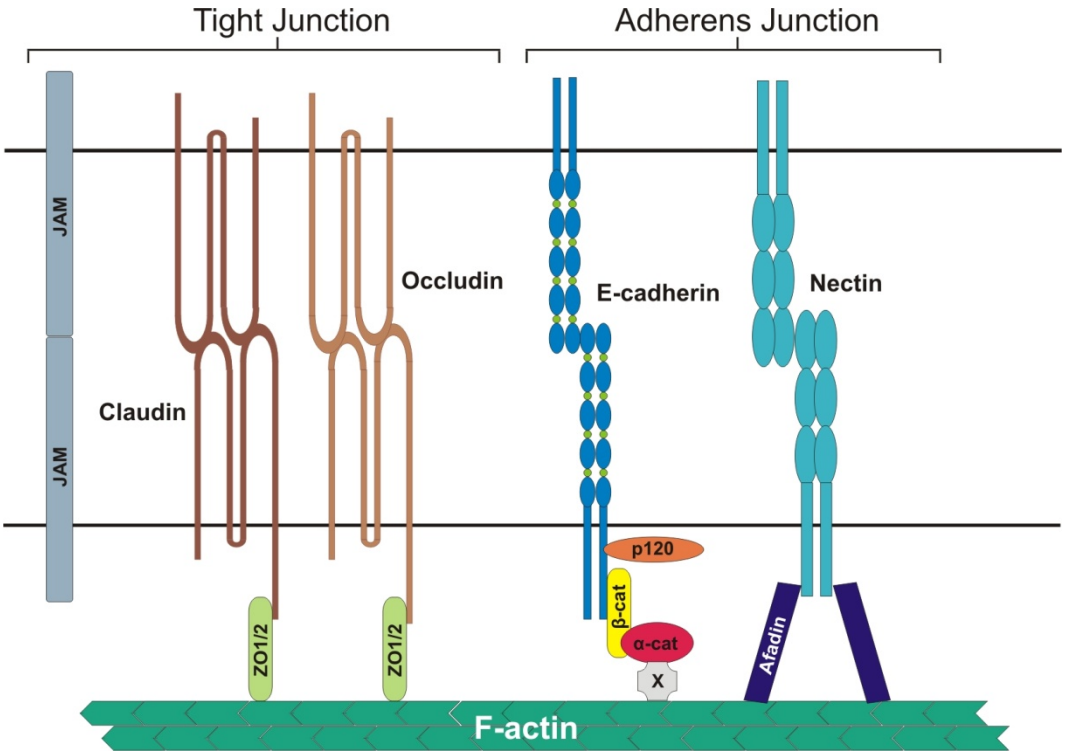

Figure 2: Schematic representation of the basic structural components of the apical junctional complex comprised of Adherens and Tight junctions.

including p120-catenin, β-catenin and α-catenin (Hartsock and Nelson, 2008). The predominant epithelial isoform E-cadherin (also known as uvomorulin) is a type I, single-pass transmembrane protein with five characteristic extracellular cadherin (EC) domains, with EC1 most membrane distal and EC5 most membrane proximal (Figure 2). The human isoform consists of 882 amino acids. E-cadherins of adjacent cells homophilically *trans*-interact dependent on Ca^{2+}. Mechanistically, a dimer of neighbouring (*cis*) EC1 domains forms an interface with an EC1 dimer from the opposing cell by swapping β strands. The interaction is anchored by the insertion of the side chain of the conserved Trp2 residue into a complementary hydrophobic pocket in the opposing molecule, resulting in the formation of *trans*-tetramers of cadherins on opposing cells. As a prerequisite, the transmembrane domains have to be rigid. Therefore, three Ca^{2+} ions have to be bound in the calcium-binding hinge in each EC-interdomain boundary (Boggon *et al.*, 2002; Haussinger *et al.*, 2004; Patel *et al.*, 2006). A recent study showed, that E-cadherin is essential for the formation but not the maintenance of AJs: Depletion of E-cadherin and Cadherin-6 from preformed epithelial junctions resulted in loss of β-catenin, but not TJ proteins in the membrane (Capaldo and Macara, 2007). E-cadherins in mature AJs are clustered laterally via their 94-amino acid cytoplasmic juxtamembrane domain (JMD). Eight highly conserved amino acids of the JMD also mediate binding to the armadillo repeats of p120-catenin (Yap *et al.*, 1998). β-Catenin binds the 72 C-terminal amino acids of E-cadherin also via its armadillo repeats in a phospho-regulated manner and the vinculin homology (VH) 1 domain of α-catenin via a region 30 amino acids N-terminal of its armadillo repeats (Perez-Moreno and Fuchs, 2006). Besides β-catenin binding, the N-terminal located VH1 domain of α-catenin mediates

homodimerization, making both events mutually exclusive. Thus, α-catenin subsists either as monomer capable of β-catenin binding or a homodimer competent for actin filament binding, but not vice-versa, disproving its function as direct linker between β-catenin and the actin cytoskeleton. Nevertheless, numerous studies indicate that AJs are somehow linked to the actin cytoskeleton, likely in a rather dynamic than static interaction (Gates and Peifer, 2005; Burridge, 2006). The linkage might be at least partially dependent on α-catenin by its interaction with actin binding proteins like vinculin, spectrin, afadin, ZO-1, α-actinin, formin-1 or EPLIN via its VH2 or VH3 domain (Gates and Peifer, 2005; Burridge, 2006; Abe and Takeichi, 2008). Furthermore, the nectin/afadin complex, the second basic adhesive unit of the AJ, might mediate linkage (Gates and Peifer, 2005). The nectin family of IgG-like adhesion receptors, consisting of the four members Nectin-1 to -4, forms lateral homodimers capable of Ca^{2+}-independent homo- and heterophilic engagement with other nectins or nectin-like receptors. Their extracellular domain consists of three IgG-like loops, a single transmembrane region and a cytoplasmic tail with a PDZ domain. Nectins seem to provide a first scaffold for AJ and TJ formation, as cadherin mediated cell-cell adhesion and TJ formation are dependent on nectins. All nectin family members are directly linked to the actin cytoskeleton by binding the PDZ domain of the actin-binding protein afadin, also known as AF-6, via a conserved C-terminal motif (Irie *et al.*, 2004).

3. The actin cytoskeleton

The eukaryotic protein actin, first isolated and characterized as myosin-ferment in 1887 (Halliburton, 1887; Finck, 1968), consists of 4 pairwise arranged subunits that sandwich an adenine nucleotide and Mg^{2+} (Aguda *et al.*, 2005). The 43 kDa monomer is also called globular actin or G-actin. In physiological conditions, Mg-ATP actin monomers can form helical polymers all arranged head-to-tail to give molecular polarity. The lifetime of these actin filaments, or shortly F-actin, is determined by the intrinsic ATPase activity of actin: irreversible hydrolysis of the bound ATP and dissociation of the γ-phosphate trigger processes leading to its destabilization and disassembly. The filament end favored for elongation by ATP actin association is called the barbed end, the one losing ADP actin the pointed end, based on the arrowhead pattern created when myosin binds to F-actin. The steady-state flux of monomers associating and dissociating is called treadmilling (Pollard and Borisy, 2003). Within the cell, this dynamic treadmilling process is regulated by a variety of proteins, some of which will be discussed in the following (Figure 3).

3.1. Actin filament assambly

The spontaneous association of actin filaments is kinetically unfavourable because actin dimers and trimers are very unstable (Pollard and Borisy, 2003). Physiologically, nucleator proteins like the actin-related protein-2/3 (Arp2/3) complex (Machesky *et al.*, 1994) or formins (Pruyne *et al.*, 2002) initiate de novo filament formation. The Arp2/3 complex nucleates branched actin filaments emerging from

existing ones upon recruitment of the nucleation promoting factors (NPFs) class I and II. Class I is comprised of the Wiskott-Aldrich syndrome proteins (WASP) along with the isoforms of the suppressor of cyclic AMP repressor (SCAR, also called WASP-family verprolin-homologous proteins (WAVE)) (Machesky and Insall, 1998), class II of i.e. cortactin (Weed *et al.*, 2000). WASP or SCAR/WAVE binding induces conformational changes, which bring the Arp2 and Arp3 subunits in close vicinity, possibly mimicking the barbed end of a filament. Furthermore, they deliver the first actin monomer (Chereau *et al.*, 2005). Cortactin seems to stabilize the y-branched organization of newly generated actin networks (Goley and Welch, 2006). There are 15 formin isoforms in mammals, i.e. murine mDia 1 and 2. All share as defining feature a FH1 and FH2 domain, which cooperatively mediate de novo nucleation of actin filaments (Pruyne *et al.*, 2002; Higashida *et al.*, 2004). Thereby, formin homodimers encircle the filament end like a donut, and recruit profilin-bound ATP actin for elongation. Once bound, formins remain continuously associated with the barbed end (Kovar, 2006). The enabled/vasodilator stimulated phosphoprotein (Ena/VASP) protein family elongates pre-existing actin filaments by interacting with the barbed ends, shielding them from capping proteins (Bear *et al.*, 2002) and mediating filament bundling (Schirenbeck *et al.*, 2006). Furthermore, Ena/VASP appears to antagonize the formation of Arp2/3 complex induced actin branching (Skoble *et al.*, 2001; Bear *et al.*, 2002) via an up to now unknown mechanism (Trichet *et al.*, 2008). The surface-attached sheetlike membrane protrusions formed by an Arp2/3 complex nucleated debranched actin meshwork is called lamellipodium. Emanating from the lamellipodium at the leading edge of the cell are thin, formin nucleated finger-like protrusions containing parallel bundles of 10 – 30 actin filaments oriented with their barbed ends toward the membrane, the so-called filopodia (Chhabra and Higgs, 2007).

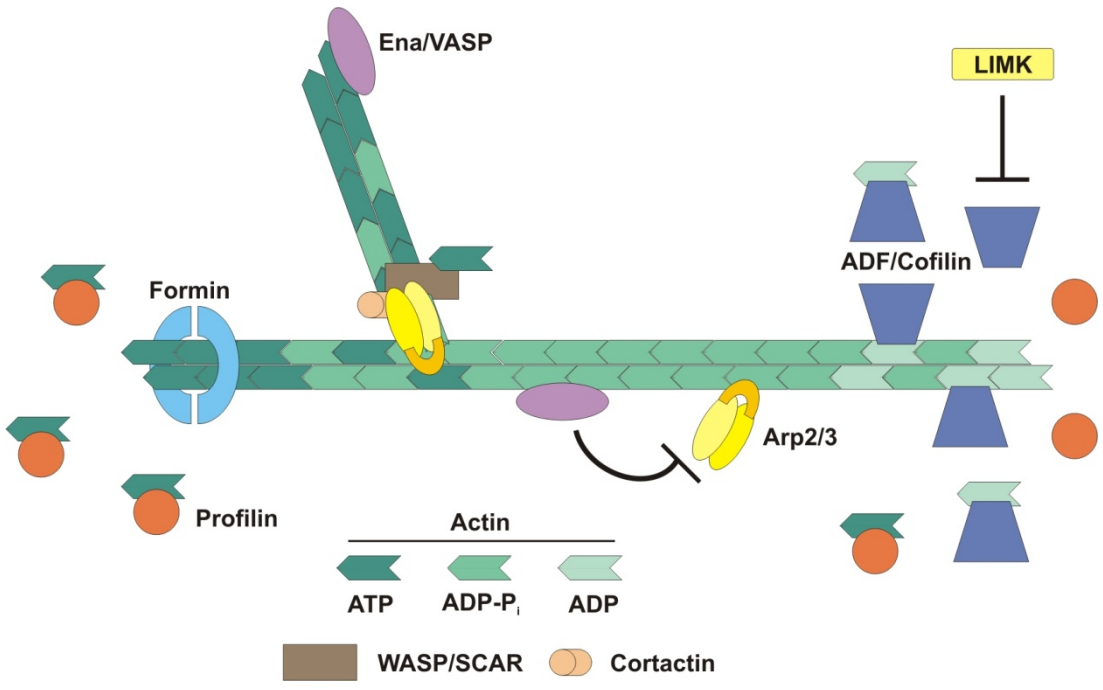

Figure 3: Scheme of selected actin binding proteins involved in actin treadmilling.

3.2. Actin filament disassembly

Debranching, severing and depolymerization of actin filaments from their pointed ends is induced by actin-depolymerizing factor (ADF)/Cofilin proteins, which bind ADP F-actin and stimulate γ-phosphate dissociation from ADP-P_i actin (Carlier *et al.*, 1997; Blanchoin *et al.*, 2000). Mechanistically, the binding induces filaments to twist by approximately 5° per subunit, which changes the thermodynamic stability of the filament leading to depolymerization (McGough *et al.*, 1997). ADF/Cofilin activity is inter alia regulated via phosphorylation by LIM kinase (LIMK) and testicular protein kinase (TESK) (Bamburg, 1999). Phosphorylation downregulates the actin interactions of ADF/cofilin (Bamburg, 1999). The small actin binding protein profilin compedes with ADF/Cofilin for ADP actin binding and promotes the dissociation of ADP (Mockrin and Korn, 1980; Vinson *et al.*, 1998). Due to the higher concentration of ATP in living cells and its higher affinity to ATP than ADP, nucleotide-free actin binds preferentially ATP. Profilin has a higher affinity for ATP actin than ADF/Cofilin, thereby renewing the ATP actin monomer pool ready for polymerization (Rosenblatt *et al.*, 1995; Pollard and Borisy, 2003).

3.3. Actin contractility

Non-muscle cells contain prominent transitory or permanent contractile bundles of actin filaments crosslinked mainly by α-actinin (Lazarides and Burridge, 1975), non-muscle myosin (Weber and Groeschel-Stewart, 1974) and tropomyosin (Lazarides, 1975). In the rigor state, myosin connected to an actin filament is tightly bound via its head to a second, parallel filament. On contraction, this interaction is weakened upon ATP binding to the myosin head. The intrinsic ATPase activity of myosin hydrolyzes the ATP, which causes a conformational change in the head that moves it to a new position where it rebinds the second filament. The phosphate dissociation of ADP-P_i induces another conformational change exerting a force to move the tightly bound myosin on the second filament leading to contraction, followed by the release of ADP to complete the cycle. Essential for this process is the phosphorylation of the regulatory light chain of myosin 2 at Ser 19, which leads to an increase in its intrinsic ATPase activity (Somlyo and Somlyo, 2003). One of the central regulators of contractility is RhoA activated coiled-coil kinase (ROCK) (Leung *et al.*, 1995; Ishizaki *et al.*, 1996; Leung *et al.*, 1996). ROCK stimulates actomyosin contractility by acting on myosin light chain 2 (MLC) in at least four ways (Figure 34): (i) direct phosphorylation of myosin light chain 2 at Ser19 (Amano *et al.*, 1996; Katoh *et al.*, 2001); (ii) inhibition of MLC phosphatase (MLCPP) (Kimura *et al.*, 1996); (iii) phosphorylation of ZIP kinase (ZIPK) which activates MLC and inhibits MLCPP (Murata-Hori *et al.*, 1999; MacDonald *et al.*, 2001; MacDonald *et al.*, 2001); (iv) activation of CPI-17, a MLCPP inhibitor (Kitazawa *et al.*, 2000; Koyama *et al.*, 2000).

3.4. Actin modifying compounds

Numerous actin modifying compounds are available to study the role of the actin cytoskeleton in signal transduction processes. These compounds modulate actin dynamics by accelerating either polymerization or depolymerization. The underlying mechanisms are sometimes quite complex. The basic effects of compounds employed in this study are shortly summarized in the following. Jasplakinolide is a cell membrane permeable actin filament stabilizer isolated from the marine sponge *Jaspis johnstoni* (Scott *et al.*, 1988; Zampella *et al.*, 1999). It also acts as inducer of actin polymerization and thereby deplets the monomeric actin pool (Bubb *et al.*, 1994). Latrunculins and cytochalasins are F-actin destabilizing compounds. Eight forms of latrunculin have been isolated from different murine sponges and nudibranchs (Spector *et al.*, 1983; Vilozny *et al.*, 2004). Latrunculin B is isolated from the sponge *Latrunculia magnifica* (Spector *et al.*, 1983) and prevents assembly and polymerization of actin monomers via specific binding in the ATP-binding cleft of monomeric actin (Spector *et al.*, 1999). Numerous cytochalasins, natural compounds derived from the marine fungus *Zygosporium masonii* (Minato and Katayama, 1970) and derivates, exist. They have various effects on actin, the most efficient is to act by capping the barbed end of actin filaments (Cooper, 1987). At higher concentrations they can also sever F-actin and sequester monomers or dimers and stimulate the ATPase activity of actin monomers (Cooper, 1987; Sampath and Pollard, 1991). Cytochalasin D is one of the best characterized cytochalasins and, in contrast to cytochalasins A and B, does not inhibit monosaccharide transport across the plasma membrane (Rampal *et al.*, 1980).

4. Small guanosine triphosphatases

Small guanosine triphosphatases (also known as small G-proteins or GTPases) are molecular switches that cycle between an inactive GDP-bound and an active GTP-bound confirmation. They possess low intrinsic GTP hydrolysis and GDP/GTP exchange activities. When active, they interact with effector proteins, which induce downstream signalling events. The GDP-GTP cycle is highly regulated by guanine nucleotide exchange factors (GEFs) and GTPase-activating proteins (GAPs). GEFs induce the release of bound GDP to be replaced by GTP and thereby turn on signalling, GAPs provide an essential catalytic group for GTP hydrolysis, which terminates signalling (Wennerberg *et al.*, 2005; Bos *et al.*, 2007). The human Ras superfamily of GTPases consists of at least 154 members divided into five principal families: Ras, Rho, Rab, Arf and Ran (Wennerberg *et al.*, 2005).

To date, there are 22 mammalian Rho family GTPases known (Jaffe, Hall 2005). The most prominent and investigated members are RhoA, Rac1 and Cdc42. To investigate the specific function of single GTPases, constitutive active and dominant mutants have been engineered. Constitutive activation for Rac1 is achieved by replacement of glycine at position 12 with valine, for RhoA by substitution of glutamine at position 63 with leucine. Both mutations reduce the intrinsic GTPase activity (Diekmann *et al.*, 1991; Khosravi-Far *et al.*, 1995).

4.1. Clostridial toxins as inhibitors of RhoGTPases

To investigate the involvement of small G-protein activation in signal transduction pathways inhibitory clostridial toxins are commonly employed. Most toxins are not selective for one GTPase (Genth *et al.*, 2008), but systematic inhibition with different toxins usually allows specific identification of the GTPase essential for signal transduction (Figure 23). Large clostridial cytotoxins are cell permeable single chain proteins sharing exceptionally high molecular masses (> 250 kDa) with substrates exclusively found in the Rho and Ras family GTPases (Schirmer and Aktories, 2004). The toxins modify their targets by stable mono-*O*-glucosylation or mono-*O*-*N*-acetylglucosaminylation, with UDP-glucose as sugar donor (Schirmer and Aktories, 2004). Prominent representatives are toxin A and toxin B derived from *Clostridium (C.) difficile*, with toxin B approximately 100 – 1000 fold more toxic to cultured cells. Toxin A and B from *C. difficile* reference strain VPI 10463 inhibit Rho family GTPases, i.e. Rho, Rac and Cdc42 (Just *et al.*, 1995; Just *et al.*, 1995). A toxin B variant, TcdBF, derived from the *C. difficile* serotype F strain 1470 glucosylates and thereby inhibits Rac1, Cdc42 and R-Ras, but not Rho (Huelsenbeck *et al.*, 2007; Genth *et al.*, 2008). C3-like ADP-ribosyltransferases are 23 - 28 kDa proteins (Wilde and Aktories, 2001), a prototype is *C. botulinum* derived C3 exoenzyme. It selectively catalyzes the ADP-ribosylation of the Rho subtype GTPases RhoA, RhoB and RhoC by modification of Asp41, which acts inhibitory (Sekine *et al.*, 1989). The usual experimentally used C3 exoenzyme consists of an enzyme domain, but lacks a cell binding and transport domain, leaving it cell impermeable. To overcome this problem, Sahai and colleagues engineered the fusion protein TAT-C3 of the HIV TAT leader sequence and C3, that permits transduction of the protein across the plasma membrane (Sahai and Olson, 2006).

5. Regulation of epithelial cell-cell adhesion

The regulation of epithelial junction association and dissociation is essential for morphogenetic processes during the development of new tissues and the controlled growth and turnover of adult tissues in response to environmental, chemical or mechanical changes and for migration (Gumbiner, 2005; Mege *et al.*, 2006). The efficient formation, maintenance and dissociation of apical junctions appear to require the force generated by actin-dependent movement. In polarized epithelial cells the actin cytoskeleton forms a cortical actin belt encircling the lateral membrane and builds stress fibres and supports focal contacts at the basal surface. The AJC is closely associated with the cortical actin belt. Altering the AJC destabilizes the actin belt and vice versa, suggesting a physical link (Peifer, 1993; Cox *et al.*, 1996; Quinlan and Hyatt, 1999). Recent studies indicate that this link is rather dynamic than static: Although TJs and nectins can directly associate with the actin cytoskeleton via ZO proteins and afadin, respectively, cortical actin was shown to be much more dynamic than the cadherin/catenin complex (Yamada *et al.*, 2005). It seems that two actin pools with distinct dynamics, stable patches and a dynamic network, regulate E-cadherin/catenin-complex stability and mobility

(Cavey *et al.*, 2008). Altogether, the cumulative effect of many weak transient interactions of actin binding proteins appears to mediate the AJC-actin cytoskeleton interaction (Gates and Peifer, 2005; Burridge, 2006). First evidence suggesting that this interaction is regulated by small G-proteins base upon the observation that Rho, Rac and Cdc42 localize to cadherin-based cell-cell contact sites (Braga *et al.*, 1997; Kodama *et al.*, 1999). Importantly, Rho family GTPases play coordinate roles during actin remodelling. Constitutive active variants of Rho, Rac1 or Cdc42 expressed in fibroblasts induce stress fibre, lamellipodia, or filopodia formation, respectively (Nobes and Hall, 1995). Indeed, epithelial MDCK cells expressing constitutive active Rac1 or Cdc42 show enhanced E-cadherin staining at cell adhesion sites and form more pronounced cortical actin belts compared to wild type MDCK cells (Takaishi *et al.*, 1997; Kodama *et al.*, 1999). Expression of dominant negative Rac or inhibition of Rho by C3 toxin interferes with epithelial cell contact formation (Braga *et al.*, 1997; Takaishi *et al.*, 1997).

5.1. Epithelial junction formation

5.1.1. Contact formation induced activation of GTPases

Up to now cell adhesion receptor induced small G-protein family signalling remains contradictory, mainly because it depends profoundly on the cellular context and assay conditions (Braga *et al.*, 1999; Braga and Yap, 2005). Homophilic E-cadherin engagement in MDCK and keratinocyte cells lead to the activation of Rac within minutes (Nakagawa *et al.*, 2001; Noren *et al.*, 2001; Betson *et al.*, 2002). Junction association upregulated Rho activity in primary keratinocytes (Calautti *et al.*, 2002) and MDCK cells (Yamada and Nelson, 2007) and Cdc42 activity in human breast adenocarcinoma epithelial MCF-7 cells (Kim *et al.*, 2000), but none of both activities in MDCK II cells (Nakagawa *et al.*, 2001; Noren *et al.*, 2001). Overall, Rac seems to be principally activated upon cadherin engagement mediated new contact formation (Yap and Kovacs, 2003). Mechanistically, *trans*-interaction of cadherin seems to activate Rac via recruitment of the tyrosine kinase c-Src and subsequent Rap1 activation through phosphorylation of Crk adaptor protein, which in turn activates C3G, a Rap1 GEF. Activated Rap1 mediates phosphatidylinositol-3 kinase (PI3K) induction, which promotes activation of the Rac GEF Vav2 (Sander *et al.*, 1998; Fukuyama *et al.*, 2006). Furthermore, the Rac GEF Tiam1 localizes to AJs to play a role in Rac activation (Sander *et al.*, 1998). Additionally, p120-catenin may act by inhibiting Rho and activating Rac and Cdc42 (Perez-Moreno *et al.*, 2006). Thus, E-cadherin engagement at nascent contacts locally recruits and activates Rac. Heterophilic and homophilic nectin engagement leads to the recruitment of c-Src, which in turn recruits C3G through Crk, leading to Rap1 activation (Fukuyama *et al.*, 2005). Rap1 then activates FRG, a GEF for Cdc42 (Fukuyama *et al.*, 2006). c-Src also phosphorylates FRG to activate Cdc42 (Fukuhara *et al.*, 2004). Cdc42 activates Vav2, which in turn activates Rac1. Thus, Rap1 recruits Cdc42 and Rac1 to initial nectin-based cell-cell contacts. Nectin-bound afadin then recruits the tight junction proteins claudin-1, occludin, JAM-1 and ZO-1 to the junction (Sato *et al.*, 2006), and JAM-1

is known to activate Rap1 (Mandell *et al.*, 2005). If and how further TJ proteins induce GTPase signalling remains to be elucidated (Braga and Yap, 2005).

5.1.2. Actin binding proteins as effectors of GTPases

The activation of GTPases at newly initiated cell contacts leads to recruitment of actin-nucleating proteins, which mediate junction maturation by new filament synthesis. The Rac effector Arp2/3 complex is associated with E-cadherin at nascent contacts. Thus, Rac activation stimulates Arp2/3 complex to drive actin assembly (Kovacs *et al.*, 2002; Kovacs *et al.*, 2002). Consistently, live-cell imaging shows that Rac1 activity and Arp2/3 complex, as well as RhoA activity and actomyosin, are restricted to zones at the edges of the expanding cell-cell contacts initiated by E-cadherin engagement in MDCK cells (Yamada and Nelson, 2007). Cortactin is also recruited to the outer margins of nascent cadherin contacts in a Rac-dependent manner (Helwani *et al.*, 2004), coupling adhesion to actin dynamics and junction assembly. N-WASP, the WASP isoform expressed in epithelial cells, bound to activated Cdc42 via the Cdc42- and Rac-interacting domain/G protein binding (CRIB/GBD) and phosphatidylinositol-4,5-bisphosphat (PI(4,5)P2) via the basic (B) domain also stimulates Arp2/3 complex-mediated actin polymerization and inhibits branch dissociation (Prehoda *et al.*, 2000; Rohatgi *et al.*, 2000; Weaver *et al.*, 2002; Kinley *et al.*, 2003). Formins are also direct effectors of RhoGTPases: mDia1 is activated by binding of RhoA and RhoC in its GTP-bound state (Lammers *et al.*, 2005; Rose *et al.*, 2005), Cdc42 binds mDia2, a formin which accumulates at the tip of filopodia, where actin polymerization takes place (Mallavarapu and Mitchison, 1999; Peng *et al.*, 2003). Formins might therefore participate in junction maturation by nucleating unbranched actin cable polymerization (Vasioukhin *et al.*, 2000; Kobielak *et al.*, 2004). However, together it seems that both Rac and Cdc42 activities are necessary for cell contact maturation. Rac induces lamellipodia formation and efficiently mediates the coalescence of cell-cell adhesion between the filopodia like a zipper, whereas Cdc42 increases the number of filopodia (Miyoshi and Takai, 2008).

5.1.3. Myosin involvement in junction formation

Myosins seem also involved in apical junction formation. Nonmuscle myosin 2 can be detected at cell-cell contacts, where it promotes adhesion and local accumulation of cadherins (Dawes-Hoang *et al.*, 2005; Shewan *et al.*, 2005). Furthermore, the actomyosin ring and its regulator ROCK are colocalized at junctions during epithelial wound healing. Myosin light chain accumulation is colocalized with afadin but not E-cadherin or α-catenin at the apical-lateral border, suggesting that a complex including ZO-1 and afadin scaffolds for assembly and localization of the ring adjacent to the wound. Claudin/ZO-1 and nectin/afadin complexes might thus anchor the actomyosin cables to cell adhesion sites (Tamada *et al.*, 2007).

5.1.4. Additional mechanisms inducing junction formation and stabilization

Independent of GTPases, E-cadherin engagement recruits Ena/VASP to the cell surface, which in turn can polymerize actin cables providing the force necessary to bring epithelial cells actively together (Vasioukhin *et al.*, 2000; Schirenbeck *et al.*, 2006; Scott *et al.*, 2006). α-Catenin recruits and regulates formins to and at AJs, respectively (Kobielak *et al.*, 2004). Furthermore, α-catenin binds ZO-1 (Itoh *et al.*, 1997) during the junction formation process supporting the formation of linear actin cables (Ikenouchi *et al.*, 2007). Initial cell-cell contacts are approached by actin filaments perpendicular through local Arp2/3 dependent polymerization, while mature contacts are characterized by a parallel orientation to the membrane (Adams *et al.*, 1998; Vasioukhin *et al.*, 2000). Essential for this switch might be α-catenin. As a monomer it binds the E-cadherin/β-catenin complex, as homodimer it competes with the Arp2/3 complex for F-actin binding. Thus, cadherin-catenin clustering at maturing junctions would generate a high local concentration of cadherin-free α-catenin, which could antagonize branching and promote linear organization of parallel bundles (Drees *et al.*, 2005). Nevertheless, the fusion protein of a C-terminal truncated E-cadherin (tEC) lacking the β-catenin binding site and α-catenin is able to link adherens junctions to the actin cytoskeleton (Nagafuchi *et al.*, 1994). Further analysis revealed that a fusion protein of tEC and amino acids 509 – 643 of the 906 amino acid protein α-catenin, the so-called adhesion modulation domain located in and downstream of the VH2 domain, is sufficient and essential for adhesion (Nagafuchi *et al.*, 1994; Imamura *et al.*, 1999). However, fusion protein expressing cells are not committed to rapid remodelling (Nagafuchi *et al.*, 1994), further reinforcing the role of α-catenin as allosteric regulator of the actin cytoskeleton. E-cadherin and nectin *trans*-interactions stabilize newly formed cell-cell adhesion: activation of Rac and Cdc42 promotes retention of E-cadherin at the plama membrane by inhibition of clathrin-dependent endocytosis (Izumi *et al.*, 2004).

5.2. Epithelial junction dissociation

5.2.1. Epithelial-Mesenchymal Transition

Epithelial-Mesenchymal Transition (EMT) is a process allowing polarized, immotile epithelial cells to convert into motile, mesenchymal cells. This process is highly conserved and an indispensable mechanism during morphogenesis. Furthermore, it is implicated in promoting carcinoma invasion and metastasis (Thiery and Sleeman, 2006). Overall, EMT can be loosely defined by three major changes in cellular phenotype: (i) Cobblestone-like polarized epithelial cells in monolayers change to spindle-shaped mesenchymal cells with migratory protrusions; (ii) epithelial differentiation markers change from cell-cell junction proteins and cytokeratin intermediate filaments to vimentin filaments and fibronectin; (iii) functional changes leading to the acquisition of the ability to migrate and invade the ECM. Thereby, not all three changes are always observed during EMT, and (iii) alone is considered as a functional hallmark of EMT (Boyer and Thiery, 1993; Hay, 1995). Vive versa, EMT is not an

irreversible switch, and the reverse process, Mesenchymal-Epithelial Transition (MET), also occurs during embryonic development and pathological processes (Boyer and Thiery, 1993; Davies, 1996). During development, tissue remodelling via EMT induces amongst others mesoderm formation (Viebahn, 1995), neuronal crest development (Nichols, 1981; Duband and Thiery, 1987; Martins-Green and Erickson, 1987; Tucker *et al.*, 1988), cardiac valve development (Markwald *et al.*, 1977; Bolender and Markwald, 1979), secondary plate formation (Fitchett and Hay, 1989) and male Müllerian duct regression (Trelstad *et al.*, 1982). EMT during tumour progression allows single carcinoma cells to disseminate from primary epithelial tumours by loosening of cell-cell adhesion and acquisition of motility in order to break away from neighbouring cells and invade adjacent cell layers (Thiery, 2002). Major extracellular signal transmitters inducing EMT are members of the transforming growth factor-β (TGF-β) superfamily. During development, TGF-β superfamily members induced EMT initiates inter alia mesoderm formation in *Xenopus*, zebrafish and mice embryos (McDowell and Gurdon, 1999; Chen *et al.*, 2006; Kimelman, 2006). Furthermore, they are involved in neural crest formation in *Xenopus*, chickens and mice (Raible, 2006; Correia *et al.*, 2007) and cardiac valve formation in chicken (Boyer *et al.*, 1999). TGF-β induced signalling has also been shown to promote EMT in carcinoma cells by allowing cells to invade into the ECM in culture and spread to distant organs in mice (Oft *et al.*, 1998; Janda *et al.*, 2002). In cultured epithelial cells, the TGF-β receptors are localized at tight junctions and interact there with regulators of epithelial polarity and TJ integrity (Barrios-Rodiles *et al.*, 2005; Ozdamar *et al.*, 2005). Phosphorylation events induced by TGF- type II receptor lead to the loss of TJs and apical-basal polarity (Ozdamar *et al.*, 2005). Together with the TGF-β pathway, EMT is regulated via a number of other signalling pathways, including the Wnt and Notch pathway and several tyrosine kinase receptor pathways including Met, epidermal-growth factor-receptor (EGFR), fibroblast-growth factor-receptor (FGFR) and platelet-derived-growth factor-receptor (PDGFR) (Yang and Weinberg, 2008). Typical epithelial markers downregulated upon EMT include E-cadherin, claudins, occludins, desmoplakin, cytokeratin-8, -9, -18 and mucin-1, whereas the mesenchymal markers smooth-muscle actin, vimentin, fibronectin, vitronectin, fibroblast-specific protein-1 (FSP-1) and FGFR2 IIIb and IIIc splice variants are upregulated (Thiery and Sleeman, 2006). For a full EMT induction several signals must be combined and present for a prolonged time period (> 4-6 days) (Cui *et al.*, 1996; Oft *et al.*, 1996; Lehmann *et al.*, 2000; Gotzmann *et al.*, 2002). Once an EMT is established, it can be maintained after withdrawal of the inducing signal by autocrine TGF-β secretion (Oft *et al.*, 1996; Oft *et al.*, 1998; Janda *et al.*, 2002).

5.2.2. Scattering

During scattering epithelial cells become migratory and fibroblastoid in shape by a integrin-dependent actomyosin traction force induced dissociation of E-cadherin mediated cell-cell contacts (de Rooij *et al.*, 2005), but fail to activate the mesenchymal gene expression program (Jechlinger *et al.*, 2002). It is induced, in i.e. MDCK cells, by Hepatocyte Growth Factor (HGF; also known as Scatter Factor)

stimulation, which activates the Met pathway (Stoker, 1989). Multiple downstream signalling cascades including Ras, mitogen-activated protein kinase (MAPK), PI3K and Rac/Cdc42 induce the changes responsible for scattering (Royal and Park, 1995; Birchmeier *et al.*, 1997; Potempa and Ridley, 1998; Tanimura *et al.*, 1998).

5.2.3. Calcium as a tool to manipulate epithelial junction dynamics

Physiologically, Epithelial-Mesenchymal Transition (EMT) and scattering of epithelial cells both induce the downregulation of epithelial markers, dissociation of cell-cell contacts and induction of motility amongst various other processes (Jechlinger *et al.*, 2002; Thiery and Sleeman, 2006). The induction of scattering or a full EMT in a cell culture model system takes up to 48 h or 4 – 6 days, respectively (Cui *et al.*, 1996; Oft *et al.*, 1996; Lehmann *et al.*, 2000; Gotzmann *et al.*, 2002; Jechlinger *et al.*, 2002). The diversity of scattering/EMT induced processes during this time makes it extremely difficult to identify a specific, potentially transient process responsible for a detected effect. The calcium switch mimics just one of the many consequences induced by scattering/EMT. These assays are commonly used to investigate epithelial junction formation and dissociation induced cellular responses. They utilise the dependency of calcium ions for cadherins and desmosomes to *trans*-interact on adjacent cells. Alteration of the extracellular calcium level below a critical threshold leads to junction dissociation (Nakas *et al.*, 1966). Gap junctions, desmosomes, TJs including the proteins ZO-1, occludin, claudin-1 and -4 and JAM-1, and AJs including E-cadherin, β-catenin, p120-catenin and afadin dissociate (Martinez-Palomo *et al.*, 1980; Peracchia and Peracchia, 1980; Kartenbeck *et al.*, 1982; Sakisaka *et al.*, 1999; Rothen-Rutishauser *et al.*, 2002; Ivanov *et al.*, 2004). Thereby, AJs and TJs are internalized via clathrin-mediated endocytosis (Ivanov *et al.*, 2004). Upon calcium depletion epithelial junctions dissociate within minutes (Rothen-Rutishauser *et al.*, 2002). Calcium can be withdrawn by either addition of calcium specific chelators like ethyleneglycol-*bis*(b-aminoethyl)-N,N,N′,N′-tetraacetic acid (EGTA) (Nakas *et al.*, 1966) or medium exchange to medium with reduced amounts of calcium (Siliciano and Goodenough, 1988). Within the latter method, the calcium does not need to be depleted completely but just below the critical concentration for junction dissociation, whereby calcium depletion induced cytotoxic effects are minimized. Dissociated junctions can be easily reformed by elevation of the calcium level above this critical concentration (Gonzalez-Mariscal *et al.*, 1985). Nowadays, the modulation of the extracellular calcium concentration is a fully accepted and widely applied method to investigate cellular responses towards alterations in epithelial dynamics, and the application of this method gave rise to many of the concepts discussed in section II.5.1..

5.3. Discrimination between adherens and tight junction mediated signalling

A calcium switch induces the complete dissociation of epithelial junctions. To further narrow down which specific component of junction is essential for signal induction is complicated originating from

the complexity of junctional networks and the interdependency of their discrete elements (see discussion). To date, just a few experimental setups allow the separate investigation of AJ and TJ mediated signalling: one approach is taking advantage of the observation that E-cadherin is essential for the formation of epithelial junctions but not the maintenance of AJs. The knockdown of E-cadherin and Cadherin-6 in already preformed epithelial junctions of MDCK cells dissociates the AJ, but not the TJ (Capaldo and Macara, 2007). Vice versa, the deletion and knockdown of ZO-1 and ZO-2, respectively, in the ZO-3 deficient EpH4 cells allows epithelial polarization and AJ formation independently of TJs (Umeda *et al.*, 2006).

6. Rho-actin-SRF pathway

6.1. Serum Response Factor

Serum response Factor (SRF) was identified in 1986 by several independent studies as the protein responsible for serum-stimulated expression of the immediately early gene *c-fos* (Gilman *et al.*, 1986; Prywes and Roeder, 1986; Treisman, 1986). The 67 kDa protein is the founding member of the MADS (MCM1, Agamous, Deficiens, SRF) family of transcription factors, which is characterized by a conserved 56 amino acid MADS-box facilitating DNA-binding, homodimerization and protein-protein interactions. SRF is encoded on a single gene and conserved in all higher eukaryotes, where it is widely expressed. The SRF MADS-box mediates DNA binding to the 10 base pair DNA consensus sequence $CC(A/T)_6GG$, the so-called CArG box, which dyadic symmetry explains the dimeric nature of binding (Shore and Sharrocks, 1995). In fibroblasts, SRF is regulated at least via two families of signal regulated cofactors, the ternary complex factor (TCF) (Hipskind *et al.*, 1991; Dalton and Treisman, 1992; Price *et al.*, 1995) and myocardin-related transcription factor (MRTF) cofactor family (Miralles *et al.*, 2003). The TCF family of the Ets domain proteins, Elk-1, SAP-1 and Net, responds to MAPK signalling (Treisman, 1994). In contrast, two members of the MRTF family, MAL (also MKL1/MRTFa) and MAL16 (also MKL2/MRTFb), respond to Rho-actin signalling (Miralles *et al.*, 2003) whereas activation by the third member myocardin seems to be constitutive (Wang *et al.*, 2001). In fibroblasts, SRF activation is responsive to extracellular stimuli like whole serum, lysophosphatidic acid (LPA), aluminium fluoride ion (AlF_4^-), phorbol myristate acetate (TPA) and the polypeptide growth factors platelet-derived growth factor (PDGF), colony-stimulating factor-1 (CSF-1) and epidermal growth factor (EGF) (Hill and Treisman, 1995). However, SRF activation via the Rho-actin-MAL pathway is responsive to whole serum, LPA and AlF_4^-, but none of the other activators (Hill *et al.*, 1995). In general, heterotrimeric G proteins transduce the signal from the membrane via both pathways to SRF (Hill *et al.*, 1995).

6.2. Regulation of SRF via the Rho-actin pathway in fibroblasts

In the fibroblast model system RhoA induced actin treadmilling regulates the transcription factor SRF via its coactivator MAL (Figure 4). Activated forms of RhoA, Rac1 and Cdc42 induce SRF, but only functional RhoA is required for signalling to SRF, as shown by inhibition of RhoA with C3 exoenzyme (Hill *et al.*, 1995). Changes in actin dynamics regulate SRF: LIM kinase-1 (LIMK-1) and LIMK-2 strongly activate SRF, presumably by stabilization of F-actin via phosphorylation mediated inactivation of Cofilin. However, LIMKs are not essential signalling mediators that activate SRF following serum stimulus. F-actin accumulation via overexpression of VASP, WASP and N-WASP or constitutive active mDia1, mDia2 and the F-actin stabilizing drug jasplakinolide also strongly activates SRF. In constrast, latrunculin B, which sequesters actin monomers, completely blocks SRF activation (Sotiropoulos *et al.*, 1999; Copeland and Treisman, 2002; Geneste *et al.*, 2002; Grosse *et al.*, 2003). The RhoA effector kinase ROCK is not sufficient for SRF activation (Sahai *et al.*, 1998). Increase of the G-actin pool without altering the G- to F-actin ratio by ectopic expression of wild type actin or the non-polymerizable actin mutants G13R or R62D abolishes serum induced SRF activation. In contrast, the hyperpolymerizable actin mutants S14C, G15S and V159N, which favour F-actin

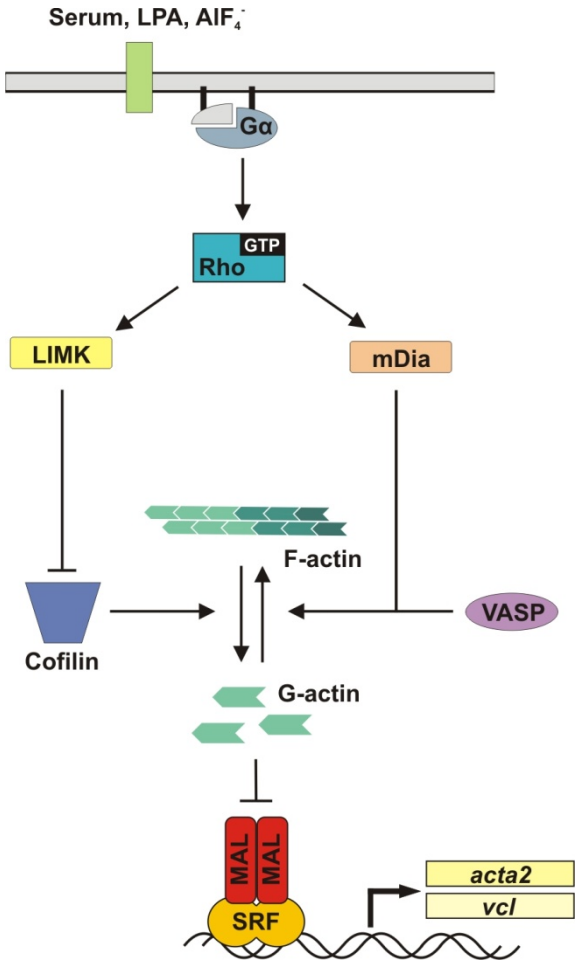

Figure 4: Regulation of the Rho-actin-SRF pathway in fibroblasts.

formation, strongly activate SRF. Together, these results indicate that a change in the G- to F-actin ratio mediating a depletion of the cellular G-actin pool is essential for signalling to SRF (Posern *et al.*, 2002; Posern *et al.*, 2004). G-actin can directly bind to the N-terminal RPEL motifs of MAL (compare Figure 40) and thereby inhibit SRF activation (Miralles *et al.*, 2003). In unstimulated cells, the actin/MAL complex rapidly shuttles between the cytoplasm and the nucleus. Upon serum stimulation induced actin polymerization it translocates to the nucleus. There it accumulates because serum stimulation efficiently blocks its export. Importantly, MAL binds to SRF but remains inactive until actin dissociates (Miralles *et al.*, 2003; Vartiainen *et al.*, 2007).

6.3. Endogenous SRF target genes

SRF induced transcription is essential for life, as homozygous *SRF*-deficient embryos die during gastrulation by not developing mesodermal cells (Arsenian *et al.*, 1998). $SRF^{-/-}$ embryonic stem cells grow, but do not display serum-induced immediate early growth response gene expression (Schratt *et al.*, 2001). Furthermore, these cells exhibit morphological perturbations dependent on the defective formation of cytoskeletal structures as well as defects in cell spreading, cell adhesion and migration (Schratt *et al.*, 2002). Besides the prototypical SRF target gene involved in cell growth, *c-fos*, in mammals approximately 160 genes harbouring a conserved CArG box element (the CArGome) have been identified as direct transcriptional targets of SRF in a computational genome wide screen, half of which have been validated experimentally (Sun *et al.*, 2006). Amongst the SRF target genes are many immediately early growth response genes encoding cytoskeletal components, signalling molecules and transcription factors (Sun *et al.*, 2006). A second major class of SRF target genes is involved in myogenesis, whereof some are expressed either in cardiac, smooth or skeletal muscle, others in multiple muscle types (Pipes *et al.*, 2006). The fact that the widely expressed SRF is required for the expression of muscle genes suggests that cofactors to initiate specific transcription exist. During myogenesis this cofactor is myocardin, which expression is largely confined to cardiac and smooth muscles of i.e. the cardiovascular system (Wang *et al.*, 2001). In general, SRF toggles between disparate programs of gene expression dependent on the signal transduction pathway (Sotiropoulos *et al.*, 1999; Gineitis and Treisman, 2001) and resulting cofactor binding (Wang *et al.*, 2001; Zaromytidou *et al.*, 2006). Activation of the MAPK pathway leads to the phosphorylation of TCF family proteins, which in turn initiate transcription by association with both, SRF and adjacent Ets-binding sites (Hipskind *et al.*, 1991). Induction of the RhoA-actin pathway promotes MAL/SRF complex formation. Thereby, MAL adds a β-strand to the SRF DNA-binding domain β-sheet region, and SRF induced DNA bending facilitates MAL-DNA contact (Zaromytidou *et al.*, 2006). Mechanistically, the cofactors compete for interaction with a common surface in the MADS-box of SRF (Miralles *et al.*, 2003; Wang *et al.*, 2004; Zaromytidou *et al.*, 2006). Amongst others, known SRF targets induced by TCF binding are the growth related *c-fos* and *egr-1* genes, the latter one encoding for early growth response protein-1. To the RhoA-actin activated MAL dependent SRF targets belong

the cytoskeletal components encoding *smooth muscle α-actin* and *vinculin* genes and *srf* itself (Sotiropoulos *et al.*, 1999).

7. Cellular model systems

The in this study mainly used Madin-Darby Canine Kidney (MDCK) cell line was derived from normal female adult Cocker Spaniel by S.H. Madin and N.B. Darby in September 1958 (Gaush *et al.*, 1966). Single cells lack apical-basal polarity, but E-cadherin mediated cluster fomation and collagen deposition at the basal surfaces of the cells leads to full polarization including the tight junction mediated intersection of the apical and lateral plasma membrane (Wang *et al.*, 1990). Furthermore, cell-cell adhesion between adjacent MDCK cells is mediated via desmosomes and gap junctions (Whitesell *et al.*, 1981; Cereijido *et al.*, 1984). MDCK cells are a widely used model system to investigate the formation and dissociation of epithelial cell-cell adhesion (Hinck *et al.*, 1994; Nathke *et al.*, 1994; Balda *et al.*, 1996; Sander *et al.*, 1998; Sakisaka *et al.*, 1999). HGF stimulation of MDCK cells in monolayer culture induces scattering (Stoker, 1989). As EMT model system EpRas cells were employed. These are oncogenic v-Ha-Ras expressing mouse mammary epithelial EpH4 cells (Oft *et al.*, 1996). Once a full EMT is established it persists in the absence of inducing signals due to an autocrine TGF-β secretion loop.

III. Aims of this PhD thesis

Epithelial cell-cell contacts are functionally and dynamically linked to the actin cytoskeleton. The dissociation of these contacts is a hallmark of Epithelial-Mesenchymal Transition, which is an essential process during morphogenesis and tumour progression. The aim of this study was to investigate whether epithelial cell-cell contacts regulate cellular gene expression. Specifically, I wanted to analyse if and how transcription controlled by serum response factor and its coactivator MAL is affected by epithelial cell-cell contact dissociation. Differential regulation of endogenous target genes, as well as promoter-reporter constructs, should be analysed for this purpose. Subsequent characterisation of the signal transduction pathway should be performed. I wanted to analyse a potential dependency on actin treadmilling, more precisely the depletion of the cellular G-actin level, and on the MAL protein. The participation of crucial small guanosine triphosphatases of the Rho family in signal transduction should be clarified, and the sufficient or required small GTPases should be identified. Effects of modifiers of F-actin function should also be tested. Moreover, the junction component within the epithelial contact critical for signal induction to SRF should be identified.

IV. Results

1. Serum stimulation does not activate SRF in confluent epithelial cells

The transcription factor SRF induces the expression of differential sets of target genes dependently on cofactor-binding. In fibroblasts, this is regulated via two known distinct signalling pathways: the Ras-MAPK pathway inducing the cofactors of the ternary complex factor (TCF) family, and the more recently discovered Rho-actin pathway inducing MAL/MKL1 (Hill and Treisman, 1995; Posern and Treisman, 2006; Zaromytidou *et al.*, 2006). To specifically determine the TCF-independent activation

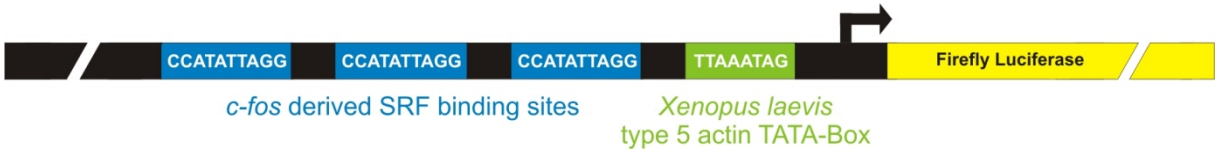

Figure 5: Scheme of the 3D.A-Luc SRF luciferase reporter plasmid used in this study. Three c-fos derived SRF binding sites in front of a Xenopus laevis type 5 actin TATA-Box drive the expression of the Firefly luciferase gene (Geneste *et al.*, 2002). The respective binding sequences are indicated in capital letters on the plasmid.

of SRF, the 3D.A-Luc reporter system was employed. This reporter consists of three *c-fos* derived SRF binding sites in front of a *Xenopus laevis* actin TATA box driving the expression of Firefly luciferase (Figure 5) (Geneste *et al.*, 2002; Miralles *et al.*, 2003). This system lacks sequences

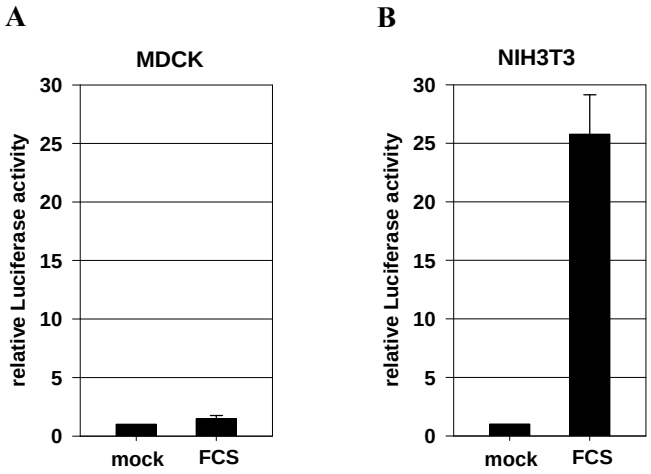

Figure 6: Epithelial cells do not activate SRF upon serum stimulation, in contrast to fibroblasts. (A) No SRF activation upon serum stimulation in epithelial MDCK cells. 1.5 x 10^6 MDCK cells were transiently transfected with the SRF reporter 3.DA-Luc (1.2 µg) and reseeded to form a confluent monolayer (600,000 per cm^2). They were serum starved at 0.5% FCS for 24 h followed by a serum stimulus to a final concentration of 15% FCS. (B) SRF activation upon serum stimulation in Fibroblasts. 3.5 x 10^4 NIH3T3 cells were transiently transfected with the same construct (20 ng), serum starved and stimulated as MDCK. Luciferase activity was always measured after 7 h. Shown is the relative luciferase activity normalized to protein amount. Error bars indicate the s.e.m. of three independent experiments. Mock, no FCS stimulus; FCS, serum addition to a final concentration of 15% FCS.

essential for TCF binding and is therefore unresponsive to the Ras-MAPK pathway (Hill and Treisman, 1995). Transiently 3D.A-Luc transfected NIH3T3 fibroblasts activated the SRF reporter upon serum stimulation (Figure 6 B), consistent with previous reports (Miralles *et al.*, 2003). By contrast, confluent epithelial MDCK cells did not significantly activate the reporter upon serum stimulation (Figure 6 A). Serum unresponsiveness was also observed in other epithelial cell lines like EpH4 mouse mammary gland or NBTII rat bladder carcinoma cells (not shown). These findings indicate that contrary to fibroblasts, epithelial cells regulate SRF-controlled genes independendly of serum. Other extracellular stimuli must mediate its regulation. Further investigations focused on how SRF is regulated in epithelial cells.

2. Calcium as a tool to manipulate the epithelial integrity of MDCK cells

Vertebrate epithelial cells form contacts to neighbouring cells via tight junctions, adherens junctions, desmosomes and gap junctions. Major components of adherens junctions and desmosomes are transmembrane proteins belonging to the cadherin familiy, which homophilically interact with their extracellular domains dependent on calcium. Reduction of the extracellular calcium level below a specific threshold leads to a dissociation of the contacts (Nakas *et al.*, 1966). Junction integrity regulated via calcium concentration can be monitored via the localization of the adherens junction component E-cadherin. During this study, I established specific protocols to dissociate and reassociate epithelial junctions by switching the extracellular calcium concentration. Epithelial canine kidney MDCK cells, maintained in normal culture medium, clustered via E-cadherin containing junctions (Figure 7, left). Calcium removal led to E-cadherin internalization and cellular detachment (Figure 7, middle) without apparently harming the cells, even if applied for several days (not shown). Readdition of calcium to the physiological concentration of 1.8 mM induced the reformation of the junctions within 15 minutes (Figure 7, right). Taken together, variation of the extracellular calcium concentration is a useful tool to regulate epithelial junction dynamics and analyse cellular responses.

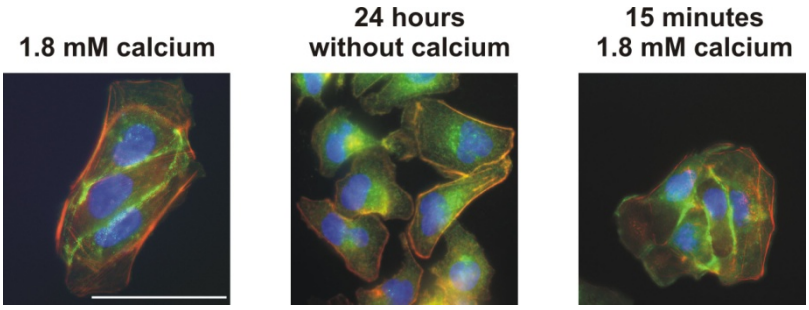

Figure 7: Calcium dependent epithelial junction dissociation and reassociation. MDCK cells (5 x 10^4 per cm^2) were maintained in normal culture medium (left) followed by a 24 h cultivation in calcium reduced medium (middle) and the readdition of calcium to physiological concentration for 15 minutes (right), fixed, and stained for E-cadherin (DECMA-1, green), F-actin (rhodamin-phalloidin, red) and DNA (blue). Bar: 25 µm.

3. SRF activity upon epithelial cell-cell contact formation

Epithelial cell-cell contact formation is known to be involved in small GTPase activation and actin reorganization (Braga and Yap, 2005). For instance, Rac and Rho were shown to be essential for the formation of cadherin dependent cell-cell adhesion and to induce the actin reorganization needed for receptor stabilization at the cell-cell contacts in epithelial cells (Braga *et al.*, 1997). Furthermore, nectin adhesion activates Cdc42 via Rap1 (Fukuyama *et al.*, 2005). ZO-1 is crucial for tight junction and polarized epithelial adherens junction formation by activation of Rac1 and the rearrangement of actin filaments (Ikenouchi *et al.*, 2007). Therefore, I carried out experiments investigating a possible connection between epithelial junction formation and SRF activation. MDCK cells (5 x 10^4 per cm^2) were transfected and grown in calcium depleted medium for 40 h. Thereafter, junction formation was induced by calcium addition, which led to an approximately 2-fold significant activation of SRF (Figure 8). E-cadherin clustering proved to be essential for activation as preincubation with the E-cadherin blocking antibody DECMA-1 abolished signal transduction (Figure 8). Furthermore, monomeric actin was identified as crucial signalling mediator. Latrunculin B inhibits actin polymerization by binding monomeric actin within the ATP-binding cleft (Spector *et al.*, 1999) still allowing actin/MAL complex formation. Ectopic expression of wild type and R62D actin increases the G-actin level independently of endogenous actin, whereby R62D is a non-polymerizable actin mutant possibly due to conformational changes mimicking free ADP-actin (Posern *et al.*, 2002). Ectopic expression of wild type (wt) or non-polymerizable mutant R62D actin as well as latrunculin B (LatB)

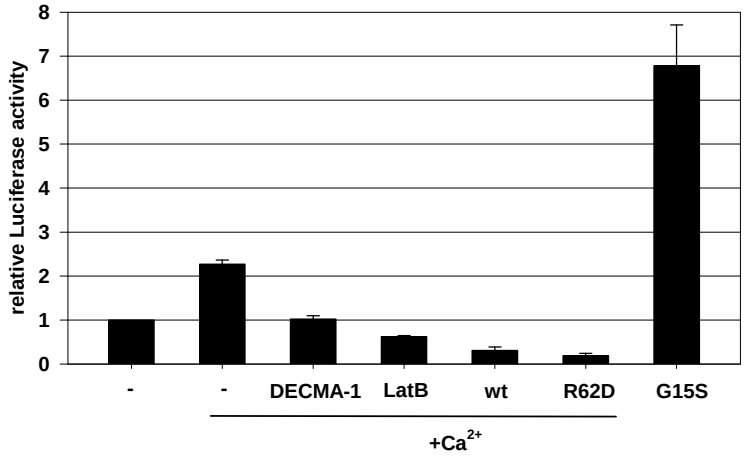

Figure 8: SRF activation induced by epithelial junction formation dependents on E-cadherin clustering and monomeric actin. MDCK cells (5 x 10^4 per cm^2) were transfected with 3D.A-Luc (60 ng), pRL-TK (50 ng) and, if indicated, with wild type (wt), R62D or G15S actin (250 ng each). Then the medium was exchanged to calcium and FCS free medium containing 0.2% BSA. After 40 h, calcium was added to a final concentration of 1.8 mM. Cells were preincubated with the E-cadherin blocking antibody DECMA-1 (1:100 dilution) for 30 minutes prior to the calcium stimulus. Shown is the relative luciferase activity normalized to pRL-TK measured after 7 h, error bars indicate s.e.m. of three independent experiments.

treatment repressed SRF induction. Conversely, the F-actin stabilizing mutant G15S (Posern *et al.*, 2004) led to a strong activation (Figure 8). Importantly, the ectopic expression of the different actins did not interfere with calcium dependent junction dissociation or formation, as visualized by E-cadherin staining (Figure 29 and Figure 31). Further investigations focused on triggering the relatively weak 2-fold SRF induction revealed no influence of cell density on inducibility (not shown). In summary, epithelial junction formation led to a small but significant SRF activation reliant on E-cadherin clustering and monomeric actin.

4. SRF activation induced by the dissociation of epithelial cell-cell contacts

Given that SRF activation during epithelial junction formation was very modest, I investigated other aspects of junction remodelling and their effects on transcription. Dissociation of epithelial cell-cell contacts is an essential process underlying the conversion of epithelial to mesenchymal cells, a process called epithelial-mesenchymal transition (EMT), and the disintegration of the epithelium. EMT is an indispensable mechanism during morphogenesis and pathologically a hallmark of malignant cancer progression initiating the dissemination of metastasis (Thiery and Sleeman, 2006). Only little is known about how epithelial cell-cell contact dissociation regulates transcription. To be able to address this question, I carried out experiments analysing epithelial junction integrity in dependence of the extracellular calcium level. The critical calcium concentration for MDCK cells grown in a confluent monolayer was between 0.04 and 0.05 mM, as visualized by immunostaining for E-cadherin (Figure 9, upper panel) and by the formation of bright circles around uncoupled epithelial cells due to their altered light scattering properties, the so-called halo effect, in phase contrast microscopy (Figure 9, lower panel). To test whether the dissociation of epithelial cell-cell contacts influences transcriptional regulation MDCK cells were transiently transfected with the 3D.A-Luc SRF luciferase reporter and seeded to form a confluent monolayer. To ensure proper junction formation cells remained then untouched for 24 – 36 h. After this, the culture medium was exchanged to medium containing the physiological (1.8 mM) or reduced amounts of calcium. SRF reporter activation, measured after 7 h, was significantly induced upon calcium withdrawal with a concentration dependent threshold of about 0.04 mM calcium. The maximum activation was detected at extracellular calcium concentrations of 0.02 mM and lower (Figure 10). The dissociation of the epithelial cell-cell contacts strictly correlated with SRF activation (Figure 9 and Figure 10). This denotes that epithelial sheet disintegration regulates transcription via SRF signalling.To ensure that the induction of the reporter by calcium withdrawal was strictly dependent on SRF, a mutant reporter lacking functional SRF binding sites was generated by replacing the sequence CCATATTAGG to CCCAATCGGG (compare Figure 5) (Hill and Treisman, 1995). The mutated reporter 2M.A-Luc was transfected into MDCK cells. The cells were seeded to form a confluent epithelial monolayer and 24h later medium was exchanged to medium

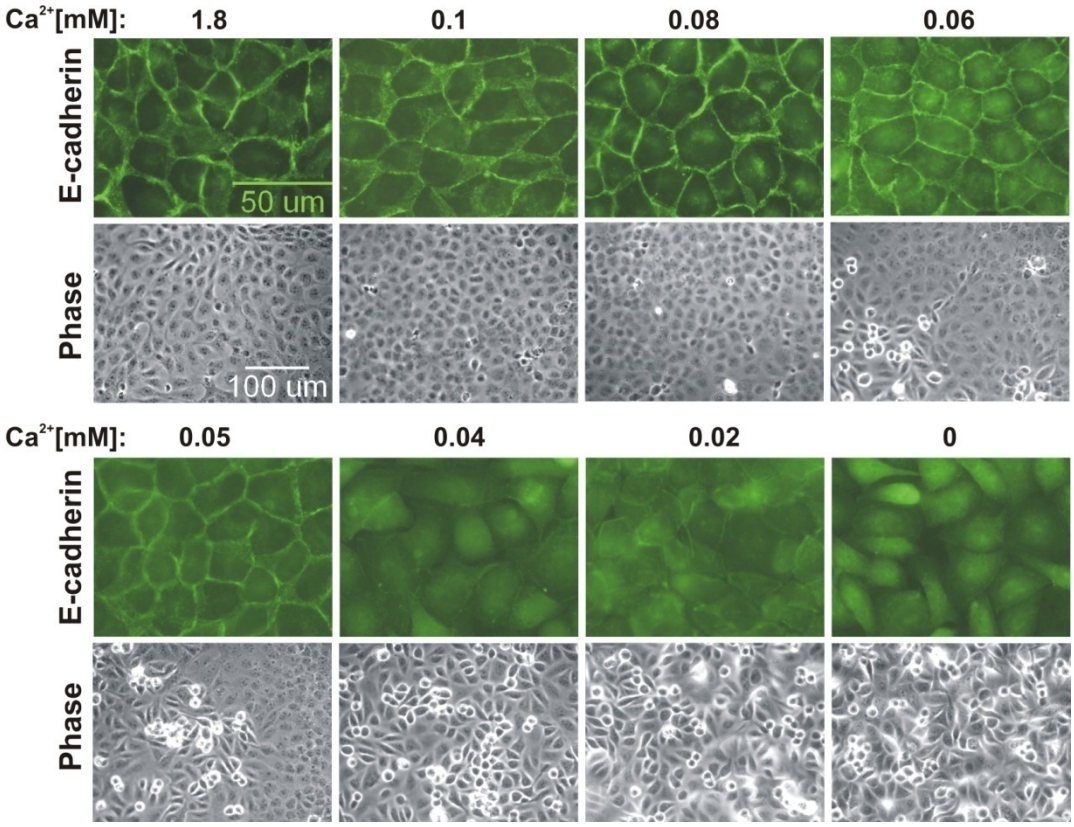

Figure 9: Epithelial cell-cell contacts dissociate upon reduction of the extracellular calcium level below a threshold of 0.05 mM. MDCK cells were seeded to form a confluent monolayer and maintained in normal culture medium for 24 h to allow proper junction formation. Then the medium was exchanged to medium with the indicated amounts of calcium. After 7 h the cells were fixed and analysed by phase-contrast microscopy (lower panel) or immunostained for E-cadherin (DECMA-1, upper panel).

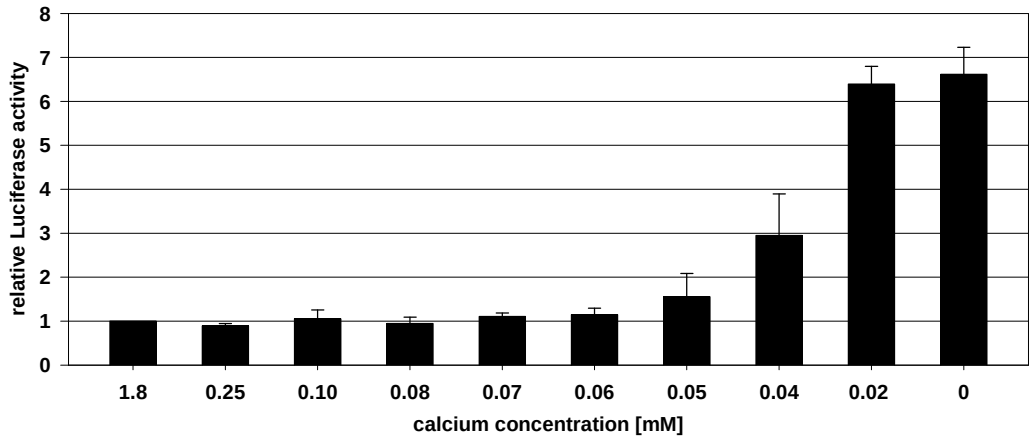

Figure 10: Dose response curve of SRF activation. MDCK cells were transiently transfected with 3D.A-Luc and reseeded to form a confluent monolayer. 24 h later the medium was exchanged to medium with the indicated amounts of calcium. Luciferase activity was measured after 7 h. Shown is the relative luciferase activity normalised to protein amount. Error bars indicate s.e.m. of three independent experiments.

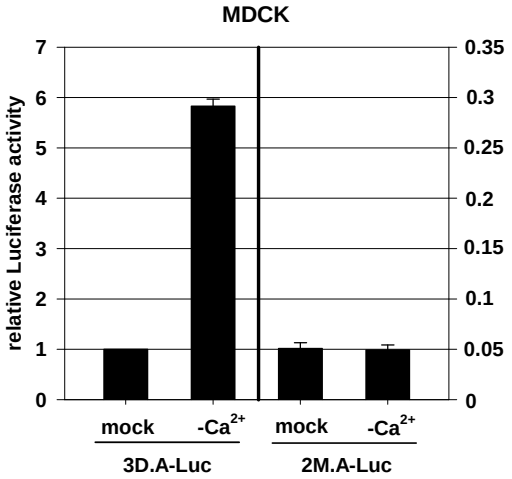

Figure 11: The induction of 3D.A-Luc upon calcium withdrawal strictly dependents on SRF binding. MDCK cells were transiently transfected either with 3D.A-Luc or a reporter harbouring mutated SRF binding sites (2M.A-Luc) and reseeded to form a confluent monolayer. After 24 h the medium was exchanged to normal calcium (1.8 mM) medium (mock) or medium containing 0.02 mM calcium (-Ca^{2+}). A mock medium exchange was performed to exclude potential alterations by addition of fresh medium or shear stress. Shown is the relative luciferase activity after 7 h normalized to protein amount, error bars indicate s.e.m. of three independent experiments. Note that the scaling for the relative luciferase activity differs for 3D.A-Luc and 2M.A-Luc.

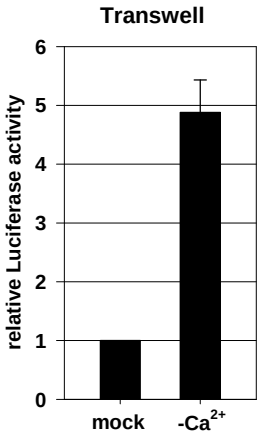

Figure 12: SRF activation in fully polarized MDCK cells grown on transwell filters. MDCK cells (1.75 x 10^5 per transwell) were transfected and treated as described in Figure 11.

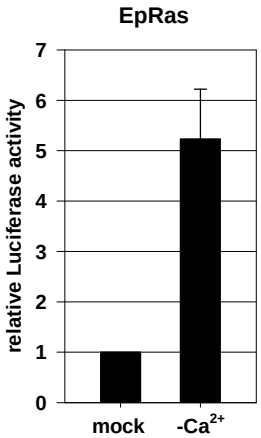

Figure 13: Contact dissociation leads to SRF activation in epithelial EpRas cells. Murine mammary gland derived EpRas cells were transfected and reseeded as MDCK. 24 h later the medium was exchanged to normal calcium medium (mock) or medium containing 0.02 mM calcium (-Ca^{2+}). Luciferase activity was measured after 7 h. Shown is the relative luciferase activity normalised to protein amount. Error bars indicate s.e.m. of three independent experiments.

containing physiological (1.8 mM) or reduced (0.02 mM) amounts of calcium. In contrast to the functional reporter, no activation of 2M.A-Luc was detected upon dissociation of epithelial cell-cell contacts (Figure 11). Furthermore, the absolute luciferase activities measured with the mutated reporter were reduced 20-fold, indicating the basal SRF activity in MDCK cells. To ensure a proper epithelial basolateral polarisation the luciferase assay was repeated with MDCK cells grown on porous transwell filters (Grunert *et al.*, 2003). Calcium withdrawal reproduced the previously obtained SRF activation (Figure 12). This indicates that junctions formed on normal uncoated tissue culture dishes are adequate to induce signalling. Depletion of calcium ions by the chelator EGTA is a commonly used method to disrupt epithelial cell-cell contacts (Nakas *et al.*, 1966; Rothen-Rutishauser *et al.*, 2002). Application of this method led to comparable results as obtained upon medium exchange (not shown), but resulted in strong cytotoxicity. An explanation for this might be the comparable long assay time of 7 h leading to a complete depletion of calcium ions, potentially intracellularly as well. In contrast, cultivation in low calcium medium did not inflict any ascertainable harm to MDCK cells for several days (not shown).

Several other epithelial cell lines including EpH4 and the EpH4-derived EpRas (Oft *et al.*, 1996) also activated the SRF reporter upon calcium withdrawal induced epithelial cell-cell contact dissociation to a similar extend as MDCK cells (Figure 13 and not shown).

5. E-cadherin deficient cell lines do not activate SRF

The formation of epithelial junctions depends on the homophilic calcium dependent *trans*-interaction of E-cadherins on neighbouring cells (Gumbiner *et al.*, 1988; Watabe *et al.*, 1994; Qin *et al.*, 2005). Numerous cancer cell lines of epithelial origin lost E-cadherin expression along with EMT induction (Vincent-Salomon and Thiery, 2003; Yang and Weinberg, 2008), amongst them the human gastric and breast cancer cell lines AGS and MDA-MB 435S, respectively (Figure 14, inset). Whereas MDA-MB 435S showed a fibroblastoid morphology (not shown), AGS cells exhibited a more epithelial, cobblestone like phenotype and formed a not fully developed epithelial sheet with some, but not all of the cells closely attached to each other (Figure 43). To investigate whether the dissociation of E-cadherin dependent junctions is essential for SRF activation, AGS and MDA-MB 435S cells were grown in confluent monolayers and subjected to calcium withdrawal. Both cell lines did not activate SRF upon calcium withdrawal (Figure 14). To assure that RhoGTPase induced SRF activation is generally functional in AGS and MDA-MB 435S cells, constitutive active variants of Rac1, RacV12, and RhoA, RhoQ63L, were cotransfected and tested for reporter activation. Both constructs induced SRF activation (Figure 14), approving a functional pathway. Furthermore, the E-cadherin deficient Chinese hamster ovary cell line CHO-K1 did not activate SRF upon calcium withdrawal (not shown). These results demonstrate that intact epithelial junctions are essential for SRF activation upon calcium withdrawal.

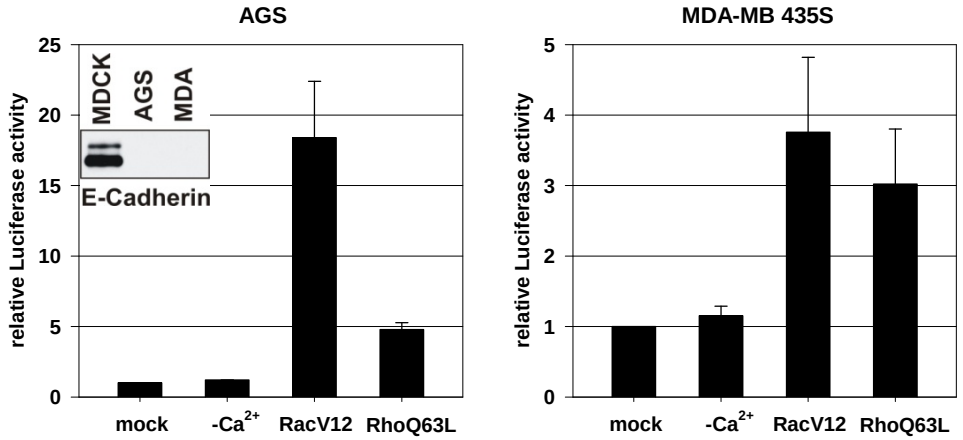

Figure 14: E-cadherin deficient cell lines do not activate SRF upon calcium withdrawal. The E-cadherin deficient cell lines AGS and MDA-MB 435S (inset) were transfected and reseeded as MDCK. For MDA-MB 435S 6 µg , for AGS 2.5 µg of either RacV12 or RhoQ63L were cotransfected to serve as positive controls proving the existence of a functional pathway. 24 h later the medium was exchanged to normal calcium medium (mock) or medium containing 0.02 mM calcium (-Ca^{2+}). Luciferase activity was measured after 7 h. Shown is the relative luciferase activity normalised to protein amount. Error bars indicate s.e.m. of three independent experiments.

6. Time course of cell-cell contact disintegration and SRF induction

To monitor the time course of SRF activation upon epithelial disintegration a new reporter plasmid was constructed. The vector pd2EGFP-N1 encodes for an EGFP with a half-life time of approximately 2 hours, because it is fused to amino acid residues 422–461 of the mouse ornithine decarboxylase, a PEST domain marking it for fast proteasomal degradation. The CMV promoter in pd2EGFP-N1 was replaced by the three *c-fos* derived SRF binding sites and *Xenopus laevis* type 5 actin TATA box from 3D.A-Luc (Figure 5 and Figure 15). Resultant, expression of the destabilized EGFP was driven by the SRF signalling.

Figure 15: Scheme of the SRF reporter plasmid used for life imaging. The SRF binding sites and TATA-Box from 3.DA-Luc (Figure 5) were cloned into pd2EGFP-N1 substituting the existing CMV promoter. Thereby, a plasmid harbouring a destabilized EGPF controlled by a SRF responsive promoter was constructed. The EGFP has a short half-life time because of fusion to a PEST domain, marking it for fast proteasomal degradation.

MDCK cells were stably transfected with this plasmid, the cell morphology and EGFP expression was analysed by time lapse microscopy. Upon calcium withdrawal of confluent cells the cell-cell-contacts opened completely within 15 minutes indicated by appearance of the halo effect. The dissociation was followed by EGFP expression after approximately 3 hours, which maintained for 7 hours and then declined again (Figure 16). A control medium exchange, whereby the physiological calcium concentration was maintained, did not change cell morphology or induce EGFP expression (Figure 16,

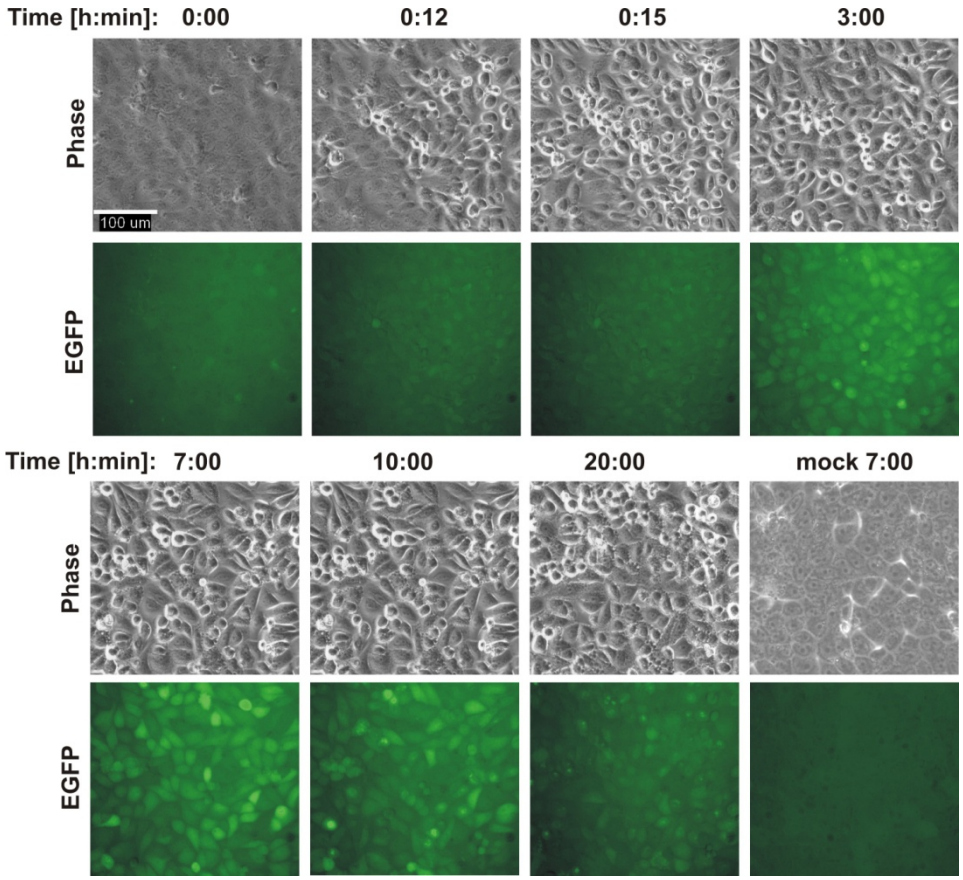

Figure 16: Calcium withdrawal induces full dissociation of epithelial junctions after 15 minutes followed by SRF activation. MDCK cells stably transfected with the life imaging SRF reporter (Figure 15) were seeded to form a confluent monolayer. 24h later living cells were analysed by microscopy monitoring cell morphology (upper panel) or EGFP expression (lower panel) after calcium withdrawal to 0.02 mM at the indicated times. Mock shows cell morphology and EGFP expression after control medium exchange to normal calcium for 7 h to exclude potential alterations by addition of fresh medium, shear stress or photocytotoxicity.

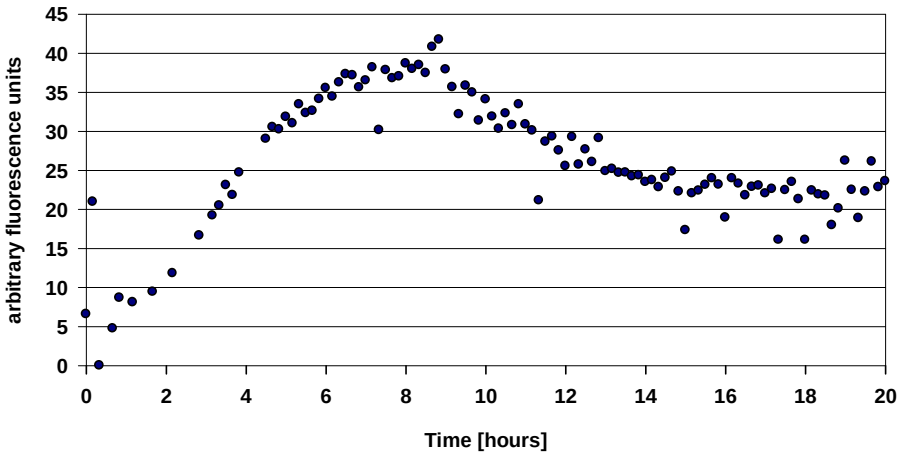

Figure 17: SRF activation upon calcium withdrawal peaks at about 8 hours. The induction profile shows the arbitrary EGFP fluorescence intensity monitored in Figure 16. It was calculated by subtraction of the measured fluorescence intensity in the mock experiment from the corresponding value upon calcium withdrawal for each time point.

mock). Quantification of the measured fluorescence intensity showed, that EGFP expression peaked at 8 hours, consistent with luciferase reporter activation (Figure 17). Several other independently isolated clones analysed showed similar results, differing just in background and signal to-noise ratio (data not shown).

7. Epithelial cell-cell contact dissociation activates the small GTPases Rac1 and RhoA

Members of the Rho GTPase family are known to be involved in epithelial junction organization and SRF regulation (Hill *et al.*, 1995; Braga and Yap, 2005). To investigate if small Rho GTPases mediate signal transduction from the dissociating epithelial cell contact towards SRF, I carried out pull-down assays precipitating the active, GTP-bound form of the activated GTPases Rho, Rac and Cdc42. To pull down Rho-GTP a fusion protein of GST and the Rho-binding domain (RBD) of the Rho effector Rhotekin, amino acids 7 – 89 of the murine protein, was used. Advantageously, Rho effectors only interact with GTP bound Rho and the RBD of Rhotekin inhibits both the intrinsic and GAP-enhanced GTPase activity of Rho (Ren *et al.*, 1999; Ren and Schwartz, 2000). The GTPase binding domain of human p21-activated kinase (PAK) 1B, amino acids 56 – 272, a Rac and Cdc42 effector protein specifically binding the GTP-loaded forms, fused to GST was used to affinity-precipitate these proteins (Sander *et al.*, 1998). To exclude any possible influence of shear stress caused by medium

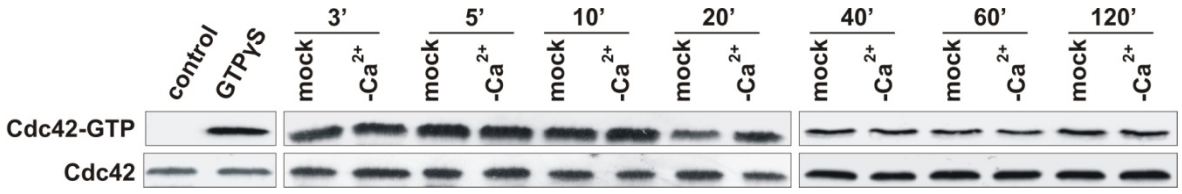

Figure 18: Cdc42 is not activated upon calcium withdrawal. MDCK cells were seeded to form a confluent monolayer. 36 h later the medium was exchanged with normal medium (mock) or medium containing 0.02 mM calcium (-Ca^{2+}). After the times indicated cells were lysed and a GST-PAK-CRIB pull down assay was employed. Uncoupled beads (control) or GTPγS incubated beads served as negative or positive control, respectively. Precipitates (Cdc42-GTP) or total lysate (Cdc42) were blotted for Cdc42.

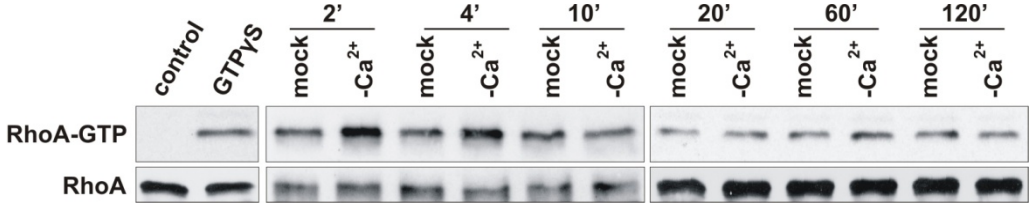

Figure 19: The transient RhoA activation upon calcium withdrawal peaks at 2 minutes. Experimental setup is identical to Cdc42 (Figure 18), except that GST-Rhothekin was employed for the pull down. Precipitates (RhoA-GTP) or total lysate (RhoA) were blotted for RhoA.

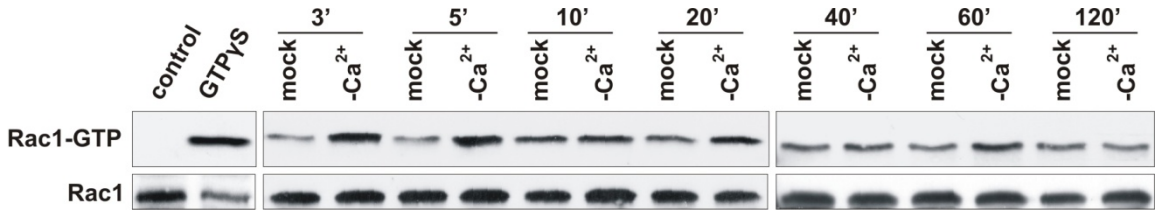

Figure 20: The transient Rac1 activation upon calcium withdrawal peaks at 3 minutes. The precipitates and total lysates obtained for Cdc42 (Figure 18) were blotted for Rac1.

exchange on the activation status of the fairly sensitive GTPases, additionally to calcium withdrawal a control medium exchange to normal calcium was performed at any given timepoint. For Cdc42, no significant activity changes were detected within 2 hours after calcium reduction (Figure 18). In contrast, GTP loading of RhoA occurred very rapidly and transient after calcium withdrawal peaking at 2 minutes with an average activation of 3.2 ± 1.0-fold (s.e.m. of 3 independent experiments), as analysed by densiometric analysis (Figure 19). The activation declined to background level after 10 minutes. Rac1 GTP-loading was as well fast and transient peaking at 3 minutes with an activation of 3.9 ± 0.9-fold going back to basal level after approximately 10 minutes (Figure 20). Over all, epithelial cell-cell contact dissociation results in a strong but transient activation of Rac1 and RhoA, but not Cdc42.

To investigate whether Rac1 and RhoA are sufficient to activate SRF in epithelial cells, the constitutive active mutants RacV12 and RhoL63 were transfected in MDCK cells and SRF activation was determined by luciferase reporter assay. Full SRF activation by either construct was detected already in the presence of calcium. It was not further triggered by calcium withdrawal, indicating the maximal possible inducibility of SRF in MDCK cells (Figure 21). Another small GTPase, Rap1, was also shown to be involved in cell-cell junction formation (Kooistra *et al.*, 2007). To analyse if Rap1 is

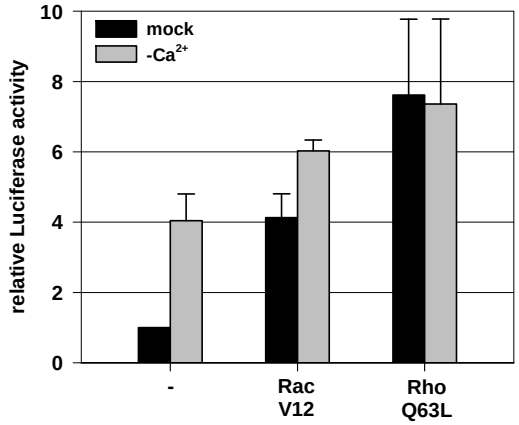

Figure 21: Constitutive active Rac1 and RhoA activate SRF. MDCK cells were transfected with constitutive active RacV12 or RhoQ63L (2.5 µg each), 3D.A-Luc (1.2 µg) and pRL-TK (1 µg) and reseeded. After 24 h the medium was exchanged for 7 h. Shown is the relative luciferase activity normalized to pRL-TK. Error bars indicate s.e.m. of three independent experiments. Mock, medium exchange to normal calcium medium; -Ca^{2+}, medium exchange to medium containing 0.02 mM calcium.

sufficient to activate SRF, a mutated version of it's GEF Epac, EpacΔcAMP, which lacks the cAMP binding site and is therefore constitutive active (de Rooij *et al.*, 1998), was assayed via luciferase reporter. Constitutive activation of Rap1 did not result in SRF activation (Figure 22), excluding Rap1 sufficiency. Recapitulatory, Rac1 and RhoA are activated upon calcium withdrawal and, in their active form, sufficient to induce SRF.

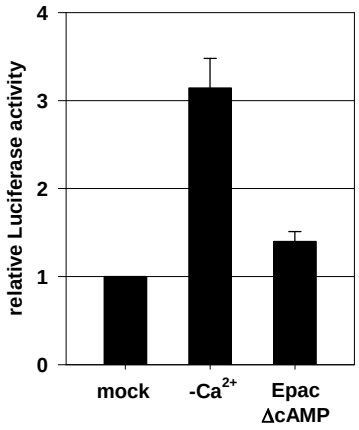

Figure 22: Activation of Rap1 does not lead to SRF reporter induction. MDCK cells were co-transfected with 2.5 µg of the constitutive active mutant EpacΔcAMP, a GEF of Rap1. Shown is the relative luciferase activity normalized to pRL-TK, error bars indicate s.e.m. of three independent experiments.

8. Active Rac1, but not Rho, induces SRF

To determine if activation of Rac or/and Rho is essential for SRF activation, I utilised the cell-permeable GTPase inhibitors TAT-C3, TcdB and TcdBF (Figure 23). TAT-C3 is a fusion protein of the HIV TAT leader sequence and the exoenzyme C3 derived from *Clostridium botulinum*. TAT permits the transduction of the protein across the plasma membrane whereas C3 selectively catalyses the ADP-ribosylation and consequent inactivation of RhoA, RhoB and RhoC (Sekine *et al.*, 1989; Sahai and Olson, 2006). TcdB is toxin B derived from *Clostridium difficile* strain VPI 10463. It

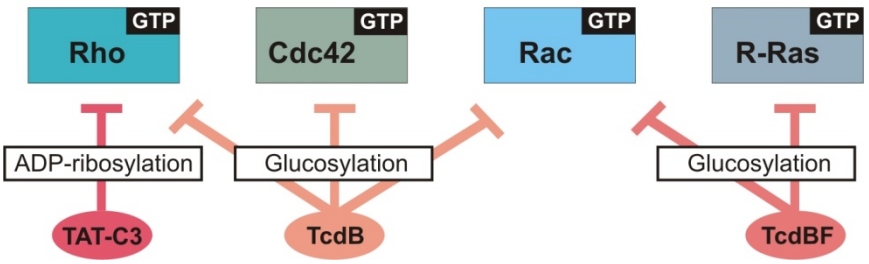

Figure 23: Inhibition spectra of the different clostridial toxins used. TAT-C3 specifically inhibits Rho by ADP-ribosylation. Both *Clostridium difficile* derived toxins inhibit by glucosylation, TcdB acts on Rho, Rac and Cdc42, TcdBF on Rac and R-Ras. Treatment of cells with each one of these inhibitors allows a specific differentiation between Rac and Rho.

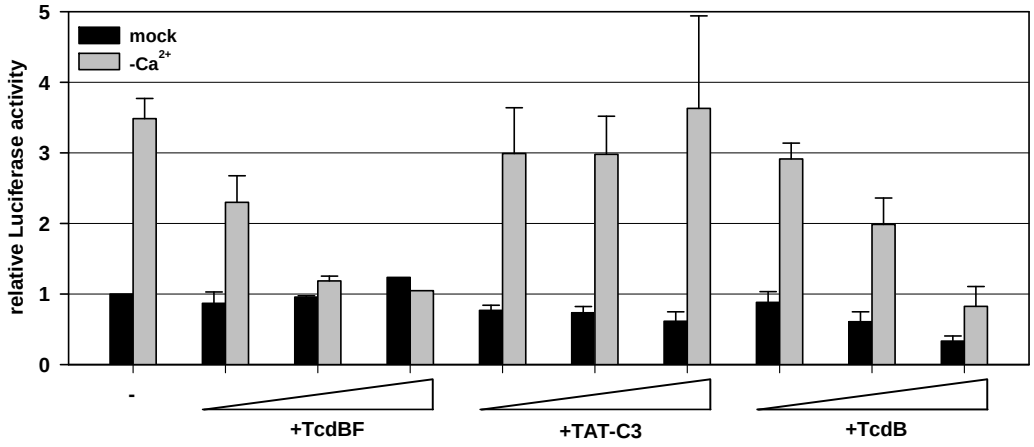

Figure 24: Rac, but not Rho is essential for SRF activation upon epithelial junction dissociation. MDCK cells were transfected and reseeded to form a confluent monolayer. Prior to medium exchange, cells were preincubated with different concentrations of TcdBF (0.1, 0.25 or 0.75 µg/mL) or TcdB (0.3, 1, 3 ng/mL) for 4 h, or TAT-C3 (0.3, 1 or 3 µM) for 15 h. Inhibitor treatment was maintained throughout the assay. Shown is the relative luciferase activity normalized to protein, error bars indicate s.e.m. of the independent experiments. Mock, medium exchange to normal calcium medium; -Ca^{2+}, medium exchange to medium containing 0.02 mM calcium.

inactivates Rho, Rac and Cdcd42 by glucosylation. TcdBF is a toxin B isoform from *Clostridium difficile* strain 1470 serotype F glucosylating specifically Rac/R-Ras. Both variants are cell-permeable (Huelsenbeck *et al.*, 2007). Treatment with each one of these inhibitors allows a specific differentiation between Rac1 and Rho (Figure 23).

Calcium withdrawal induced SRF activation was inhibited in a concentration dependent manner by TcdBF and TcdB, but not by TAT-C3, as measured by luciferase reporter (Figure 24). GTPase pull-down assay were performed to confirm functionality of the inhibitors in MDCK cells. After 4 h TcdBF pretreament, Rac1 remained inactive upon calcium withdrawal. No GTP-loading of RhoA was detected neither after 15 h preincubation with TAT-C3 nor after 4 h preincubation with TcdB. In constrast, preincubation with TcdBF did not hinder RhoA activation (Figure 25). Additionally underlining functionality, TAT-C3 hindered serum stimulation induced SRF activation in NIH3T3 fibroblasts in a concentration dependent manner (Figure 26). Importantly, immunostaining for E-cadherin analysed by confocal microscopy revealed that none of the inhibitors interfered with junction

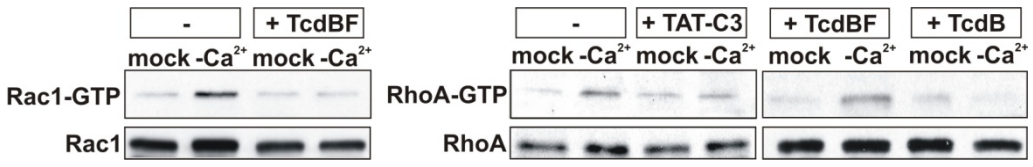

Figure 25: The clostridial toxins used are specific. GTPase pull-down assays for Rac and Rho were performed as described in Figure 19 and Figure 20. Where indicated, cells were preincubated with TcdBF (0.25 µg/mL) or TcdB (1 ng/mL) for 4 h, or TAT-C3 (1 µM) for 15h prior to medium exchange. The activity of Rac and Rho was measured 5 or 2 minutes after medium exchange, respectively. Mock, medium exchange to normal calcium medium; -Ca^{2+}, medium exchange to medium containing 0.02 mM calcium.

formation (Figure 27) or dissociation (not shown). TAT-C3 was preferred to C3 in this study, because expression of the cell- impermeable C3 abrogated already junction formation making calcium withdrawal induced dissociation impossible. Over all, this suggests that Rac1 rather than RhoA is essential for SRF activation induced by epithelial cell-cell contact dissociation.

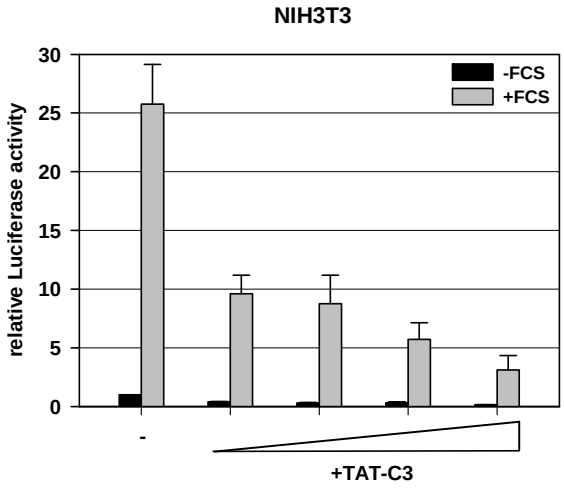

Figure 26: TAT-C3 inhibits serum stimulation induced SRF activation in NIH3T3 fibroblasts. 3.5 x 10^4 cells were transfected with 3D.A-Luc (20 ng) and pRL-TK (50 ng) and serum starved at 0.5% FCS for 20 h. They were incubated with different concentrations of TAT-C3 (0.1, 0.3, 1 or 3µM) for 15 h prior to stimulation with 15% FCS. Shown is the relative luciferase activity after 7 h normalized to pRL-TK, error bars indicate s.e.m. of three independent experiments.

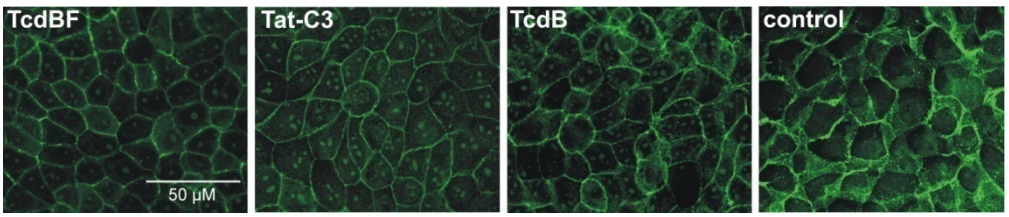

Figure 27: Treatment with the clostridial toxins does not interfere with epithelial junction formation. Confluent MDCK cells were incubated with TcdBF (0.25 µg/mL) or TcdB (1 ng/µL) for 11 h, or TAT-C3 (1 µM) for 22 h in medium with normal calcium concentration prior to fixation and analysis for E-cadherin localization via confocal immunofluorescence microscopy.

9. Dissociating epithelial cell-cell contacts activate SRF via monomeric actin

In fibroblasts, serum stimulation of SRF is regulated by monomeric G-actin, which binds to and thereby inhibits the SRF co-activator MAL (Vartiainen *et al.*, 2007; Guettler *et al.*, 2008). To test if this finding is also valid in epithelial cells, the monomeric actin level in MDCK cells was elevated by latrunculin B treatment or ectopic expression of wild type or non-polymerizable R62D actin. All stimuli significantly and efficiently reduced SRF activation upon calcium withdrawal (Figure 28).

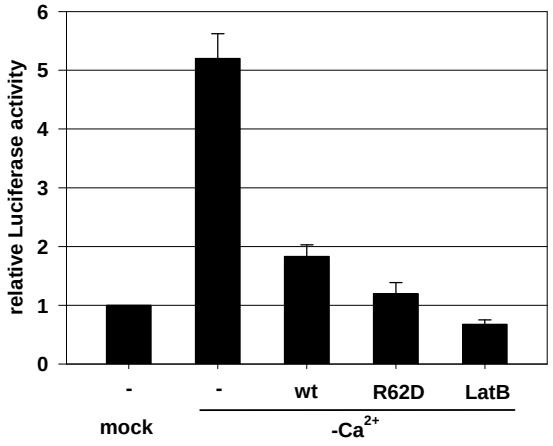

Figure 28: SRF activation is dependent on monomeric actin. MDCK cells were transfected with 3D.A-Luc (1.2 µg), pRL-TK (1 µg) and, where indicated, with 2.5 µg of wild type actin (wt) or the non-polymerizable actin mutant R62D and reseeded to form a confluent monolayer. Latrunculin B (LatB, 1 µM) was added 30 minutes before medium exchange. Shown is the relative luciferase activity normalized to pRL-TK, measured after 7 h, error bars indicate s.e.m. of 4 independent experiments.

Importantly, neither wt nor R62D actin influenced epithelial junction formation or dissociation as visualized by E-cadherin staining (Figure 29), excluding an indirect effect on SRF regulation by alteration of junctional dynamics. Vive versa the F-actin stabilizing mutant G15S activated SRF already fully in physiological calcium concentration (Figure 30) without interfering with junctional dynamics (Figure 31). To monitor changes in the endogenous G- to F-actin ratio upon cell-cell contact dissociation ultracentrifugation experiments were carried out (Posern *et al.*, 2002). Therefore, confluent MDCK cells were lysed 1 h after calcium withdrawal and Triton soluble and insoluble fractions were separated at 100.000 x g containing G- or F-actin, respectively, and analysed by Western blotting. As controls served latrunculin B and jasplakinolide, the latter acts as inducer of actin polymerization by depletion of the monomeric actin pool and filament stabilizer (Bubb *et al.*, 1994). Expectedly, latrunculin B treated cells contained mainly Triton soluble monomeric actin whereas jasplakinolide treatment almost completely depleted this pool, indicating that the assay is functional. Upon calcium withdrawal the G- to F-actin ratio shifted slightly but reproducibly by 8%, depleting the monomeric actin pool (Figure 32). Furthermore, changes in the F-actin cytoskeleton could be visualized by phalloidin staining. At calcium concentrations permissive for cell-cell-contact formation the majority of F-actin was localized at the contact. Below the threshold concentration of 0.04 mM the contacts dissociated, leading to a formation of thicker cortical actin bundles (Figure 33). Taken together, this data suggest that SRF activation by dissociating epithelial cell-cell contacts is dependent on changes in actin dynamics, particularly the depletion of the monomeric G-actin pool.

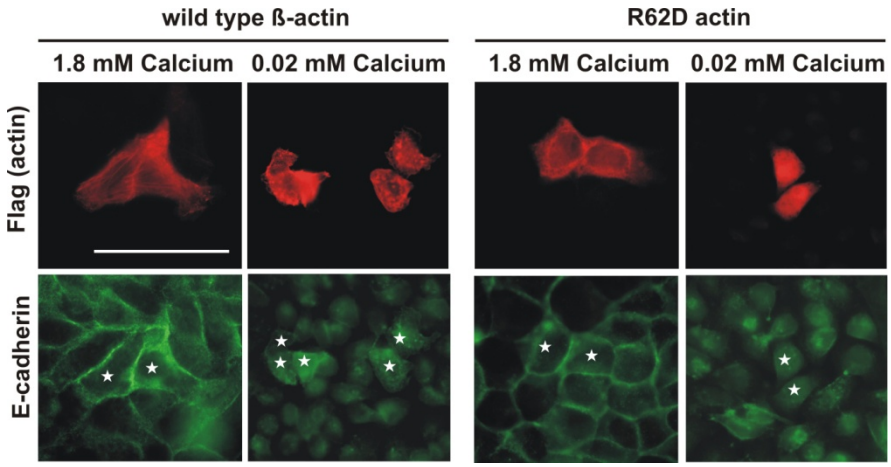

Figure 29: Ectopic expression of wild type or R62D actin does not interfere with epithelial junction formation or dissociation. Cells were transfected with Flag-tagged wild type or R62D actin and reseeded to form a confluent monolayer. 24 h later, the medium was exchanged as indicated and after 7 h incubation cells were fixed and stained for Flag (upper panel) and E-cadherin (DECMA-1, lower panel). Transfected cells are marked by stars. Bar: 50 µm)

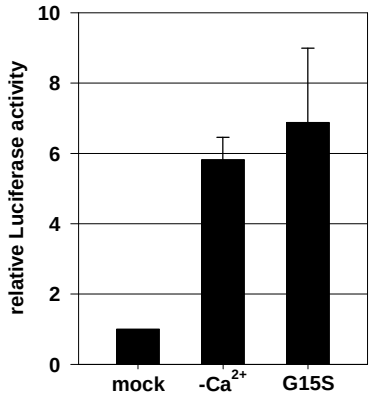

Figure 30: The F-actin stabilizing actin mutant G15S fully activates SRF in the presence of calcium. MDCK cells were, where indicated, co-transfected with 2.5 µg G15S. Further steps were performed as described in Figure.

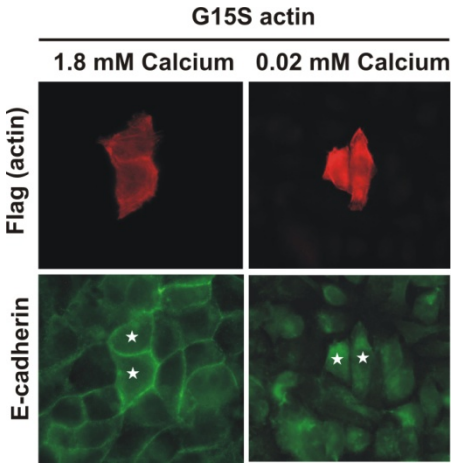

Figure 31: Ectopic expression G15S actin does not interfere with epithelial junction dynamics. The experiment was carried out as described in Figure. Stars mark transfected cells. Bar: 50 µm.

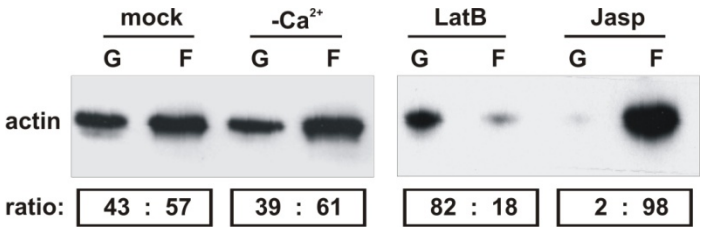

Figure 32: Calcium withdrawal induced shift in the G- to F-actin ratio, depleting the monomeric actin pool. Confluent MDCK cells were maintained in medium with normal (mock) or 0.02 mM (-Ca^{2+}) calcium for 1 h .Where indicated, cells were pretreated with 3 µM latrunculin B (LatB) or 0.5 µM jasplakinolide (Jasp) for 30 minutes. Triton-soluble and -insoluble fractions were separated by 100,000 x g, and supernatant (G) and pellet (F) were blotted for actin. Densitometric analysis of the ratio in percent is shown below.

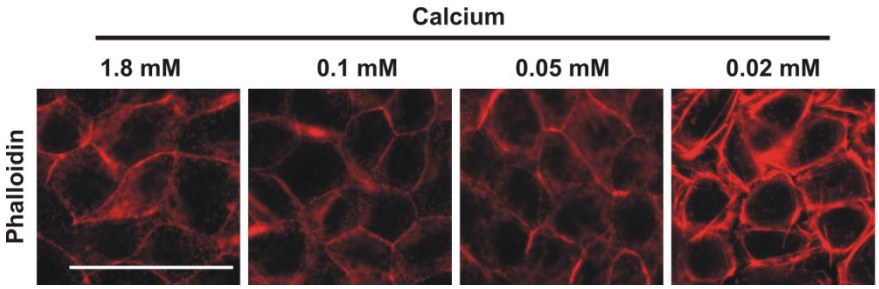

Figure 33: Correlation of the F-actin cytoskeleton reorganization with calcium level. Confluent MDCK cells were incubated in medium containing the indicated amounts of calcium for 7 h, then fixed and stained for F-actin with rhodamin-phalloidin. Bar: 50 µm.

10.Actomyosin contractility is not sufficient to activate SRF

The RhoA activated coiled-coil kinase (ROCK) is the central regulator of actomyosin contractility, acting on myosin light chain (MLC) in multiple ways (Figure 34) (Pellegrin and Mellor, 2007). The formation of apical contractile actomyosin rings was shown to drive epithelial junction disassembly in calcium depleted cells (Ivanov *et al.*, 2004). Furthermore, hepatocyte growth factor (HGF)-triggered integrin-dependent actomyosin contraction induces cell scattering mimicking EMT including junctional dissociation in MDCK cells (de Rooij *et al.*, 2005). Therefore, I investigated the effects of actomyosin contraction on SRF regulation. Contractility was repressed by two small molecules: Y-27632, a ROCK inhibitor (Uehata *et al.*, 1997) or Blebbistatin, an inhibitor of non-muscle myosin II ATPase activity (Straight *et al.*, 2003; Kovacs *et al.*, 2004). Preincubation with both small molecules led to an abrogation of SRF activation upon calcium withdrawal (Figure 35). To examine the effects accountable for the absence of inducibility E-cadherin and phalloidin micrographs after Blebbistatin

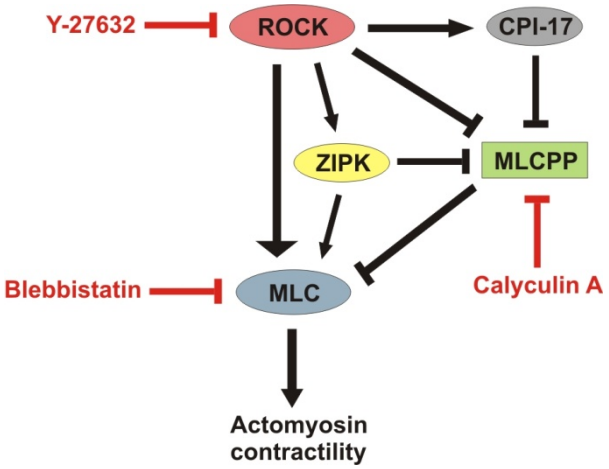

Figure 34: Scheme describing the regulation of actomyosin contractility by ROCK and the points of action for interfering substances used in this study. ROCK stimulates actomyosin contractility by acting on myosin light chain (MLC) in several ways: (i) direct phosphorylation; (ii) inhibition of MLC phosphatase (MLCPP) (iii) phosphorylation of ZIP kinase (ZIPK) which activates MLC and inhibits MLC phosphatase; (iv) activation of CPI-17, a MLCPP inhibitor. Actomyosin contraction is inhibited by Y-27632 and Blebbistatin inhibiting ROCK or MLC, respectively. Calyculin A hinders MLCPP, thereby stimulating contraction.

treatment were analysed. This revealed a strong reduction of E-cadherin internalization upon calcium withdrawal, as was reported before (Ivanov *et al.*, 2004). Nevertheless, Rac1 and RhoA were, however, still activated upon calcium withdrawal, as determined by small GTPase pull-down assays (Figure 36). In physiological calcium concentration F-actin organization was diffuse with reduced amounts of stress fibers. Upon withdrawal no obvious reorganization and formation of thick cortical bundles took place (Figure 37). This indicates that SRF activation needs actomyosin contractility as a prerequisite, as otherwise F-actin remodelling and junction dissociation can not occur properly.

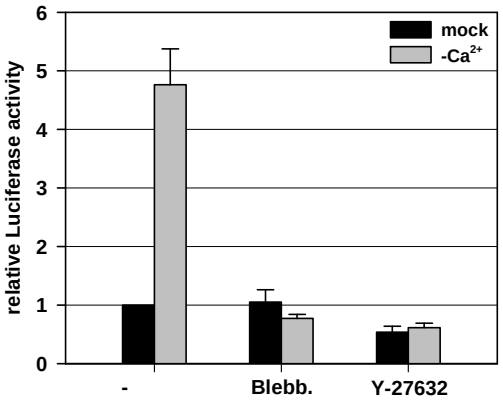

Figure 35: Actomyosin contractility is a prerequisite for SRF activation. MDCK cells were transfected and treated as before. Where indicated, cells were pretreated with Blebbistatin (100 µM, 2.5 h) or Y-27632 (20 µM, 30 minutes). The inhibitors were maintained on the cells throughout the assay. Luciferase assay was performed as before.

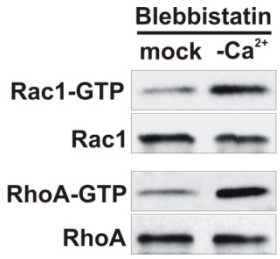

Figure 36: Calcium withdrawal induced Rac1 and RhoA activation is not dependent on actomyosin contractility. Pull-down assays for Rac and Rho were performed as described in Figure and Figure, either 5 or 2 minutes after medium exchange, respectively. Cells were pretreated with 100 µM Blebbistatin for 2.5 h.

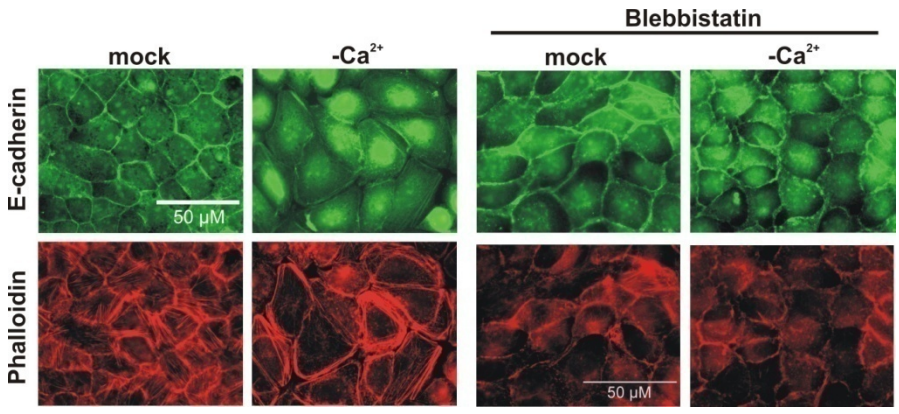

Figure 37: Blebbistatin treatment interferes with epithelial junction internalization and F-actin reorganization. Confluent MDCK monolayers were preincubated with Blebbistatin (100 µM, 2.5 h) prior to medium exchange and treatment was maintained throughout the assay. After 7 h cells were fixed and stained for E-cadherin (upper panel) and F-actin (rhodamin-phalloidin; lower panel).

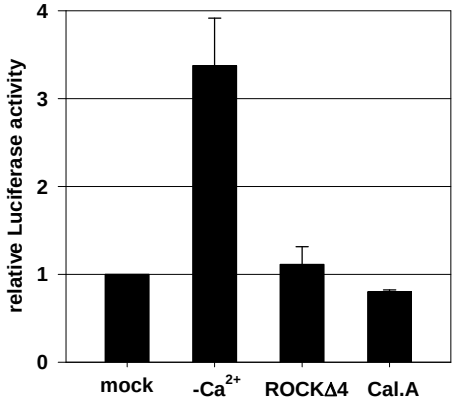

Figure 38: Forced actomyosin contraction does not activate SRF. MDCK cells were, if indicated, co-transfected with 2.5 µg ROCKΔ4 or pretreated with 5 nM calyculin A for 30 minutes (Cal.A; maintained throughout the assay). Further treatment and luciferase readout were performed as described before.

To investigate whether actomyosin contractility plays a direct role in SRF activation by transmitting signals experiments inducing stress fiber formation were carried out. ROCKΔ4 is constitutive active by truncation and calyculin A inhibits myosin light chain phosphatase and protein phosphatases PP1 and PP2A (Ishihara *et al.*, 1989; Resjo *et al.*, 1999). Overexpression of ROCKΔ4 or calyculin A treatment did not induce SRF (Figure 38), despite both stimuli forced formation of thick actin fibers as visualized by phalloidin staining (Figure 39). This results demonstrate that actomyosin contraction is a prerequisite, but not sufficient for SRF activation.

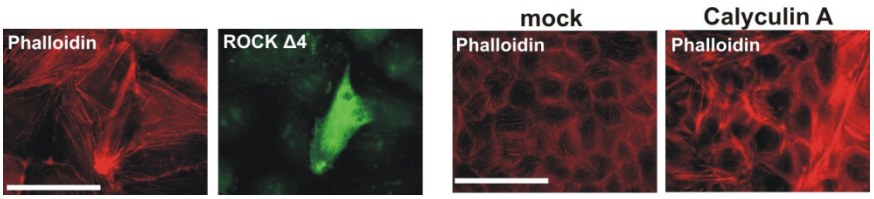

Figure 39: ROCKΔ4 and calyculin A induce stress fiber formation. (A) 5 x 10^4 MDCK cells were transfected with ROCKΔ4 and 36 h later fixed and stained for myc (ROCKΔ4) and F-actin (phalloidin). (B) Confluent MDCK cells were, if indicated, treated with calyculin (5 nM) for 7.5 h. Cells were fixed and stained for F-actin (phalloidin). Bars: 50 µM.

11. SRF activation upon epithelial cell-cell contact dissociation is dependent on MAL

To investigate the role of MAL regarding SRF activation upon cell-cell contact dissociation MDCK cells were transiently transfected with full length (fl) or mutant MAL constructs (Figure 40). MAL fl was sufficient to activate the SRF luciferase reporter in physiological calcium concentration, full activation was achieved upon calcium withdrawal (Figure 41). A constitutive active version of MAL, MALΔN, which lacks the N-terminal RPEL motives responsible for actin binding and thereby inhibition (Miralles *et al.*, 2003), activated SRF fully even in the presence of calcium (Figure 41).

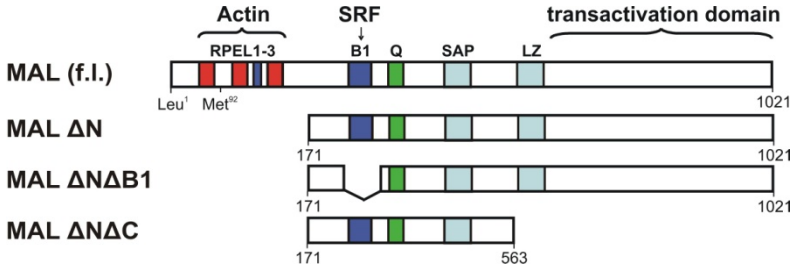

Figure 40: Scheme of MAL and the MAL mutants used in this study. Full length MAL (MAL (f.l.)) is a 1021 amino acid protein with 3 N-terminal located RPEL motives responsible for actin binding, a B1 domain allowing SRF binding, a Q domain strengthening affinity to SRF without direct contact, a SAP domain predicted to bind DNA and a leucine zipper (LZ) domain for dimerization and transactivation. All mutants lack the N-terminal RPEL motif and are insensitive to inactivation by actin binding. Therefore, MAL ΔN acts constitutive active. MAL ΔNΔB1 and MAL ΔNΔC function as dominant negatives, the first one by titrating out the endogenous MAL by dimerization without SRF binding, the latter one by binding SRF not allowing dimerization and transactivation.

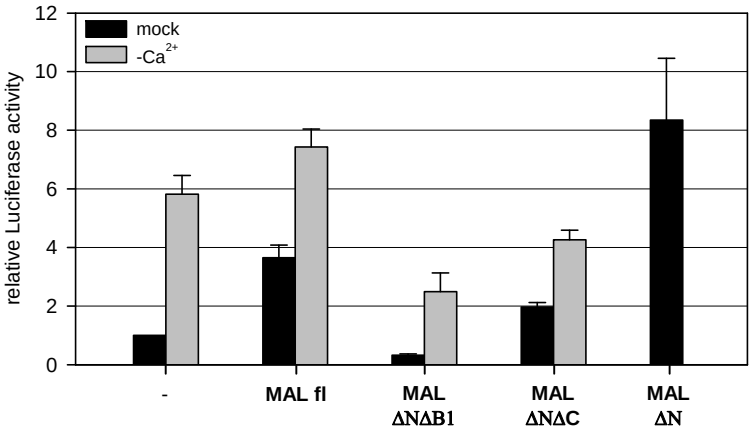

I
b **Figure 41: MAL is sufficient and essential for SRF activation.** MDCK cells were co-transfected with 0.4 µg MAL(f.l.), 2.5 µg MAL ΔNΔB1, 2.5 µg MAL ΔNΔC or 0.4 µg MAL ΔN. Medium exchange was performed as before. Luciferase activity is normalized to pRL-TK. Error bars are s.e.m. of three independent experiments.

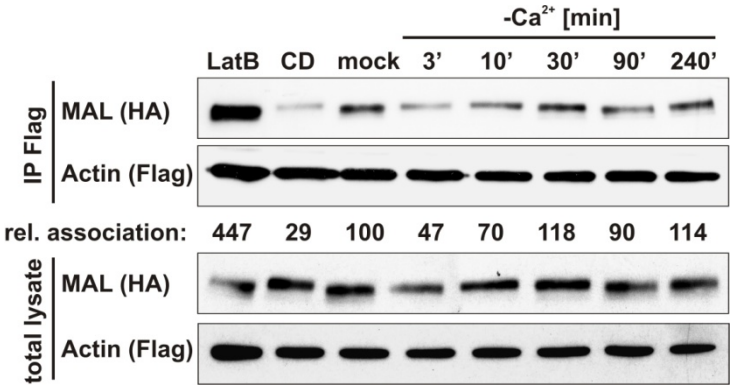

Figure 42: Dissociation of the actin-MAL complex upon epithelial cell-cell contact dissociation. 1 x 10^7 MDCK cells were electroporated with 10 µg Flag-actin and 10 µg HA-MAL and seeded to form a confluent monolayer. 36 h later the medium was exchanged to normal (mock) or 0.02 mM calcium (-Ca^{2+}). After the times indicated cell lysates were immunoprecipitated with anti Flag, blotted and visualized with antibodies against Flag- or HA-tag. Latrunculin B (LatB, 3 µM) or cytochalasin D (CD, 10 µM) were added 30 minutes prior to lysis. Relative association was calculated from densiometric analysis.

domain. MALΔNΔC binds SRF constitutively but can not dimerize and transctivate (Figure 40) (Miralles *et al.*, 2003; Zaromytidou *et al.*, 2006). Both constructs significantly reduced SRF activation upon calcium withdrawal, whereat MALΔNΔB1 showed a stronger inhibitory effect than MALΔNΔC (Figure 41).

The dissociation of the inhibitory actin/MAL complex is the critical step for MAL regulating SRF in fibroblasts (Vartiainen *et al.*, 2007). To determine if this finding also applies to epithelial cells, I conducted co-immunoprecipitation experiments investigating complex integrity. First attempts to immunoprecipitate endogenous proteins were difficult to reproduce, most likely due to unspecific actin binding to the sepharose beads. Therefore, MDCK cells were transiently transfected with tagged proteins: Flag-actin, which was immunoprecipitated, and HA-MAL. As expected, latrunculin B treatment strengthened the complex compared to mock medium exchange, densiometric analysis revealed approximately 4.5 fold. Vice versa cytochalasin D (CD) treatment, which acts by capping the barbed end of actin filaments and sequestration of monomers in a way that prevents interaction with MAL (Cooper, 1987; Sotiropoulos *et al.*, 1999), reduces complex integrity to about 30% (Figure 42). Calcium withdrawal led to a fast and transient dissociation of the actin/MAL complex peaking at about 3 minutes and a complete reassociation after 30 minutes. Additionally, MAL shifts upward upon complex dissociation, maybe due to phosphorylation or other posttranslational modifications (Figure 42). Overall, the results demonstrate that the actin/MAL complex dissociates upon epithelial cell contact disintegration and that MAL is sufficient and essential for SRF activation.

12.Adherens junctions seem to be essential for SRF activation

Calcium withdrawal induced epithelial junction dissociation leads to changes in actin dynamics, which in turn mediate SRF activation. Within the epithelial junction Adherens and Tight junctions are linked to the actin cytoskeleton (Miyoshi and Takai, 2008). To investigate whether AJs and/or TJs are essential for SRF activation, the E-cadherin deficient AGS cell line was stably transfected with wild type E-cadherin or empty vector as control and analysed via microscopy with respect to AJC protein localisation and luciferase reporter assay concerning SRF activation. Control transfected AGS cells grown others loosely attached to each other, visualized by the partial obliteration of cell-cell borders in phase in a confluent monolayer formed not fully developed epithelial sheets with some cells very closely and contrast microscopy (Figure 43, vehicle). Immunofluorescence analysis of these cells confirmed the complete loss of E-cadherin expression and revealed the lack of the AJ proteins β-catenin and afadin at the cell membrane, although expressed. In contrast, the TJ marker ZO-1 was detected, while not completely homogeneously distributed at cell-cell junctions (Figure 43, vehicle). Upon calcium withdrawal, the partially interconnected cells dissociated completely. Along with this,

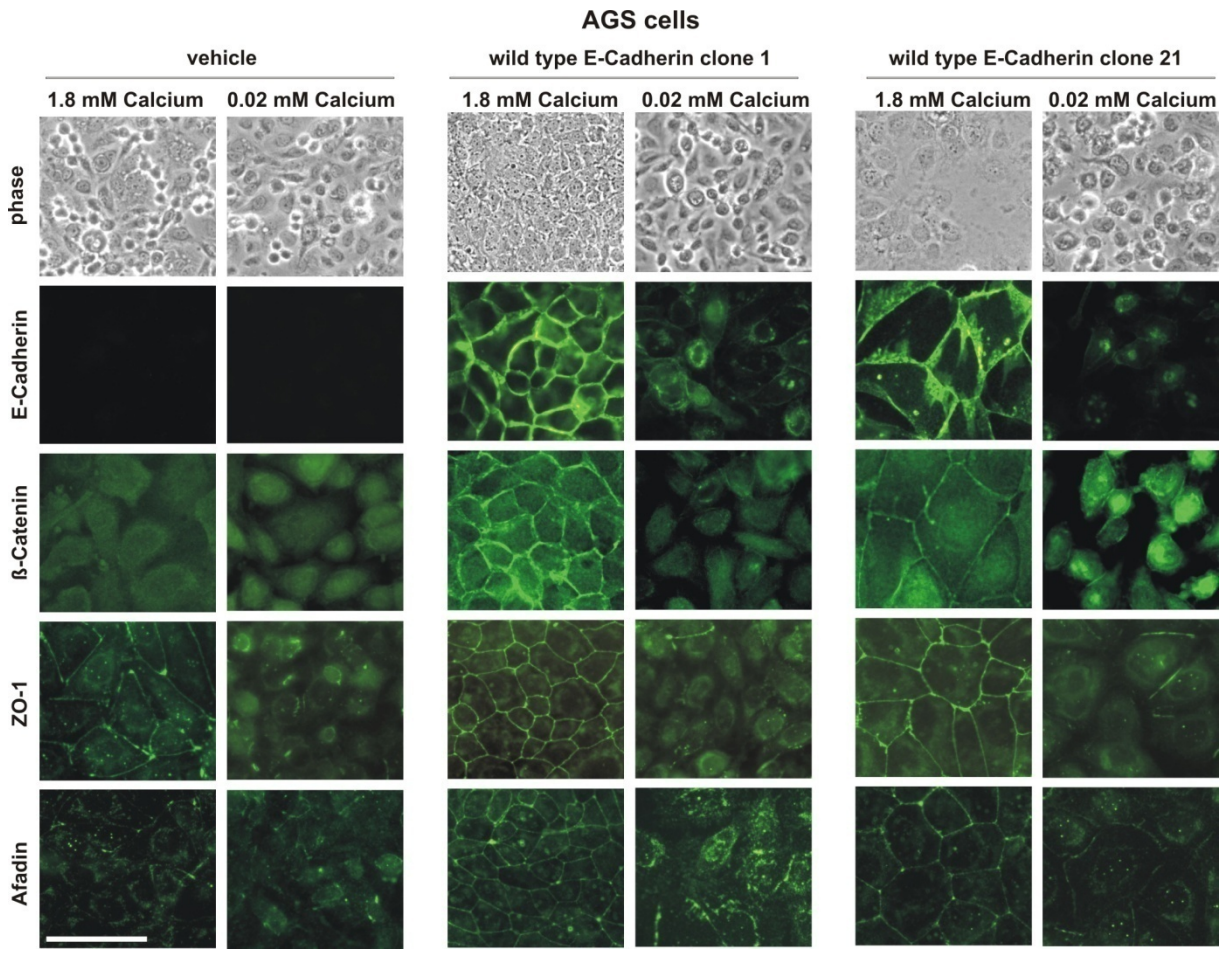

Figure 43: AJC analysis of AGS cells stably transfected with wild type E-cadherin or empty vector as control. Independently isolated clones of AGS cells stably transfected with wild type E-cadherin (clone 1 and clone 21) or empty vector as control (vehicle) were seeded to form a confluent monolayer and maintained in normal culture medium (1.8 mM calcium) for 48 h to allow proper junction formation. Then the medium was exchanged to medium with 0.02 mM calcium. After 7 h the cells were fixed and analysed by phase-contrast microscopy (phase) or immunostained for E-cadherin (ECCD-2), β-catenin, ZO-1 or afadin. Bar: 50 µm

ZO-1 dislocated from the membrane indicating the dissociation of TJs (Figure 43, vehicle). SRF was not activated upon calcium withdrawal (Figure 44, vehicle). Two independently isolated monoclonal AGS cell lines stably expressing E-cadherin, clone 1 and 21, fully developed epithelial sheets as visualized by the complete obliteration of cell-cell borders in phase contrast microscopy (Figure 43). Furthermore, they revealed a proper localization of E-cadherin and relocalization of β-catenin and afadin to the membrane. ZO-1 showed a more prominent membrane staining compared to control AGS cells (Figure 43). Calcium withdrawal induced the epithelial sheet dissociation as indicated by the appearance of the halo effect and the dislocation of E-cadherin, β-catenin, afadin and ZO-1 from the plasma membrane (Figure 43). Upon junction dissociation both, clone 1 and 21, activate SRF significantly approximately 3- or 1.5-fold, respectively (Figure 44). However, the basal SRF activity in the presence of calcium of clone 1 is around 50% reduced compared to control AGS cells. These data suggest that the calcium withdrawal induced dissociation of AJ but not TJ proteins leads to the activation of SRF. Further, AJ proteins complexed in the AJC might repress SRF activity.

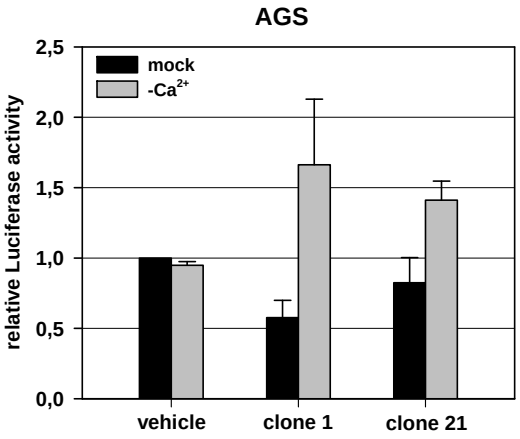

Figure 44: AGS cells stably expressing E-cadherin activate SRF upon calcium withdrawal. Stably control (vehicle) and E-cadherin (clone 1 and clone 21) transfected AGS cells were cotransfected with luciferase reporter and reseeded as MDCK. 48 h later the medium was exchanged to normal calcium medium (mock) or medium containing 0.02 mM calcium (-Ca^{2+}). Luciferase activity was measured after 7 h. Shown is the relative luciferase activity normalised to protein amount. Error bars indicate s.e.m. of three independent experiments.

13.Induction of endogenous SRF target genes

In fibroblasts, vinculin (*vcl*) and smooth muscle α-actin (*acta2*) are known endogenous SRF target genes regulated via the actin-MAL but not the MAPK-TCF pathway (Gineitis and Treisman, 2001; Du *et al.*, 2004). To test whether calcium withdrawal also induces these genes endogenously, I carried out quantitative real-time RT-PCR experiments in murine EpRas cells. EpRas cells subjected to junctional dissociation also induced the SRF reporter (Figure 13) but are of murine and not canine origin, simplifying experimental feasibility.

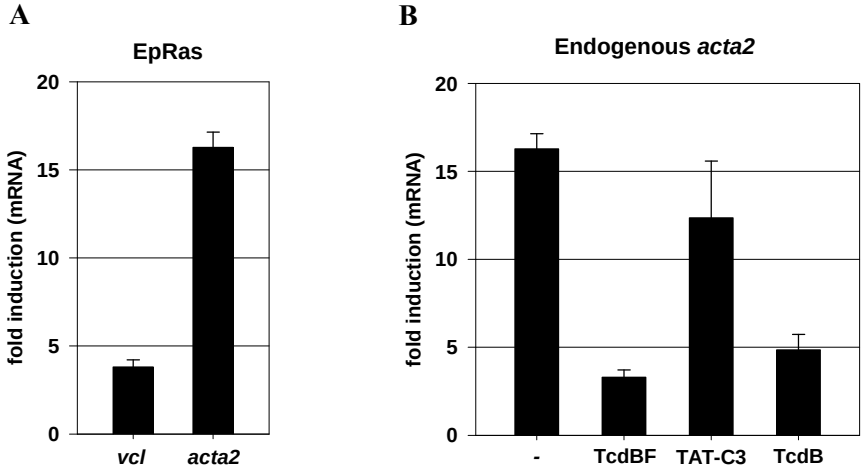

Figure 45: Rac1-dependent activation of SRF endogenous target genes upon epithelial disintegration. (A) RNA was isolated from confluent EpRas cells 3 hours after medium exchange and SRF endogenous target gene induction of vinculin (*vcl*) and smooth muscle α-actin (*acta2*) was analysed by quantitative real-time RT-PCR. Shown is the fold induction obtained after medium exchange to 0.02 mM calcium normalized to an exchange to normal calcium. (B) Effect of Rac1 and RhoA inhibition on *acta2* induction, determined as in (A). Where indicated, cells were pretreated with TcdBF (0.25 µg/mL, 4 h), TAT-C3 (1 µM, 15 h), or TcdB (0.3 ng/mL, 4 h). Error bars indicate s.e.m. of 3 independent experiments.

Vcl and *acta2* mRNAs were upregulated 3 hours after calcium withdrawal to 0.02 mM compared to control medium exchange approximately 4.5- and 16-fold, respectively (Figure 45). Furthermore, the induction for endogenous *acta2* was blocked significantly by inhibition of Rac1 with TcdBF and TcdB. In contrast, exclusive inhibition of Rho by TAT-C3 did not result in a significant blockage of acta2 mRNA transcription (Figure 45). Together, these data confirm that actin-MAL-SRF pathway induced endogenous genes are regulated upon epithelial cell-cell contact dissociation dependent on Rac1, but not Rho, consistent with the results obtained in MDCK cells with luciferase assays.

14.SRF activation upon junction dissociation independent of calcium

Next investigations were carried out to test whether junction disintegration independent of calcium withdrawal leads to SRF activation. Addition of HGF to MDCK cells disrupts epithelial interactions and promotes cell scattering from preformed epithelial sheets (Figure 46 B) (Gherardi *et al.*, 1989). As monitored by luciferase reporter, this led to a significant 2-fold activation of SRF (Figure 46 A). EpRas cells undergo EMT when treated with transforming growth factor β (TGFβ) (Oft *et al.*, 1996), thereby disintegrating their epithelium. TGFβ treatment for 72 h induced SRF significantly around 3-fold, also measured with luciferase assay (Figure 47). Summarizing, both tested calcium-independent physiological ligands mediating epithelial disintegration activate SRF. This supports the idea that SRF activation is a general response to epithelial cell-cell contact dissociation.

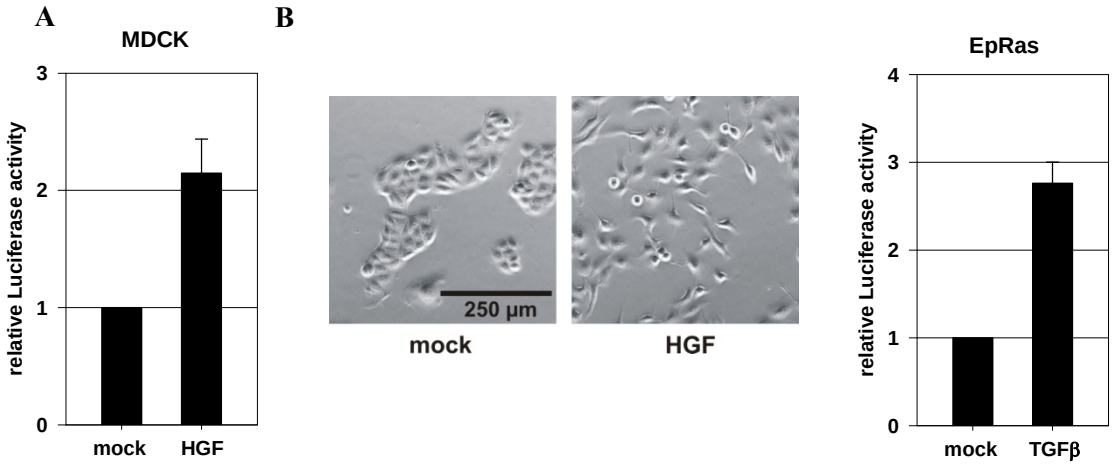

Figure 46: HGF induces SRF and scattering of MDCK cells. (A) MDCK cells were transfected and 24 h later HGF (40 ng/mL) was added for 24 h prior to analysis of luciferase activity. Shown is the relative luciferase activity normalized to protein amount, error bars indicate s.e.m. of 3 independent experiments. (B) Phase contrast images of cells in (A) prior to lysis.

Figure 47: Epithelial disintegration induced by EMT activates SRF. EpRas cells were transfected and reseeded (identical to MDCK)**.** 24 h later EMT was induced by addition of TGFβ (5 ng/mL) for 72 h. Shown is the relative luciferase activity ± s.e.m. of 3 independent experiments.

V. Discussion

Within this study I show that the dissociation of cell-cell contacts, presumably Adherens junctions, in confluent epithelial monolayers leads to SRF dependent target gene expression. Thereby, the small GTPase Rac, G-actin and MAL/MRTF were shown to be required and sufficient for signal transduction (Figure 48). I show that the dissociation of epithelial junctions precedes SRF activation with a specific threshold at 0.05 mM extracellular calcium. Junction dissociation leads to a transient activation of both Rac and RhoA, but not Cdc42. By usage of clostridial toxins Rac is identified as the essential signal transducer. SRF activation correlates with changes in the actin cytoskeleton and the dissociation of the G-actin/MAL complex. Elevation of the cellular G-actin level by ectopic expression of non-polymerizable actin mutants or latrunculin B treatment blocks SRF reporter activation, whereas the depletion of the G-actin level by expression of an F-actin stabilizing mutant leads to SRF reporter activation. During this process, actomyosin contractility is a prerequisite, but not sufficient for SRF activation. Dominant negative MAL blocks and constitutive active MAL activates the SRF reporter, respectively. Upon junction dissociation two known MAL dependent endogenous SRF target genes encoding for vinculin and smooth muscle α-actin are expressed (Figure 48). Furthermore, I demonstrate that epithelial junction formation leads to an, although weak, significant and reproducible SRF reporter induction. The induction requires E-cadherin *trans*-engagement and signalling depends on depletion of G-actin.

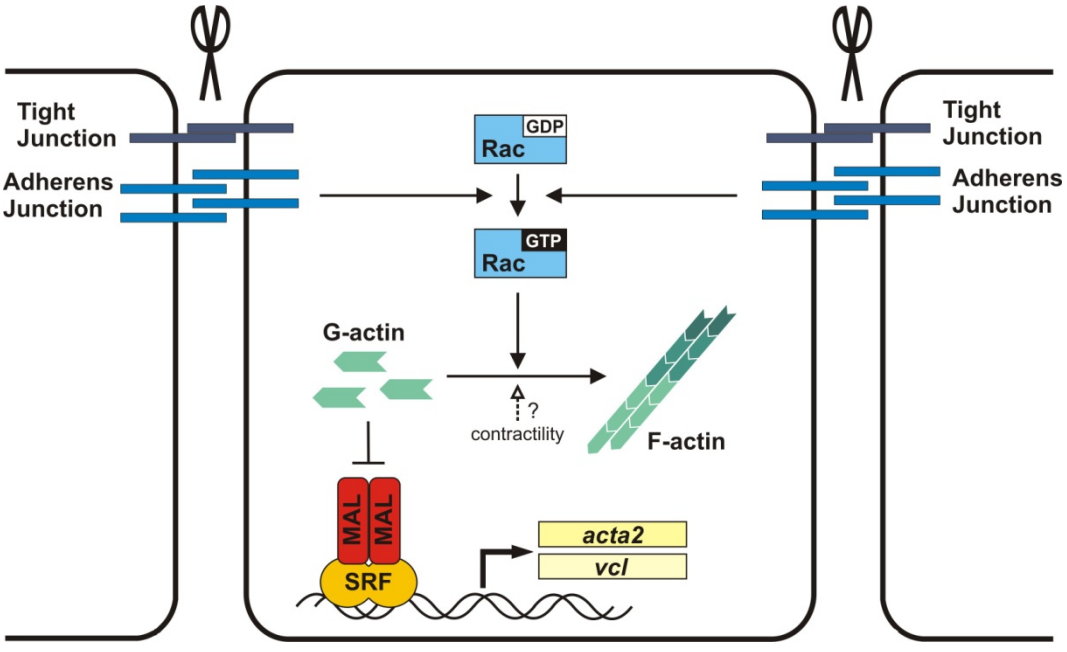

Figure 48: Model of the regulation of SRF target gene expression upon epithelial junction dissociation. The disassembly of epithelial cell-cell contacts transiently activates, presumably via Adherens junctions, the small GTPase Rac, which in turn alters the actin treadmilling cycle. This releases MAL from its inhibitory complex with G-actin leading to the activation of SRF and subsequent transcription of endogenous SRF target genes like *vinculin* (*vcl*) and *smooth muscle α–actin* (*acta2*). Actomyosin contractility is a prerequisite for appropriate actin remodeling during this process, but is not sufficient for SRF activation.

Serum stimulation of confluent epithelial cell monolayers does not trigger the activation of SRF (Figure 6), raising the question how SRF-controlled genes are regulated in epithelia. Both, epithelial junction formation and dissociation are known to cause changes in the actin cytoskeleton, which is an essential signalling event in serum-stimulated fibroblasts (Volberg *et al.*, 1986; Gumbiner *et al.*, 1988; Sotiropoulos *et al.*, 1999). I therefore investigated whether junction remodelling has an impact on SRF regulation. Epithelial junction formation induces the SRF reporter 2-fold (Figure 8). This activation is hindered by preincubation with the E-cadherin blocking antibody DECMA-1 (Figure 8), clearly identifying junction formation rather than other potential calcium induced side-effects as the essential signal transmitter. Regardless, the specific junctional component essential for induction can not be identified by this experiment, since DECMA-1 hinders besides AJ also TJ and desmosomal junction formation (Gumbiner *et al.*, 1988; Watabe *et al.*, 1994). In addition, actin mutant expression and latrunculin B treatment showed that changes in the G- to F-actin ratio, leading to the depletion of the cellular monomeric actin pool, are essential for signal transmission to SRF (Figure 8). The F-actin stabilizing mutant G15S is thought to maximally induce MAL-dependent SRF transcription (G.P. and S.B.). This maximal inducibility is in confluent epithelial MDCK cells around 6 to 7-fold (Figure 8 and Figure 30). However, upon epithelial junction formation the induction is, although reproducible and significant, just around 2-fold. In parallel I made the observation that epithelial junction dissociation activates SRF to the same extend as G15S (Figure 10). Further, I focused my investigations on this exciting finding.

By employment of the calcium switch method I dissociate epithelial junctions, thereby mimicking one aspect of a full EMT. To assure that the calcium withdrawal induced junction dissociation and not secondary effects induce SRF activation several experiments were carried out. The titration of extracellular calcium showed that epithelial junction disintegration strictly correlates with SRF activation (Figure 9 and Figure 10), indicating a direct interdependence. Normal and cancer cell lines lacking E-cadherin expression fail to activate SRF upon calcium withdrawal despite the possession of a functional pathway (Figure 14 and not shown). Upon stable expression of E-cadherin in the E-cadherin-deficient gastric cancer cell line AGS AJs are reformed and activate SRF in response to calcium withdrawal (Figure 43 and Figure 44). Finally, a HGF or TGF-β mediated calcium withdrawal independent junction dissociation activates SRF. These observations prove that SRF activation is a direct consequence of junction dissociation induced signalling.

The AJC is known to regulate GTPases of the Rho family and is dynamically connected to the cortical actin belt of confluent epithelial cells (Braga, 2002). Calcium withdrawal as well as HGF or TGF-β treatment leads to the dissociation of the complete AJC including AJs and TJs. To clarify whether AJs or TJs are essential for signalling to SRF, I utilised the E-cadherin deficient human gastric cancer cell line AGS. Adjacent AGS cells grown in a confluent monolayer lack E-cadherin/β-catenin and nectin/afadin complex dependent AJs. Although the detected ZO-1 membrane staining appears to be slightly reduced compared to E-cadherin expressing AGS cells, they do possess fully

developed TJs between most cells (Figure 43). Calcium withdrawal of these cells induces TJ dissociation, probably by disassembly of the calcium dependent desmosomal cadherins. Importantly, this is not associated with SRF activation (Figure 44), suggesting that neither desmosome nor TJ disassembly regulates SRF. Conversely, stable expression of E-cadherin in AGS cells leads to the formation of fully developed AJs (Figure 43), whose dissociation induces SRF (Figure 44). These results suggest that components of the AJ rather than the TJ mediate SRF activation.

Several additional experiments can further support the idea of AJs as essential signal transducers to SRF. ZO-1 deleted and ZO-2 depleted epithelial EpH4 cells are well polarized and form fully functional AJs, but completely lack TJs (Umeda *et al.*, 2006). If these cells fail to activate SRF upon calcium withdrawal an involvement of TJs in SRF activation can be ruled out. The knockdown of E-cadherin and Cadherin-6 in preformed epithelial junctions was shown to disrupt AJs, but not TJs (Capaldo and Macara, 2007). A calcium switch in depleted cells can narrow down the potential signal transducers to the AJ components excluding α-catenin or even E-cadherin alone (Capaldo and Macara, 2007). Hence, I constructed shRNA expression vectors for transfection or amphotrophic infection targeting both mRNAs (Table 12 and not shown). The plasmid delivery efficiency for both methods turned out to be around 5 – 10% in MDCK cells and the resulting knockdown was not complete. Thus, knockdown cells were forming partial junctions with adjacent untransfected/uninfected cells mediated by their residual E-cadherin and Cadherin-6. Corollary, SRF was still activated in these cells upon calcium withdrawal (not shown). Currently, I am engineering a stable cell line carrying an inducible shRNA expression vector targeting E-cadherin and Cadherin-6 to overcome this problem.

To further differentiate between E-cadherin/catenin and nectin/afadin complex mediated signalling to SRF, calcium switch experiments in afadin depleted AGS cells, which stably express E-cadherin, can be carried out. However, afadin-independent E-cadherin mediated junction formation would be a prerequisite for this experiment.

A further dissection to identify the specific AJ component crucial for signalling proves difficult, as targeting of either β-catenin, α-catenin, p120-catenin or afadin induces severe defects in AJs and TJs, which usually lead to the complete loss of polarization and cell-cell contacts (Behrens *et al.*, 1993; Ikeda *et al.*, 1999; Ireton *et al.*, 2002; Capaldo and Macara, 2007). However, the fusion protein of a C-terminal truncated E-cadherin lacking the β-catenin binding site and specific parts of α-catenin is able mediate adhesion and connects to the actin cytoskeleton (Nagafuchi *et al.*, 1994; Imamura *et al.*, 1999). Calcium switch experiments with AGS cells stably expressing these fusion proteins would allow the identification or exclusion of β-catenin, formin-1, vinculin, α-actinin or EPLIN as essential signal transducer (Kobielak and Fuchs, 2004; Abe and Takeichi, 2008). During this study I engineered the cDNA constructs encoding for several different E-cadherin/α-catenin fusion proteins (Table 12 and not shown). AGS cell lines stably transfected with the cDNAs expressed the fusion proteins but, however, failed to correctly localize them to the membrane (not shown). Further transfections will be carried out to isolate clones with correctly localized fusion proteins. Overall, the

suggested experiments will allow the identification of the specific AJC component essential for signal transduction to SRF.

Ezrin, belonging to the ezrin-radixin-moesin (ERM) protein family, and merlin, which is encoded by the *neurofibromatosis type-2* (*NF2*) gene and is a close relative to the ERM family, are both known to localize to the AJC and regulate cell-cell adhesion (Gould *et al.*, 1989; Rouleau *et al.*, 1993; Trofatter *et al.*, 1993; Lallemand *et al.*, 2003; Pujuguet *et al.*, 2003; Van Furden *et al.*, 2004). Both, ezrin and merlin, are also connected to the actin cytoskeleton (Gould *et al.*, 1989; Gronholm *et al.*, 1999; Brault *et al.*, 2001; James *et al.*, 2001), regulate the actin polymerization function of N-WASP (Manchanda *et al.*, 2005) and can signal via Rho familiy GTPases (Maeda *et al.*, 1999; Kissil *et al.*, 2003; Pujuguet *et al.*, 2003). These observations prompted me to investigate a potential involvement of these two proteins in the regulation of SRF. Unexpectedly, overexpression of none of the therefore constructed constitutive active and dominant negative ezrin or merlin constructs (Table 12) has an impact on SRF regulation in epithelial MDCK cells (not shown). Further, the serum inducibility of SRF in subconfluent or confluent NIH3T3 cells is not influenced by any overexpressed construct (not shown). Together, these results give as yet no indication for a regulatory function of ezrin or merlin towards SRF.

The relationship between epithelial junctions and small Rho family GTPases has been studied extensively, but mainly during junction formation (for details refer to Introduction). Here, I provide evidence that the small GTPases Rac1 and RhoA are quickly and transiently GTP loaded upon epithelial junction dissociation mediated by medium exchange to 0.02 mM calcium. By contrast, EGTA induced calcium depletion for 30 minutes has previously been shown to inhibit Rac activation in MDCKII or Fisher rat thyroid cells, whereas RhoA remained unchanged in MDCKII cells (Nakagawa *et al.*, 2001; Balzac *et al.*, 2005). This apparent discrepancy is probably explained by the very transient activation of Rac1 and RhoA, which previously might have been missed, junction-independent effects of EGTA, consistent with the in my study observed toxicity upon extended treatment, or cell type specific differences. Already within the two strains of MDCK cells major junctional differences exist: strain I cells are derived from an early passage and form tight epithelia with a transepithelial resistance > 3000 ohm/cm^2, whereas strain II cells predominate in later stages and formed cell layers are "leaky" with a resistance of around 100 ohm/cm^2 (Richardson *et al.*, 1981; Balcarova-Stander *et al.*, 1984; Hansson *et al.*, 1986).

Constitutive active variants of both Rac1 and RhoA are both sufficient to activate SRF in epithelial cells (Figure 21). However, by using clostridial toxins I show that Rac but not Rho is the essential signal transducer to SRF. Dominant negative constructs of both Rho and Rac were not employed in this study, because expression of both interferes already with junction formation (not shown) (Braga *et al.*, 1997; Jou and Nelson, 1998). In addition, overexpression of RacN17 or RhoN19 may not be as specific as previously anticipated (Wells *et al.*, 2004). Within this study, the clostridial toxins were used in concentrations and times to efficiently block their specific GTPase target (Figure 25) but to not

interfere with existing junctions (Figure 27) or their calcium withdrawal induced dissociation (not shown). The finding that dissociating epithelial junctions specifically require Rac for SRF activation contrasts the situation in fibroblasts, which induce SRF upon serum stimulation specifically dependent on Rho (Hill *et al.*, 1995). Confluent epithelial cells are serum stimulation insensitive (Figure 6). Rac inhibition in NIH3T3 fibroblasts by TcdBF treatment leads to quick cell rounding and detachment. Yet, the detached cells are viable and do not show a concentration-dependent reduction of serum-induced SRF activation (not shown). These observations suggest that serum stimulation and epithelial disintegration utilise distinct pathways, which merge at the level of G-actin to induce SRF dependent gene expression.

Due to their very rapid activation, Rac1 and RhoA seem to be GTP-loaded as a direct consequence of junction dissociation. Cell culture medium containing less than 0.05 mM calcium withdraws the calcium ions required for E-cadherin-rigidity. The thereby induced conformational changes in E-cadherin might directly, or indirectly via connected AJC proteins, mediate GTPase activation. Regardless of the inducing AJC component, the increase in Rac1-GTP is likely achieved by either activation of a GEF or inactivation of a GAP. Several Rac GEFs colocalize with the AJC and might potentially activate Rac upon AJC dissociation. In nonmotile MDCK cells the Rac1-specific GEF Tiam1 is localized to the sites of cell-cell contact, whereas it localizes to lamellae of migrating cells (Sander *et al.*, 1998). It is required for TJ formation (Chen and Macara, 2005; Nishimura *et al.*, 2005), and endogenous levels of Tiam1 are essential for the maintenance of epithelial integrity (Malliri *et al.*, 2004). Overall it seems contradictory that the same Rac1-specific GEF that mediates junction formation and promotes their maintenance could potentially get activated upon junction dissociation. Nevertheless, a complex interplay with other GTPases like Cdc42 with respect to junction formation or RhoA concerning junction dissociation, respectively, does not allow a complete exclusion of Tiam1 as potential signal transducer from dissociating junctions to Rac1.

The GEF Vav2 is known to target four Rho family GTPases: Rac1, RhoA, RhoG and Cdc42 (Schuebel *et al.*, 1998; Abe *et al.*, 2000). It is bound and activated by cytoplasmic p120-catenin, whereby p120-catenin shuttles between a cytoplasmic pool and an E-cadherin-bound state. Activated Vav2 in turn induces Rac1-GTP loading. Factors that perturb cell-cell junctions lead to an increase in cytoplasmic p120-catenin (Noren *et al.*, 2000). Therefore, the dissociation of the AJC might induce Rac1-GTP loading via Vav2 by increasing the cytoplasmic p120-catenin pool and thereby induce SRF activation. To clarify a potential involvement of Tiam1 or Vav2 in epithelial junction dissociation mediated Rac1 activation detailed experimental analyses have to be carried out.

The multidomain protein Trio contains two functional GEF domains, one for Rac and the other one for Rho (Debant *et al.*, 1996). It was shown that on the onset of myoblast fusion Trio is complexed with M-cadherin and Rac1 (Charrasse *et al.*, 2007). Potentially Trio is associated with E-cadherin in epithelial cells, where it gets activated upon junction dissociation and in turn promotes Rac1- and RhoA-GTP loading. Preliminary studies carried out within this lab show that Rac1 and Trio

colocalize in the cytoplasm and translocate to the membrane upon calcium withdrawal. Furthermore, a transient interaction between Trio and E-cadherin was detected upon calcium withdrawal (Schächterle, 2008). Whether this is connected to SRF activation remains to be elucidated.

Additionally, a multitude of GAPs and other GEFs exist, whereof each individual GAP and GEF has a certain specificity profile for individual members of a G-protein family (Bos *et al.*, 2007). Whether these are linked to the AJC and might be the essential signal transmitter remains to be elucidated. Furthermore, contact dissociation might translocate Rac1 or deactivate a guanosine nucleotide dissociation inhibitor (GDI) to allow GTP-loading.

Accompanying Rac1, RhoA is also fast and transiently GTP-loaded after junctional dissociation (Figure 19), but conversely not required for SRF activation (Figure 24 and Figure 45). An explanation for this observation might be connected with the finding that RhoA mediates the disassembly of epithelial apical junctions by inducing the ROCK signalling pathway (Samarin *et al.*, 2007). The disassembly and subsequent endocytotic internalization of the AJC following calcium withdrawal as well as HGF induced scattering of MDCK cells depends on ROCK-dependent actomyosin contractility (Sahai and Marshall, 2002; Ivanov *et al.*, 2004; de Rooij *et al.*, 2005; Samarin *et al.*, 2007). Consistent with this, inhibition of actomyosin contractility by Blebbistatin hinders junction internalization (Figure 37), although the *trans*-interacting junctional proteins still disengage upon calcium withdrawal to induce both Rac1- and RhoA-GTP loading (Figure 36). Hence, RhoA might regulate the internalization and degradation of the AJC via ROCK induced actomyosin contractility. Since only the increase of RhoA-GTP loading is completely blocked upon TAT-C3 treatment (Figure 25), the remaining basal RhoA activity seems to be sufficient to induce this process.

Upon AJC disintegration, Rac gets activated and signals to SRF by depleting the monomeric actin pool. This might be facilitated by the regulation of actin treadmilling towards induction of actin polymerization. Actin treadmiling is regulated during lamellipodial extension by Rac1-GTP via binding and activation of PAK1 (Manser *et al.*, 1994), which in turn activates LIMK. Active LIMK then phosphorylates and thereby inactivates Cofilin, which, when active, catalyzes the debranching, severing and depolymerization of actin filaments (Carlier *et al.*, 1997; Edwards *et al.*, 1999; Blanchoin *et al.*, 2000). Rac is also known to induce Arp2/3 dependent actin polymerization via WAVE family proteins, which are complexed amongst others to NCK-associated protein (Nap1) or Abl interactor 1 (Abi1) (Eden *et al.*, 2002; Innocenti *et al.*, 2004). However, if these Rac effectors are also activated upon AJC disassembly to induce actin remodelling remains to be determined.

In line with my findings, a very recently published study by Fan and colleagues shows that the smooth muscle α-actin promoter, which is regulated by MAL-SRF signalling, is induced upon disruption of epithelial junctions (Fan *et al.*, 2007). Both, inhibition of non-muscle myosin II by Blebbistatin or ROCK by the specific inhibitor Y-27632 blocks SRF activation in my or smooth muscle α-actin promoter in their study, respectively (Figure 35) (Fan *et al.*, 2007). I show, however, that Blebbistatin treatment induces the disassembly of cellular F-actin and abrogates cytoskeletal

changes provoked by calcium withdrawal (Figure 37). Thus, a basal level of ROCK induced actomyosin contractility is required for maintaining the integrity and treadmilling of the actin cytoskeleton as prerequisite for signal transduction from Rac to MAL. Fan and colleagues conclude from their observations that cell contacts regulate MAL-SRF-dependent smooth muscle α-actin promoter activation via Rho-ROCK-induced actomyosin contraction. Contradictory to that, I show that forced actomyosin contraction by inhibition of myosin light chain phosphatase with Calyculin A or overexpression of constitutive active ROCK is not sufficient to activate SRF in epithelial cells (Figure 38 and Figure 39), precluding a direct role for actomyosin in SRF regulation. Further supporting this, ROCK also fails to induce SRF in fibroblasts (Sahai *et al.*, 1998). By contrast, ectopic expression of the F-actin stabilizing mutant G15S or activated mDia1, which do not facilitate contraction but ROCK-independent actin polymerization are sufficient to induce SRF even in the presence of calcium (Figure 30 and not shown). Additionally, more general effects of Blebbistatin on gene expression cannot be ruled out. These results clearly indicate that the depletion of the cellular G-actin level mediated by changes in the actin treadmilling cycle rather than Rho-ROCK induced actomyosin contraction provides the essential signal which induces SRF.

The induction of SRF upon both junction formation and dissociation might seem unexpected. However, both processes are dependent on actin remodelling. The highly dynamic process of epithelial junction formation is an orchestrated interplay of filopodia formation and lamellipodia extension (Mege *et al.*, 2006). Hypothetically, the associated actin polymerization might deplete the cellular G-actin pool, which releases MAL from its inhibition. In a positive feedback loop this might lead to the SRF dependent expression of cytoskeletal components to refill the cellular pool. Furthermore, proteins required for junction formation might be induced. In line with this, a very recent study demonstrates that SRF deleted endothelial cells show defects in actin polymerization and intercellular junctions (Franco *et al.*, 2008). Moreover, SRF is shown to be essential for the expression of VE-cadherin in endothelial cells (Franco *et al.*, 2008). The just 2-fold SRF activation upon junction formation might be sufficient to refill the cellular pools and allocate the needed junctional proteins. However, it remains unclear whether VE-cadherin expression depends on MAL and if epithelial and endothelial systems are comparable.

Calcium withdrawal leads to the dissociation of epithelial junctions, which induces a slight shift of the G- to F-actin ratio towards F-actin (Figure 32) and actin remodelling (Figure 33). Mechanistically, these effects lead to the SRF activation. During EMT the dissociation of junctions is a key aspect and prerequisite for its most important hallmark, the conversion of a predominantly stationary epithelial cell into a motile one (Boyer and Thiery, 1993; Hay, 1995). In this study, two endogenous MAL-SRF target genes encoding for smooth muscle α-actin and vinculin were shown to be upregulated upon calcium withdrawal induced epithelial junction dissociation (Figure 45). Smooth muscle α-actin is expressed in mobile mesenchymal cells after EMT and is a prototypical EMT marker (Thiery and Sleeman, 2006). The ubiquitously expressed actin-binding protein vinculin seems to

stabilize focal adhesions and thereby suppress cell migration (Ziegler *et al.*, 2006). However, along the lamella of motile cells short lived small matrix adhesions, the so-called focal complexes, are formed (Rottner *et al.*, 1999). Some of the focal complexes mature to focal adhesions, which anchor the cell in the ECM, allowing the contractile actomyosin system to pull the cell body, trailing the edge forward and restrain the migration process (Huttenlocher *et al.*, 1996; Lauffenburger and Horwitz, 1996; Small *et al.*, 1996). Initial focal complexes contain no or few vinculin. Upon development to stable focal adhesions, vinculin is recruited, and seems to be substantial to maintain migration (Lee and Jacobson, 1997; Zaidel-Bar *et al.*, 2003; Munevar *et al.*, 2004). Overall, both induced target genes seem to be required for migration. Therefore, the junction dissociation induced MAL and subsequent SRF activation seems to enhance EMT, pointing towards a feed-forward loop. Along this line, MAL/SRF-mediated transcription might promote the pathological EMT observed during carcinoma invasion and metastasis.

The hypothesis of MAL/SRF in supporting EMT is futher strengthened by the phenotype of SRF deleted mice. Mouse embryos lacking SRF expression develop normally until day 6.5 of embryogenesis, but die afterwards by not developing mesodermal cells (Arsenian *et al.*, 1998). In wild type animals, during days 5.5 to 6.5 ectodermal cells are converted into migrating mesodermal cells (Beddington and Smith, 1993). Thus, epithelial remodelling might activate MAL and SRF during gastrulation to promote developmental EMT and mesoderm formation. To experimentally challenge this hypothesis i.e. *Xenopus laevis* embryos can be injected with the 3D.A-Luc SRF luciferase reporter plasmid. An increase of luciferase activity upon the onset of mesoderm formation – at embryonic stage 10 to 11 – would clearly identify MAL/SRF signalling as essential for embryonic development.

However, calcium withdrawal does not induce the full genetic program required for migration, as calcium depleted MDCK cells remain stationary for several days (not shown). Nevertheless, it might activate a SRF dependent subset of migratory genes, which just in concert with other EMT induced signalling cascades are sufficient for migration. Supporting this idea, the TGF-β mediated full EMT in EpRas cells leads along with junction dissociation to SRF activation (Figure 47). Furthermore, Morita and colleagues show in a recently published paper that MAL cooperates with Smad3 and SRF to regulate TGF-β mediated EMT (Morita *et al.*, 2007). However, the deeper analysis of the potential dualistic nature of MAL/SRF regulated target genes, which point on the one hand towards junction formation and immobility, on the other hand towards the induction of migration, is an exiting task which remains to be elucidated.

VI. Materials and Methods

1. Materials

1.1. Laboratory hardware

ABI 3730 sequencer	Applied Biosystems (Darmstadt)
Agarose gel electrophoresis system Horizontal-Elpho	Workshop MPI of Biochemistry (Martinsried)
Amaxa Nucleofector device	Amaxa (Cologne)
Balances	Kern 572, Kern & Sohn GmbH (Balingen) Mettler AE200, Mettler Toledo (Giessen)
Celloshaker	Renner GmbH (Dannstadt)
Centrifuges	Eppendorf 5417R (Wesseling-Berzdorf) Eppendorf 5417C (Wesseling-Berzdorf) Beckman Coulter Allegra 6KR (Krefeld) Sorvall Evolution RC, Thermo Fisher Scientific (Schwerte) Hettich Universal 16 (Kirchlengern) Beckman TL-100 Ultracentrifuge (Krefeld)
Dark Reader®	Clare Chemical Research (Dolores, USA)
Duomax 1030	Heidolph (Kelheim)
Polyacrylamide gel electrophoresis casting stand, casting frames, glass plates, combs & sample loading guide	Bio-Rad (Munich)
Polyacrylamide gel electrophoresis system Vertical Elpho "B"	Workshop MPI of Biochemistry (Martinsried)
Elisareader	BioTek (Winooski, USA)
Fireboy plus	Integra Biosciences (Fernwald)
GelAir dryer	Bio-Rad (Munich)
Gel chambers	Workshop MPI for Biochemistry (Martinsried)
Genepulser XCell™	BioRad (Munich)
Icemachine	Ziegra (Isernhagen)
IDA gel documentation system	Raytest (Straubenhardt)
Immersol™ 518F	Zeiss (Jena)
Incubator HERAcell® 150i	Thermo Fisher Scientific (Schwerte)
LightCycler instrument	Roche (Penzberg)
Microplate Luminometer LB 96V	EG and G Berthold (Schwerzenbach, CH)
Microscopes	Zeiss Axio Observer.A1 (Jena) Zeiss Axiovert 200M (Jena) Leica TCS SP2 Confocal Laser Scanning Microscope (Wetzlar)
Microwave	Siemens (Munich)
Power supply	Consort EV 261 (Turnhout, B)
Sonicator Sonoplus HD70	Bandelin (Berlin)
Spectrophotometer	BioPhotometer, Eppendorf (Wesseling-Berzdorf) Nanodrop ND 1000, Thermo Fisher Scientific (Schwerte)
Sterile Lamin Air Hood	Lamin Air Model 1.2, Heraeus (Hanau) Lamin Air HA 2472 GS, Holten (Allerod, DK)
Thermocycler	Biometra T3000 (Göttingen)
Thermomixer Comfort	Eppendorf (Wesseling-Berzdorf)
Vortex Genie 2™	Bender and Hobein (Zurich, CH)
Western Blotting Chamber Mini Trans-Blot Cell	Bio-Rad (Munich)

Table 1: List of laboratory hardware used in this study.

1.2. Chemicals and reagents

Acrylamide	Serva (Heidelberg)
Agar (Difco™)	BD Biosciences (Heidelberg)
Agarose	Eurogentec (Cologne)
Alexa Fluor® 546 phalloidin	Molecular Probes (Eugene, USA)
Ampicillin	Roche (Mannheim)
Antipain	Fluka (Buchs, SUI)
Aprotinin	Sigma-Aldrich (Steinheim)
Ammonium peroxodisulfate (APS)	Bio-Rad (Munich)
Bisacrylamide	Serva (Heidelberg)
Blasticidine S hydrochloride	Sigma-Aldrich (Steinheim)
Bovine serum albumin (BSA)	Sigma-Aldrich (Steinheim)
Bradford reagent	Sigma-Aldrich (Steinheim)
Bromphenol blue	Sigma-Aldrich (Steinheim)
Chelex® 100 Chelating Ion Exchange Resin	Bio-Rad (Munich)
Chloramphenicol	Merck (Darmstadt)
Chlorophenolred-β-D-galactopyranosid	Merck (Darmstadt)
Chloroquine	Sigma-Aldrich (Steinheim)
Complete™ Protease Inhibitor Cocktail Tablets	Roche (Mannheim)
Coomassie Brilliant Blue G-250	Serva (Heidelberg)
4',6-diamidino-2-phenylindole hydrochloride (DAPI)	Roche (Mannheim)
1,4-Diazabicyclo[2.2.2]octane (DABCO®)	Sigma-Aldrich (Steinheim)
Dimethyl sulfoxide (DMSO)	Riedel-de Haën (Seelze)
Dithiothreitol (DTT)	Sigma-Aldrich (Steinheim)
Doxycycline, Hyclate	Calbiochem (Nottingham,GB)
Ethanol p.a.	Riedel-de Haën (Seelze)
Ethidium bromide	Roth (Karlsruhe)
Gelatine from cold water fish skin	Sigma-Aldrich (Steinheim)
G418	Invitrogen (Karsruhe)
4-(2-Hydroxyethyl)piperazine-1-ethanesulfonic acid (HEPES)	Biomol (Hamburg)
Hoechst 33258	Sigma-Aldrich (Steinheim)
Isopropanol	Fluka (Buchs, SUI)
Isopropyl thiogalactopyranoside (IPTG)	Fermentas (St. Leon-Rot)
Kanamycin	Invitrogen (Karlsruhe)
Leupeptin	Serva (Heidelberg)
Lipofectamine® (GibCo)	Invitrogen (Karsruhe)
Lipofectamine 2000® (GibCo)	Invitrogen (Karsruhe)
Methanol	Fisher Scientific (Schwerte)
Mowiol 4-88	Sigma-Aldrich (Steinheim)
N,N,N',N'-Tetramethylethylenediamine (TEMED)	Serva (Heidelberg)
Nonidet® P-40 Substitute (NP-40)	Fluka (Buchs, CH)
Paraformaldehyde (PFA)	Sigma-Aldrich (Steinheim)
Pepstatin	Roche (Mannheim)
Phenylmethanesulfonyl fluoride (PMSF)	Sigma-Aldrich (Steinheim)
Puromycin Dichloride	Calbiochem (Nottingham,GB)
Rhodamine phalloidin	Molecular Probes (Eugene,USA)
Sodium azide	Serva (Heidelberg)
Sodium dodecyl sulfate (SDS)	Serva (Heidelberg)
Sodium fluoride	Sigma-Aldrich (Steinheim)
Sodium orthovanadate	Sigma-Aldrich (Steinheim)
TransFast™	Promega (Madison, USA)
Tris	Sigma-Aldrich (Steinheim)
Triton X-100	Roth (Karlsruhe)

Tryptone (Bacto™)	BD Biosciences (Heidelberg)
Tween 20	Sigma-Aldrich (Steinheim)
Yeast extract (Bacto™)	BD Biosciences (Heidelberg)

Table 2: List of chemicals and reagents used in this study.

All other chemicals were purchased in analytical grade from Merck (Darmstadt).

1.3. Drugs and inhibitors used in cellular assays

The drugs and inhibitors listed in Table 3 were preincubated in the concentration indicated in the corresponding figure legends.

Drug/Inhibitor	Description	Source/Reference
(-)-Blebbistatin	specific small molecule inhibitor of skeletal muscle and nonmuscle myosin II adenosine triphosphate (ATPase) activity	Merck (Darmstadt)
Calyculin A	derived from the marine sponge *Discodermia calyx*, inhibits myosin light chain phosphatase and protein phosphatases PP1 and PP2A	Merck (Darmstadt)
Cytochalasin D	isolated from the marine fungus *Zygosporium masonii,* acts by capping the barbed end of actin filaments, severs F-actin and sequester monomers or dimers and stimulate the ATPase activity of actin monomers	Merck (Darmstadt)
Jasplakinolide	derived from the marine sponge *Jaspis johnstoni*, actin filament stabilizer inducer of actin polymerization and thereby deplets the monomeric actin pool	Merck (Darmstadt)
Latrunculin B	derived from marine sponge *Latrunculia magnifica*, prevents assembly and polymerization of actin monomers via specific binding in the ATP-binding cleft of monomeric actin	Merck (Darmstadt)
TAT-C3	C3 exoenzyme derived from *Clostridium botulinum*, selectively inhibits the Rho subtype GTPases RhoA, RhoB and RhoC by ADP-ribosylation of Asp41, fused to the HIV TAT leader sequence to permit plasma membrane trasnduction	E.Sahai, CRUK (London, GB)
TcdB	Toxin B derived from *Clostridium difficile* reference strain YPI10463, inhibits Rho family GTPases, i.e. Rho, Rac and Cdc42 by stable glucosylation, with UDP-glucose as sugar donor	H. Genth, MHH (Hannover)
TcdBF	Toxin B variant derived from *Clostridium difficile* strain 1470 serotype F, glucosylates and thereby inhibits Rac1, Cdc42 and R-Ras, but not Rho.	H. Genth, MHH (Hannover)
Y-27632	small molecule inhibitor of ROCK	Sigma-Aldrich (Steinheim)

Table 3: List of drugs and inhibitors used in this study.

1.4. Kits and miscellaneous materials

Amaxa Nucleofection Kit L	Amaxa (Cologne)
Cellophane	Pütz Folien (Taunusstein)
Coverslips	Hartenstein (Würzburg)
Chromatography paper 3MM	Whatman (Dassel)
CryoTube™ vials	Nunc (Roskilde, DK)
Dual-Glo™ Luciferase Assay Kit	Promega (Madison, USA)
ECL Plus™	GE Healthcare (Munich)
Electroporation cuvettes (0.2 cm)	Bio-Rad (Munich)
Electroporation cuvettes (0.4 cm)	Bio-Rad (Munich)
Flag M2 agarose beads	Sigma-Aldrich (Steinheim)
Glutathione Sepharose beads	GE Healthcare (Munich)
Hyperfilm MP	GE Healthcare (Munich)
LightCycler® FastStart DNA Master SYBR Green I mix	Roche (Penzberg)
Micro BCA Protein Assay Kit	Pierce (Sankt Augustin)
Parafilm	Pechiney Plastic Packaging (Chicago, USA)
Plastic ware	BD Falcon (Heidelberg) Eppendorf (Wesseling-Berzdorf) Greiner bio-one (Frickenhausen) Nunc (Roskilde, DK)
Precision Plus Protein™ Dual Color Standard	Bio-Rad (Munich)
Protein A-Sepharose	GE Healthcare (Munich)
Protein G-Sepharose	GE Healthcare (Munich)
PVDF membrane Immobilion-P Transfer 0.45 µm	Millipore (Billerica, USA)
QIAquick Gel Extraction Kit	Qiagen (Hilden)
QIAquick MinElute Gel Extraction Kit	Qiagen (Hilden)
QIAquick PCR Purification Kit	Qiagen (Hilden)
QIAquick MinElute PCR Purification Kit	Qiagen (Hilden)
QIAGEN Plasmid Mini Kit	Qiagen (Hilden)
QIAGEN Plasmid Maxi Kit	Qiagen (Hilden)
QIAGEN RNeasy Mini Kit	Qiagen (Hilden)
Reverse-iT-1st-Strand-Synthesis-Kit	ABgene (Hamburg)
SmartLadder DNA marker	Eurogentec (Cologne)
Sterile filter 0.22 µm, cellulose acetate	Thermo Fisher Scientific (Schwerte)
Sterile filter 0.45 µm, cellulose acetate	Thermo Fisher Scientific (Schwerte)
Thrombin CleanCleave™ Kit	Sigma-Aldrich (Steinheim)
Vivaspin 20 column	Satorius Stedim Biotech (Aubagne Cedex, F)
Western Lightning™ Chemoluminescence Reagent Plus	PerkinElmer (Boston, USA)

Table 4: List of kits and miscellaneous materials used in this study.

1.5. Media, buffers and solutions

1.5.1. Bacterial media

Luria-Bertani (LB) broth (1% Tryptone, 0.5% yeast extract, 1% NaCl. pH 7.2) was used for cultivation of *Escherichia* (*E.*) *coli* bacteria. If required, 100 µg/mL Ampecillin, 70 µg/mL Kanamycin or 34 µg/mL Chloramphenicol were added to the medium after autoclavation. For plate preparation, 1.5% Agar was added.

1.5.2. Cell culture media

All cell lines used in this study were cultured in Dulbecco's Modified Eagle Medium (DMEM) supplemented with 4.5 mg/mL glucose (high glucose) and L-glutamine (all obtained from Invitrogen (Gibco™)), and were further supplemented with 4 – 10% fetal calf serum (FCS), 2 mM L-glutamine, 1 mM sodium-pyruvate, 50 U/mL penicillin and 50 µg/mL streptomycin (all obtained from Invitrogen (Gibco™)). Freeze medium consisted of 90% FCS and 10% DMSO.
For calcium switch experiments (3.3) the culture medium was exchanged to medium with reduced calcium. Calcium reduced medium was prepared as normal medium, but with calcium free DMEM and FCS and supplemented with the desired amount of calcium (usually 0.02 mM). Calcium free DMEM was obtained from Invitrogen (Gibco™), calcium free FCS was generated using Chelex® 100 chelating ion exchange resin according to Brennan and colleagues (Brennan *et al.*, 1975).

1.6. Buffers and solutions

All buffers and solutions were prepared in bi-distilled water if not indicated otherwise.

Acrylamide solution (30/0,8)	30 % (w/v) acrylamide 0.8 % (w/v) bisacrylamide
Annealing buffer	20 mM Tris-HCl pH 7.5 100 mM NaCl 2 mM EDTA
Blocking solution	10% (v/v) FCS 1% (v/v) gelatin 0.05% (v/v) Triton X-100 in PBS
5x Bradford solution	20% (v/v) Bradford solution (prepared according to manufacturer's instructions) 10% (v/v) H_2O 20% (v/v) ethanol 50% (v/v) H_3PO_4 after mixing filter through paper filter
2 x BBS solution	50 mM BES 280 mM NaCl 1.5 mM Na_2HPO_4 pH 6.96
Coomassie R-250 solution	0.25 % (w/v) Serva Blue R 45 % (v/v) methanol 10 % (v/v) acetic acid
Coomassie destaining solution	10 % (v/v) methanol 10 % (v/v) acetic acid
DNA loading buffer (6x)	30 % (v/v) glycerol 0.3 % (w/v) bromophenole blue 0.3 % (w/v) xylene cyanol 100 mM EDTA

GTPase lysis buffer	50 mM Tris-HCl pH 7.5 1% (v/v) Triton X-100 500 mM NaCl 10 mM $MgCl_2$ 0.5% (w/v) sodium desoxycholate 0.1% (w/v) SDS
GTPase wash buffer	50 mM Tris-HCl pH 7.5 1% (v/v) Triton X-100 500 mM NaCl 10 mM $MgCl_2$
LacZ buffer	1 mM $MgSO_4$ 45 mM β-MESH in PBS
Laemmli buffer (3x)	10 mM EDTA 3 % (w/v) SDS 20 % (v/v) glycerol 0.05 % (w/v) bromophenole blue 3 % (v/v) β-Mercaptoethanol
Milk	4% (w/v) milk powder in TBST buffer
PAK-pulldown buffer	20 mM Tris HCl pH 8.0 150 mM NaCl 5% (v/v) glycerin 10 mM $MgCl_2$ 1% (v/v) NP-40
PBS	137.0 mM NaCl 27.0 mM KCl 80.9 mM Na2HPO4 1.5 mM KH2PO4 pH 7.4
Radioimmunoprecipitation Assay (RIPA) buffer	20 mM Tris HCl pH 8.0 150 mM NaCl 5% (v/v) glycerin 10 mM $MgCl_2$ 1% (v/v) Triton X-100 0.5% (w/v) desoxycholat 0.1% (v/v) SDS
Strip buffer	65 mM Tris/HCl, pH 6.8 2 % (w/v) SDS 100 mM β-Mercaptoethanol
TAE buffer	40 mM Tris/Acetate pH 8.0 1 mM EDTA
TBE buffer	90 mM Tris/HCl, pH 8.0 90 mM boric acid 3 mM EDTA

TBS buffer	20 mM Tris/HCl, pH 7.5 150 mM NaCl
TBST buffer	20 mM Tris/HCl, pH 7.5 150 mM NaCl 0.1% (v/v) Triton X-100
TE (10/0,1)	10 mM Tris/HCl, pH 8.0 1 mM EDTA
TPE lysis buffer	50 mM Tris-HCl pH 7.5 1% (v/v) Triton X-100 150 mM NaCl 5 mM Mg_2Cl_2 1 mM DTT
Transformation buffer	50 mM $CaCl_2$ 10 mM PIPES 15% (v/v) glycerol pH 6.6 (+ NaOH)
Tris-Glycin-SDS buffer	25 mM Tris/HCl, pH 8.8 192 mM glycine 1 % (w/v) SDS
TX buffer	20 mM Tris HCl pH 8.0 150 mM NaCl 5% (v/v) glycerin 10 mM $MgCl_2$ 1% (v/v) Triton X-100
UZ buffer	20 mM HEPES pH 7.7 50 mM NaCl 1 mM EDTA 0.5% (v/v) Triton X-100
Western blotting buffer	25 mM Tris 190 mM glycine 20% (v/v) methanol 0.1% (v/v) SDS (for proteins > 80 kDa)

Table 5: List of buffers and solutions used in this study.

1.7. Oligonucleotides

All oligonucleotides were purchased from Eurofins MWG Operon (Ebersberg).

1.7.1. Sequencing primers

The oligonucleotides listed in Table 6 served as primers used in the sequencing reaction (VI.2.2.7) together with the indicated plasmids (VI.1.8.1).

Plasmid	Primer name	Sequence (5' → 3')
pGL3	GLprimer2	CTTTATGTTTTTGGCGTCTTCCA
	RVprimer4	GACGATAGTCATGCCCCGCG
pd2EGFP-N1	pd2EGFP_N	CGTCGCCGTCCAGCTCGACCA
pcDNA3	pcDNA3-for	CACTGCTTACTGGCTTATCG
	BGH Seq-	TAGAAGGCACAGTCGAGG
pcDNA3-E-cadherin-α-catenin fusions	EC forw	CTCCTGGCCTCAGAAGACA
	EC rev	TGCAATCCTGCTTCGACAG
	ECAC forw	CACCAACCCTCATGAGTGTC
	EC991	ACTGGGCTGGACCGAGAGAGTTT
	EC1501	GTGGGCCAGGAAATCACATCCTA
	EC2101	GTCGAAGCAGGATTGCAAATTC
	AC302	GTGATTTGATGAAGGCTGCTG
	AC831	ACTGGCATATGCACTCAATAAC
	AC1350	TCGAATGTCTGCAAGCCAGTTAG
	AC1850	TGGTATATGATGGCATCCGGGAC
	AC2336	GCCAAGAAAATTGCTGAGGCAG
pSUPER & pSUPERIOR	pSUPER 5#1	GACAGGGGAGTCCCGCC
pSUPER.retro	pSUPER.retro 5#2	CGATCCTCCCTTTATCCAGC
pSUPERIOR-TKD	NotI sequencing	ATGTGCTGCAAGGCGAT
	PciI sequencing	CTCACTGACTCGCTGCG

Table 6: Oligonucleotides employed for sequencing reactions.

1.7.2. Cloning primers

The primers listed in Table 7 were used to amplify cDNA in a PCR reaction (VI.2.2.10) and transfer it into a vectro of interest, thereby engineering a construct listed in Table 12. Besides the sequence complementary to the desired cDNA, they harbour an endonuclease restriction site flanked by six randomly chosen bases to allow endonuclease binding. If desired, the forward primers contain the Kozak sequence GCCACC to enhance ribosomal binding.

Const.	Direction	Primer name	Sequence (5' → 3'; restriction sequence underlined)	RS
flEC	forward	tEC3forw	AATCATGCTAGCGCCACCATGGGCCCTTGG	NheI
	reverse EcoRV	flEC5for	GCTTCGGATATCCTAGTCGTCCTCGCC	
tEC	forward	tEC3forw	see flEC	
	reverse	tEC5forw	CGAGTCGATATCATTTCCAATTTC	EcoRV
flAC	forward EcoRV	flAC3for	GGCCATGATATCATGACTGCTGTC	
	reverse	flAC5for	CCGTAAGCGGCCGCGATGCTGTCCAT	NotI
3tAC	forward	3tAC3for	GGCCATGATATCGATGACTTCTTG	EcoRV
	reverse	see flAC		

Const.	Direction	Primer name	Sequence (5' → 3'; restriction sequence underlined)	RS
MDAC	forward	see 3tAC		
	reverse	MDAC5for	CCGTAAGCGGCCGCAAAGTCAGAGTC	NotI
Ral	forward	Ral_Koz_ATG	GTGCTGGAATTCGCCACCATGGGCAC GAGCCGCGCT	EcoRI
	reverse	Ral_ATG	TGCATGCTCGAGTCGACCCGTCCG	XhoI
TKD	forward	5'PciI	GCGCACATGTAGAATTCGAACGCTGA CGTCATCA	PciI
	reverse	3'PciI	TCTCACATGTACCGGGCCCCCCCT	PciI
	forward	5'NotI	GCGCGCGGCCGCGTAGAATTCGAACG CTGACGTCATCA	NotI
	reverse	3'NotI	GCGCGCGGCCGCGTACCGGGCCCCCCCT	NotI

Table 7: Cloning primers used in this study. RS, restriction site

1.7.3. Mutagenesis primer

The oligonucleotides listed in Table 8 were used for mutagenesis (VI.2.2.11).

Construct	direction	Primer name	Sequence (5' → 3'; mutations underlined)
NF2-BBA	PCR1 forward	pcDNA3-for	see 1.7.1
	PCR1 reverse	BBA center rev	GTAATTCTCTCCTCCCACGCTGCCGCAGCC GCCGCAGCCAGATTTATTACC
	PCR2 forward	BBA center forw	GGGTAATAAATCTGGCTGCGGCGGCTGCG GCAGCGTGGGAGGAGAGAATTA
	PCR2 reverse	BGH Seq-	see 1.7.1
p2M.A-Luc	PCR1 forward	P1 3forw	GATGTCCCAATCGGGACATCTAATTGGAT GTCCCAATCGGGACATCTAATTCGAGCTC GCC
	PCR1 reverse	P1 5rev	CCAGCGGTTCCATCT
	PCR2 forward	P2 3forw	AGTGCAAGTGCAGGT
	PCR2 reverse	P2 5rev	GATGTCCCGATTGGGACATCCAATTAGAT GTCCCGATTGGGACATCCAATTCGTAATC ATG

Table 8: Oligonucleotides used for mutagenesis.

1.7.4. Small hairpin RNA encoding oligonucleotides

Sense strand (ss) and antisense strand (as) oligonucleotide were annealed and cloned in the small hairpin RNA (shRNA) expression vector of interest (VI.1.8.1). Upon transfection in mammalian cells the corresponding shRNA is expressed.

Construct	Oligo.	Sequence (5' → 3')
shRNA A against E-cadherin	E-Cad PA ss	gatccccGGACGTGGAAGATGTGAATttcaa gagaATTCACATCTTCCACGTCCtttttggaaa
	E-Cad PA as	agcttttccaaaaaGGACGTGGAAGATGTGAAT tctcttgaaATTCACATCTTCCACGTCCggg

Construct	Oligo.	Sequence (5' → 3')
shRNA B against E-cadherin	E-Cad PB ss	gatccccGTCTAACAGGGACAAAGAAttcaa gagaTTCTTTGTCCCTGTTAGACtttttggaaa
	E-Cad PB as	agcttttccaaaaaGTCTAACAGGGACAAAGAA tctcttgaaTTCTTTGTCCCTGTTAGACggg
shRNA against Cadherin-6	Cad6 ss	gatccccGCGGCTACAGTCAGAATTAttcaa gagaTAATTCTGACTGTAGCCGCtttttggaaa
	Cad6 as	agcttttccaaaaaGCGGCTACAGTCAGAATTA tctcttgaaTAATTCTGACTGTAGCCGCggg

Table 9: Oligonucleotides annealed to give shRNAs. Capital letters indicate the silencing sequence, small letters the stem. ss, sense strand; as, antisense strand

1.7.5. Quantitative real-time RT-PCR primer

The oligonucleotides listed in 1.7.5 were used as primers in quantitative real-time RT-PCR (VI.2.2.12) for expression analysis in mouse.

Gene	direction	Sequence (5' → 3')
hprt	forward	TCAGTCAACGGGGGACATAAA
	reverse	GGGGCTGTACTGCTTAACCAG
acta2	forward	TGACGCTGAAGTATCCGATAGA
	reverse	GTACGTCCAGAGGCATAGAGG
vinculin	forward	GGCCGGACCAACATCAGTG
	reverse	ATGTACCAGCCAGATTTGACG

Table 10: Oligonucleotides used as primers in quantitative real-time RT-PCR analysis.

1.8. Plasmids

1.8.1. Basic vectors

Plasmid	Description	Source
pcDNA3	mammalian expression vector, Amp^r, Neo^r, CMV promotor, BGH poly A, high copy number plasmid, F1+ origin	Invitrogen (Karlsruhe)
pcDNA6-TR	tetracycline repressor protein expression vector, Amp^r, $Blast^r$, CMV promoter for high expression level	Invitrogen (Karlsruhe)
pEF plink	mammalian expression vector, pUC12 backbone, EF1α enhancer/promoter, Amp^r	G. Posern (Sotiropoulos *et al.*, 1999)
pEF-Flag plink	like pEF plink, with 5' Flag-tag	G. Posern (Sotiropoulos *et al.*, 1999)

Plasmid	Description	Source
pGL3-Basic	reporter vector encoding for firefly (*Photinus pyralis*) luciferase, Amp^r	Promega (Madison, USA)
pRL-TK	internal control reporter for pGL3, herpes simplex virus thymidine kinase promoter driving *Renilla reniformis* luciferase expression, Amp^r	Promega (Madison, USA)
pSUPER	shRNA expression vector, Amp^r, $Puro^r$, H1 promoter	OligoEngine (Seattle, USA)
pSUPER.retro	shRNA expression vector for retroviral infection, Amp^r, $Puro^r$, H1 promoter	OligoEngine (Seattle, USA)
pSUPERIOR	doxycycline inducible shRNA expression vector, Amp^r, $Puro^r$, modified H1 promoter	OligoEngine (Seattle, USA)
pd2EGFP-N1	cDNA of EGFP, destabilized by C-terminally fused mouse ornithine decarboxylase PEST domain	BD Biosciences (Heidelberg)

Table 11: List of basic vectors used in this study.

1.8.2. Modified vectors

The vectors engineered in this study were generated by cloning, mutagenesis or shRNA encoding oligonucletide insertion into the basic vectors (VI.1.8.1). Vectors are mammalian expression vectors, if not indicated otherwise.

Plasmid	Description	Source/Reference
p2M.A-Luc	control SRF reporter derived from p3D.A-Luc, in which two SRF binding sites were made insensitive (CCATATTAGG mutated to CCCAATCGGG) (Hill and Treisman, 1995) and the third one deleted	this study
p3D.A-EGPF-N1	SRF promoter from p3D.A-Luc replacing the CMV promoter in pd2EGFP-N1, thereby driving the expression of the destabilized EGFP	this study
p3D.A-Luc	three *c-fos* derived SRF binding sites in front of a *Xenopus laevis* type 5 actin TATA-Box in pGL3-basic driving the expression of the *Firefly* luciferase gene	G. Posern (Geneste *et al.*, 2002)
pcDNA3-flEC	cDNA of full length E-cadherin	this study
pcDNA3-tEC-flAC	cDNA of truncated E-cadherin (amino acids 1 – 809) lacking the β-catenin binding site fused to full length α-catenin	this study

Plasmid	Description	Source/Reference
pcDNA3-tEC-3tAC	cDNA of truncated E-cadherin (amino acids 1 – 809) lacking the β-catenin binding site fused to the C-terminal part of α-catenin (amino acids 509 – 906)	this study
pcDNA3-tEC-MDAC	cDNA of truncated E-cadherin (amino acids 1 – 809) lacking the β-catenin binding site fused to the adhesion modulation domain of α-catenin (amino acids 509 – 643)	this study
pcDNA3-mDia1 FH1FH2	cDNA of murine mDia1, constitutive active truncation, myc-tagged	R. Fässler, MPI Biochemistry (Martinsried)
pcDNA3-NF2	cDNA of human wild type NF2	H. Morrison, FLI (Jena)
pcDNA3-NF2-S518A	cDNA of human NF2, constitutive active because not phosphorylatable, subcloned from pUHD10-3-NF2-S518A	this study
pcDNA3-NF2-S518D	cDNA of human NF2, dominant negative by mimicking constitutive phosphorylation, subcloned from pUHD10-3-NF2-S518D	this study
pcDNA3-NF2-BBA	cDNA of NF2 with amino acids 177 – 183 mutated to alanine (within the FERM domain), dominant negative, derived by mutagenesis from pcDNA3-NF2	this study
pcDNA3-RhoQ63L	cDNA of RhoA, constitutive active by replacement of Q63 with L	R. Fässler, MPI Biochemistry (Martinsried)
pcDNA3-ROCKΔ4	cDNA of murine ROCK, constitutive active truncation, myc-tagged	R. Fässler, MPI Biochemistry (Martinsried)
pcDNA3.1-EzrinR579A	cDNA of human Ezrin, dominant negative, by replacement of R579 with A myc-tagged, Amp^r, Neo^r	H. Morrison, FLI (Jena)
pcDNA3.1-EzrinT567D	cDNA of human Ezrin, constitutive active by mimicking constitutive phosphorylation by replacement of T567 with D myc-tagged, Amp^r, Neo^r	H. Morrison, FLI (Jena)
pEF-Flag-G15S	cDNA of β-actin, hyperpolymerizable by replacement of G15 with S, Flag-tagged	G. Posern (Posern *et al.*, 2004)
pEF-Flag-R62D	cDNA of β-actin, nonpolymerizable by replacement of R62 with D, Flag-tagged	G. Posern (Posern *et al.*, 2002)

Plasmid	Description	Source/Reference
pEF-Flag-wt-actin	cDNA of wild type β-actin, Flag-tagged	G. Posern (Posern *et al.*, 2002)
pEF-MAL-HA (f.l.)	cDNA of murine full length MAL, HA-tagged	G. Posern (Miralles *et al.*, 2003)
pEF-MAL-ΔN	cDNA of murine MAL, constitutive active N-terminal truncation (amino acids 1 – 171), HA-tagged	G. Posern (Miralles *et al.*, 2003)
pEF-MAL-ΔNΔB1	cDNA of murine MAL, dominant negative truncation (amino acids 1 – 171 and 316 – 341), HA-tagged	G. Posern (Miralles *et al.*, 2003)
pEF-MAL-ΔNΔC	cDNA of murine MAL, dominant negative truncation (amino acids 1 – 171 and 563 – 1021), HA-tagged	G. Posern (Miralles *et al.*, 2003)
pEF-RacV12	cDNA of Rac1, constitutive active by replacement of G12 with V	G. Posern (Hill *et al.*, 1995)
pEGFP-N2-wtE-cadherin	cDNA of human wild type E-cadherin N-terminally fused to EGFP, Kan^r, Neo^r	Birgit Luber, TUM (Munich)
pGEX-2T-PAK CRIB	cDNA of amino acids 68 – 151 of human PAK1, bacterial expression plasmid, Amp^r (Martinsried)	A. Ullrich, MPI Biochemistry
pGEX-2T-Rhotekin RBD	cDNA of amino acids 7 - 90 of murine Rhotekin RBD, bacterial expression plasmid, Amp^r	A. Ullrich, MPI Biochemistry (Martinsried)
pGEX-KG TAT-C3	cDNA of *Clostridium botulinum* C3 N-terminally fused to the HIV-TAT sequence, bacterial expression plasmid, Amp^r	E. Sahai, CRUK (London, GB)
pMT2-HA-EpacΔcAMP	cDNA of human Epac, constitutive active truncation, HA-tagged, SV40 promoter, Amp^r	G. Posern (Posern *et al.*, 2000)
pOTB7-CTNNA1	cDNA of human α-catenin 1, cloning vector, $Chloramphenicol^r$	RZPD (Berlin)
pSUPER-EcadA	shRNA A against E-cadherin	this study
pSUPER-EcadB	shRNA B against E-cadherin	this study
pSUPER-Cad6	shRNA against Cadherin-6	this study
pSUPER.retro-EcadA	shRNA A against E-cadherin	this study
pSUPER.retro-EcadB	shRNA B against E-cadherin	this study

Plasmid	Description	Source/Reference
pSUPER.retro-Cad6	shRNA against Cadherin-6	this study
pSUPERIOR-EcadA	shRNA A against E-cadherin	this study
pSUPERIOR-EcadB	shRNA B against E-cadherin	this study
pSUPERIOR-Cad6	shRNA against Cadherin-6	this study
pSUPERIOR-TKD	shRNA A against E-cadherin, insertion of H1 promoter and shRNA B against E-cadherin via NotI, insertion of H1 promoter and shRNA against Cadherin-6 via PciI	this study
pUHD10-3-NF2-S518A	cDNA of human NF2, constitutive active because not phosphorylatable, in the reverse tetracycline-dependent transactivator cloning vector pUHD10-3, Amp^r	H. Morrison, FLI (Jena)
pUHD10-3-NF2-S518D	cDNA of human NF2, dominant negative by mimicking constitutive phosphorylation, compare pUHD10-3-NF2-S518A	H. Morrison, FLI (Jena)

Table 12: List of modified vectors used in this study.

1.9. Peptides

The HAV peptide (H-IAKYILYSHAVSSNGNAVED-NH_2) was synthesized and purified using standard Fmoc chemistry by the core facility of the Max Planck Institute of Biochemistry (Martinsried).

1.10. Antibodies

1.10.1. Primary antibodies

The antibodies listed in Table 13 were used as primary antibodies in immunoblot or immunofluorescence (IF) analysis. The IF-row specifies which fixation method was used for immunofluorescence staining with M for Methanol, P for 4% PFA, - indicated that neither M nor P worked and n/a for not tested. If a costaining with actin wanted to be obtained, cells had to be fixated with the PFA method as organic solvents erase the actin signal.

Antibody	Origin/Description	Source	IF
Actin (clone C4)	mouse, monoclonal	MP Biomedicals (Aurora, USA)	n/a
AF-6	mouse, monoclonal, raised against human AF-6 aa 1091-1223	BD Biosciences (Heidelberg)	M

Antibody	Origin/Description	Source	IF
β-Catenin	mouse, monoclonal, binds C-terminal part of β-catenin	BD Biosciences (Heidelberg)	M&P
Cdc42	mouse, monoclonal, raised against human Cdc42 aa 1-191	BD Biosciences (Heidelberg)	n/a
E-cadherin (ECCD-2)	rat, monoclonal, binds extracellular domain	Merck (Darmstadt)	M
E-cadherin (clone 36)	mouse, monoclonal, raised against human E-cadherin aa 735-883	BD Biosciences (Heidelberg)	M&P
E-cadherin (DECMA-1)	mouse, monoclonal, blocking antibody,does not recognize human E-cadherin	Sigma-Aldrich (Steinheim)	M&P
Flag M2	mouse, monoclonal	Sigma-Aldrich (Steinheim)	P
Flag M2 p.c.	see Flag M2, peroxidase conjugate	Sigma-Aldrich (Steinheim)	n/a
HA	mouse, monoclonal, recognizes the influenza hemagglutinin epitope	BAbCO (Richmond, USA)	P
HA p.c. (3F10)	see HA, peroxidase conjugated	BAbCO (Richmond, USA)	n/a
MRTF-A (H-140)	rabbit, polyclonal, raised against human MRTF-Aaa 761-900	Santa Cruz (Santa Cruz, USA)	-
MRTF	rabbit, polyclonal, recognizes MRTF-A and MRTF-B	homemade (Posern Lab)	P
c-Myc (9E10)	mouse, monoclonal	Cancer Research UK	P
Rac1	mouse, monoclonal, raised against human Rac1 aa 1-192	BD Biosciences (Heidelberg)	n/a
RhoA (26C4)	mouse, monoclonal, raised against human RhoA aa 120-150	Santa Cruz (Santa Cruz, USA)	n/a
ZO-1	rabbit, polyclonal, raist against the N-terminal region of human ZO-1	Zymed (San Francisco, USA)	M

Table 13: Primary antibodies used in immunoblot or immunofluorescence analysis. The IF-row specifies which fixation method was used for immunofluorescence staining: M, Methanol; P, 4% PFA; -, neither M nor P worked; n/a, not tested.

1.10.2. Secondary antibodies

For immunoblot analysis the horseradish peroxidase (HRP) conjugated anti-IgG antibodies listed in Table 14 were used in this study.

Antibody	Dilution	Source
Polyclonal goat anti-mouse-HRP	1:7500	DakoCytomation (Glostrup, DK)
Polyclonal swine anti-rabbit-HRP	1:3000	DakoCytomation (Glostrup, DK)
Polyclonal goat anti-rat-HRP	1:5000	Jackson ImmonuResearch (Newmarket, GB)

Table 14: Secondary horseradish peroxidase (HRP) conjugated anti-IgG antibodies used in immunoblot analysis.

For immunofluorescence analysis the fluorescent dye conjugated anti-IgG antibodies listed in Table 15 were used in this study.

Antibody	Dilution	Source
Alexa Fluor® 350 goat anti-rabbit	1:1000	Molecular Probes (Eugene, USA)
Alexa Fluor® 488 goat anti-mouse	1:1000	Molecular Probes (Eugene, USA)
Alexa Fluor® 546 goat anti-mouse	1:1000	Molecular Probes (Eugene, USA)
Alexa Fluor® 546 goat anti-rabbit	1:1000	Molecular Probes (Eugene, USA)
Polyclonal swine anti-rabbit-FITC	1:30	DakoCytomation (Glostrup, Denmark)
Polyclonal swine anti-rabbit-TRITC	1:40	DakoCytomation (Glostrup, Denmark)
Polyclonal goat anti-rat-Cy3	1:100	Jackson ImmonuResearch (Newmarket, GB)

Table 15: Secondary fluorescent dye conjugated anti-IgG antibody used for immunofluorescence analysis. FITC, Fluorescein Isothiocyanate; TRITC, Tetramethylrhodamine Isothiocyanate; Cy3, Carbocyanin 3.

1.11. Enzymes

Enzyme	Source
Antarctic Phosphatase	NEB (Frankfurt/Main)
DNA Polymerase I, Large (Klenow) Fragment	NEB (Frankfurt/Main)
DNAse I, RNAse free	Roche (Mannheim)
Phusion™ High-Fidelity DNA-Polymerase	Finnzymes (Espoo, FI)
Restriction Endonucleases	NEB (Frankfurt/Main) MBI (Fermentas, St. Leon-Rot)
T4-DNA Ligase	NEB (Frankfurt/Main)
Trypsin (Gibco)	Invitrogen (Karsruhe)

Table 16: Enzymes used in this study.

1.12. Cells

1.12.1. Bacterial strains

The following *Escherichia coli* (*E.coli*) strains were used for transformations to amplify plasmids (DH5α) and for protein expression (Rosetta^{TM}).

Strain	Genotype/Properties	Origin
DH5α	F^- φ80dlacZM15 (lacZYA-argF)U169 deoR recA1 endA1 endA1 hsdR17(r k^- m k^+) phoA supE44 thi-1 gyrA96 relA1 λ^-	Invitrogen (Karlsruhe)
Rosetta^{TM} (DE3)	BL21 derivatives, express 6 additional tRNAs rarely occuring in *E. coli*; F^- ompT $hsdS_B$ (r_B- m_B-) gal dcm (DE3) pRARE Cam^R	Novagen (Madison, USA)

Table 17: Bacterial strains used in this study.

1.12.2. Mammalian cell lines

The following eukaryotic cell lines were used in this study.

Cell line	Description	Origin/Reference
AGS	human gastric adenocarcinoma cells, E-cadherin deficient	ATCC (Manassas, USA)
CHO-K1	chinese hamster ovary cells, E-cadherin deficient	ATCC (Manassas, USA)
EpH4	normal mouse mammary epithelia cells	H.Beug, IMP (Vienna, A)
EpRas	EpH4 cells stably expressing v-Ha-Ras. Cells undergo EMT upon TGF-β treatment (Oft *et al.*, 1996).	H.Beug, IMP (Vienna, A)
MDA-MB 435S	metastatic human breast cancer cells, E-cadherin deficient	ATCC (Manassas, USA)
MDCK	canine kidney normal epithelial cells	ATCC (Manassas, USA)
NIH3T3	mouse embryonic fibroblasts	R.Treisman, CRUK (London, GB)
PhoenixA	amphotropic retrovirus producing cell line derived from the Human Embryonic Kidney (HEK) 293T cell line	A.Ullrich, MPI Biochemistry (Martinsried)

Table 18: Mammalian cell lines used in this study. ATCC, American Type Culture Collection.

1.13. Scientific software

Software	Source
AIDA	Raytest (Staubenhardt)
KC4	BioTek (Winooski, USA)
MetaVueTM Imaging Software	Molecular Devices (Downingtown, USA)
MetaMorphTM Imaging Software	Molecular Devices (Downingtown, USA)
SigmaPlot	SPSS Science Software (Erkrath)
SoftWoRx	Applied Precision (Issaquah, USA)
WinGlow	EG and G Berthold (Schwerzenbach, CH)

Table 19: Scientific software used in this study.

2. Molecular biology methods

2.1. Microbiological techniques

2.1.1. Cultivation and maintenance of bacterial strains

E. coli strains were grown at 37 °C for 12 – 16 h either in LB medium or on LB agar plates supplemented with the for selection appropriate antibiotics. For short-term storage, *E. coli* cultures were kept on LB agar plates at 4 °C. For long-term storage 1 mL glycerol stocks consisting of overnight culture in 50 % (v/v) glycerol were stored in CryoTube^{TM} vials at -80 °C.

2.1.2. Generation of competent bacteria

To generate electrocompetent bacteria a well isolated bacterial colony grown on a fresh LB agar plate was inoculated in 5 mL LB medium and incubated shaking (180 rpm) at 37°C over night. The next day the overnight culture was diluted 1:100 in fresh LB medium and incubated as before until the cell density reached the optical density of 0.5 at 600 nm. At this point the bacteria were harvested by centrifugation at 1200 x g and 4°C for 10 minutes. Then the supernatant was decanted and the bacteria resuspended in sterile ice-cold 10% glycerol (same amount than supernatant decanted) and incubated for 20 minutes on ice. Afterwards the bacteria were pelleted as before and resuspended in 10% glycerol ($1/10^{th}$ of the amount of decanted supernatant) followed by another incubation on ice for 20 minutes. Thereafter the bacteria were pelleted again as before and resuspended in 10% glycerol ($1/5^{th}$ of the amount of decanted supernatant). The now electrocompetent bacteria were shock frozen in 40 µL aliquots in liquid nitrogen and stored at -80°C. Newly generated competent bacteria were tested for efficiency by transformation of 0.1 ng of a known plasmid, which should result in 10^8 – 10^9 colonies per µg DNA.
To generate chemically competent bacteria a 2 mL over night culture of bacteria in LB medium was diluted 1/100 in fresh LB medium and incubated while shaking (180 rpm) at 37°C until the OD reached 0.2. The bacteria solution was incubated for 10 minutes on ice, centrifuged at 400 x g and 4°C for 10 minutes and the resulting pellet resuspendend in 25 mL cold transformation buffer. The suspension was inbcubated for 20 minutes on ice and centrifuged as before, the pellet this time resuspended in 2.5 mL cold transformation buffer. The now chemically competent bacteria were snap-frozen in 50 µL aliquots and stored at -80°C. Newly generated competent bacteria were tested for efficiency by transformation of 0.1 ng of a known plasmid, which should result in 10^7 – 10^8 colonies per µg DNA.

2.1.3. Transformation of competent bacteria

Competent bacteria were either transformed by electroporation or the "heat shock" method.
For each electroporation 50 µL of electrocompetent bacteria were thawed on ice and supplemented with 1 – 2 µL ligation reaction. The mixture was then transferred into an ice-cold 0.2 cm electroporation cuvette and electoporated with the Genepulser XCell^{TM} at 2.5 kV, 25 µF and 200 Ohm. Immediately afterwards 500 µL of SOC medium were added, followed by an incubated on a rotating wheel at 37°C for 1 h. Thereafter 200 µL of the mixture were plated on a LB agar plate with the appropriate antibiotics.
For each heat shock induced transformation 50 µL of chemically competent bacteria were thawed on ice and incubated with the whole ligation reaction for 10 minutes on ice. For the following heat shock, the cells were incubated at 42°C for 90 seconds pursued by another incubation on ice for 5 minutes. Then 200 µL LB medium were added and the cells were incubated on a rotating wheel at 37°C for 1 h. Afterwards the mixture was plated on a LB agar plate with the appropriate antibiotics.

2.1.4. TAT-C3 purification

TAT-C3 was purified according to the large scale protein production described by E. Sahai and colleagues (Sahai and Olson, 2006) with a modified, calcium-free thrombin cleavage buffer (1 mM $MgCl_2$, 1 mM DTT in TBS).

2.2. DNA modification

2.2.1. Plasmid preparation

Plasmids were prepared using the QIAGEN Plasmid Mini Kit for small amount of DNA and the QIAGEN Plasmid Maxi Kit for larger amounts of DNA according to manufacturer's instructions.

2.2.2. Restriction digestion of DNA

For restriction digestion approximately 0.5 – 2 µg of DNA were digested with the endonuclease of interest at the concentration/temperature and with the buffer recommended by the manufacturer. For analytical digestions, the reaction volume was 20 µL incubated for 1 h, for preparative digestions 50 µL incubated for 3 h – over night.

2.2.3. Blunt end creation

DNA polymerase I, large (Klenow) fragment fills-in 5' overhangs and removes 3' overhangs to create blunt ends. The DNA fragment or plasmid of choice was incubated with DNA polymerase I, large (Klenow) fragment according to manufacturer's instructions. Aferwards, the DNA was purified by agarose gel electrophoresis or directly via the QIAquick PCR Purification Kit or QIAquick MinElute PCR Purification Kit.

2.2.4. Dephosphorylation of DNA 5'-termini

To prevent self-ligation of vector termini generated by restriction digestion, the 5'- termini of vectors were dephosphorylated with Antarctic Phosphatase according to manufacturer's protocols. The reaction was stopped by either heat inactivation at 65°C for 5 minutes or direct purification of the DNA via the QIAquick PCR Purification Kit or QIAquick MinElute PCR Purification Kit.

2.2.5. Ligation of DNA fragments

Before ligation, the fragments were purified by agarose gel electrophoresis followed by gel extraction with the QIAquick Gel Extraction Kit. Dephosphorylated and QIAquick PCR Purification Kit purified vector fragments were directly used for ligation. For ligation, 20 - 200 ng of vector and the 3 – 6 fold molar amount of insert were incubated together with 400 U of T4 DNA Ligase and T4 Ligase buffer in a total of 20 µL at 14°C over night or at RT for 1 – 2 h. As control, the ligation was performed as described above with the difference that the insert fragment was missing. Immediately after incubation the cells were transformed into competent *E. coli DH5α*.

2.2.6. Generation of shRNA expressing plasmids

For annealing 3 µg of sense and the corresponding antisense shRNA oligonucleotide strand were mixed in a total of 50 µL Annealing buffer. The mixture was heated to 95°C for 10 minutes and then cooled down with 0.01°C per second to 4°C in a Biometra T3000 Thermocycler. The annealed shRNAs habouring a BglII and HindIII overhang were purified via agarose gel electrophoreses and extracted. The insertion into the desired shRNA expression vector was done according to manufacturer's instructions.

2.2.7. Sequencing

DNA samples were sequenced on an ABI 3730 sequencer by the core facility of the Max Planck Institute of Biochemistry (Martinsried).

2.2.8. Agarose gel electrophoresis

DNA fragments and plasmids were separated by agarose gel electrophoresis (Sambrook, 1989). For gel preparation 0.7 – 2 % (w/v) agarose in TAE or TBE buffer was boiled and afterwards supplemented with 0.01% (v/v) ethidium bromide. After gel polymerization, DNA samples were mixed with the corresponding amount of DNA loading buffer and loaded on the agarose gel together with the SmartLadder DNA marker for size determination. Electrophoresis was performed in TAE or TBE buffer, according to gel preparation, at 70 – 120 V for 20 – 60 minutes in a agarose gel electrophoresis sytem Horizontal-Elpho. After electrophoresis, the DNA was visualized at 302 nm and photographs were taken with the IDA gel documentation system. If the separated DNA fragments or plasmids were used for further experiments, they were visualized with a Dark Reader® at 460 nm to avoid the introduction of mutations.

2.2.9. Isolation of DNA fragments and plasmids from agarose gels

The DNA fragments or plasmids of interest were cut out of the gel with a sterile blade and purified using the QIAquick Gel Extraction Kit according to manufacturer's instructions.

2.2.10. DNA amplification by Polymerase Chain Reaction

DNA fragments of interest were exponentially amplified via Polymerase Chain Reaction (PCR) by a repeated cycle of denaturation, primer annealing and polymerase-driven primer elongation (Mullis and Faloona, 1987). The PCR reaction was carried out employing the Phusion™ High-Fidelity DNA-Polymerase according to manufacturer's instructions with the primers denoted in Table 7 for cloning and Table 8 for mutagenesis in a Biometra T3000 Thermocycler. PCR products were analysed via agarose gel electrophoreses and positive products were extracted from the gel (VI.2.2.8 and VI.2.2.9).

2.2.11. Mutagenesis by PCR

Mutagenesis was performed as described by Sambrook and colleague according to the protocol "Rapid and Efficient Site-directed Mutagenesis by the Single-tube Megaprimer PCR Method" (Sambrook, 2001). The first PCR was performed as described in section VI.2.2.10. The second PCR was performed with 1 ng product of the first PCR.

2.2.12. Quantitative real-time RT-PCR

Cellular RNA was isolated with the QIAGEN RNeasy Mini Kit and cDNA was synthesised with the Reverse-iT-1st-Strand-Synthesis-Kit according to manufacturer's instruction. For cDNA synthesis 1 µg of RNA and anchored oligo-dT primers were used. For cDNA quantitation one fortieths of the RT reaction was mixed with gene specific primers (0.5 µM) (VI.1.7.5), $MgCl_2$ (3 mM) and LightCycler® FastStart DNA Master SYBR Green I mix (1.5 µl) to a total volume of 15.5 µl. The PCR was carried out on a LightCycler instrument according to the manufacturer's instructions. Calculation was done using the $\Delta\Delta C_t$ method (Winer *et al.*, 1999).

3. Methods in mammalian cell culture

3.1. General cell culture methods

CHO-K1, EpH4, EpRas, MDCK, NIH3T3 and PhoenixA cell lines were cultivated in a HERAcell® 150i CO_2 incubator in a 90% air and 10% CO_2 atmosphere, the MDA-MB 435S cell line in a 95% air and 5% CO_2 atmosphere, all at 37°C. All working steps were carried out in sterile Lamin Air hoods. All cells were routinely cultured in fresh DMEM containing 4.5g/L D-glucose and L-glutamine additionally supplemented with 10% FCS (4% FCS for EpRas), 2 mM L-glutamin, 1 mM sodium pyruvat, 50 U/mL penicillin and 50 µg/mL streptomycin and passaged constantly. Prior to seeding cells were counted manually in a Neubauer counter chamber. For long time storage cells were transferred in freeze medium to CryoTube™ vials and after stepwise freezing stored in liquid nitrogen.

3.2. Generation of monoclonal cell lines

To generate monoclonal cell lines stably harbouring one or several vectors of interest, cells were transfected with Lipofectamine® (VI.3.5.2), split on the following day 1:8 and supplemented with the corresponding antibiotics (VI.1.8.1 and VI.1.8.2) as indicated in Table 20 for selection. Single surviving colonies were expanded and analysed by Western blotting (VI.5.5 and VI.5.6) and/or immunofluorescence techniques (VI.6).

Antibiotic		AGS	MDCK
Blasticidine	selection	-	5 µg/mL
	maintenance	-	3 µg/mL
G418	selection	600 µg/mL	600 µg/mL
	maintenance	300 µg/mL	300 µg/mL
Puromycin	selection	-	1 µg/mL
	maintenance	-	1 µg/mL

Table 20: Concentrations of antibiotics used to select monoclonal cell lines.

3.3. Calcium switch

Calcium switch experiments were carried out to induce the dissociation and reformation of epithelial junctions.
To investigate cellular responses mediated by junction formation cells were transfected as described in section VI.3.5.2. and immediately afterwards starved in calcium and FCS free medium containing 0.2% BSA for 40 h. Junction formation was induced by readdition of calcium to the physiological concentration of 1.8 mM.
To investigate cellular responses mediated by junction dissociation cells were either transfected as described in section VI.3.5 and then reseeded or directly seeded to from a confluent monolayer. The medium of cells grown in confluent monolayers was refreshed every 24 h. 24 – 36 h after (re)seeding the medium was exchanged to normal medium as control or reduced calcium medium containing 0.02 mM calcium (or as otherwise indicated in the figure legend).

3.4. Serum stimulation

Serum stimulation of NIH3T3 was done as previously described (Posern *et al.*, 2002). For MDCK, cells were seeded to form a confluent monolayer and then serum starved and stimulated as NIH3T3 cells.

3.5. Methods to introduce DNA in mammalian cells

3.5.1. Calcium phosphate mediated transfection

The PhoenixA retrovirus producing cell line was transfected with the calcium phosphate method as described before (Sambrook, 2001). 18-24 hours prior transfection 6 x 10^6 cells per 10 cm plate were seeded in 10 mL medium without Penicillin/Streptomycin. 1 hour prior to transfection the cell medium was replaced with 9 mL fresh media for each 10 cm plate supplemented with 25 µM chloroquine. For each transfection, 500 µL $CaCl_2$ (250mM) were mixed with 20 µg of retroviral vector DNA. This mixture was added dropwise while swirling on vortex to 500 µL 2 x BBS solution to initiate precipitation. After 20 minutes of incubation at RT, the mixture was added dropwise into the cell medium while swirling the cells. The transfected cells were incubated at 3% CO_2 and 37°C to enhance precipitate formation. 24 h post transfection the cells were washed once with medium and cultured in fresh medium without Penicillin/Streptomycin.

3.5.2. Lipofection

AGS, CHO-K1, EpH4, MDCK and NIH3T3 cell lines were transfected with Lipofectamine®, the EpRas cell line with Lipofectamine 2000® and MDA-MB 435S cell line with Transfast according to manufacturer's instructions. The individual cell numbers seeded 18 – 24 h prior to infection, total amount of DNA transfected and amount of transfection reagent (TR) used are summarized in Table 21.

	12 well	6 well	6 cm plate	10 cm plate	
AGS/CHO-K1/ EpH4/EpRas/ MDCK	5.0 x 10^4 500 ng 2,5 µL	1.5 x 10^5 1 µg 5 µL	1 x 10^6 2 µg 10 µL	1.5 x 10^6 5 µg 25 µL	cell-number [DNA] [TR]
MDA-MB 435S	-	-	-	1 x 10^6 15 µg 45 µL	cell-number [DNA] [TR]
NIH3T3	3.5 x 10^4 500 ng 2 µL	-	-	1 x 10^6 7.5 µg 20µL	cell-number [DNA] [TR]

Table 21: Cell numbers, the amount of DNA and Transfection reagent used for lipofection of mammalian cell lines.

3.5.3. Electoporation

For each electroporation 5 x 10^6 MDCK cells in 500 µL normal medium were transferred together with 20 µg DNA in a 0.4 cm wide electroporation cuvette. Cells were electroporated in the square wave modus 3 times at 250 V for 20 ms, with a 100 ms break between the pulses, in a Genepulser XCell™. Afterwards, 1 mL of fresh prewarmed medium was added immediately, before the cells were reseeded in a 6 cm plate in a total of 3 mL medium.

3.5.4. Nucleofection

MDCK cells were nucleofected in an Amaxa Nucleofector device according to manufacturer's instructions. Briefly, for each nucleofection 2.5 x 10^6 MDCK cells were trypsinized, centrifuged at 90 x g for 10 minutes, resuspended in 100 µL Nucleofector solution L and mixed with a total of 4.1 µg DNA. Then the cells were transferred in the nucleofector cuvette and nucleofected with program A-024. Immediately afterward 500 µL prewarmed medium was added and the cells were reseeded.

3.5.5. Retroviral infection

One 10 cm plate of PhoenixA cells per well of target cells in a 6 cm plate was transfected with the calcium phosphate method. 24h post transfection the cells were washed once with medium and then cultured in 6.5 mL DMEM without Penicillin/Streptomycin at 7% CO_2 and 32°C to enhance virus stability. 48 h post Phoenix cell transfection the target cells, either 1 x 10^5 NIH3T3 cells or 1.5 x 10^6 MDCK cells per 6 cm plate seeded 24h prior to infection in normal medium, were infected. Therefore, the supernatant from the 10 cm plate of transfected Phoenix cells was filtered through a 0.45 µm PVDF-filter to remove cells and concentrated to 1 mL by centrifugation at 2000 x g in a PBS-equilibrated vivaspin 20 column. The 10 cm plate of Phoenix cells was supplemented with 6.5 mL of fresh medium and further incubated at 7% CO_2 and 32°C for a second round of infection. During the centrifugation the medium from the target cells was removed and 1 mL of medium supplemented with 8 µg/mL polybrene was added. When the supernatant was concentrated to 1 mL, it was after membrane rinsing removed from the vivaspin column and added to the target cells, which were after gentle swirling incubated at 7% CO_2 and 32°C. 9 h later the target cells were infected a second time identically, except that the old medium from the target cells was just removed half, and after readdition of 4 µg/mL polybrene the 1 ml concentrate was added. 24 h post infection the medium of the target cells was replaced by normal medium. 48 h post infection the infection efficiency was monitored by EGFP expression of a control infection.

4. Gene reporter assays

4.1. Luciferase reporter assay

For luciferase reporter assays AGS, CHO-K1, EpH4, MDCK, MDA-MB 435S and NIH3T3 cells were transfected as described in section VI.3.5 with p3D.A-Luc encoding for the Firefly luciferase gene, pRL-TK encoding for the Renilla luciferase gene and additional plasmids of interest as indicated in the figure legends.
The luciferase reporter assay was carried out with reagents from the Dual-Glo™ Luciferase Assay Kit. After the treatment of interest the cells were washed twice with ice-cold PBS and lysed by incubation in 50 µL Passive Lysis Buffer (PLB) per 12 well or transwell filter on ice for 10 minutes. Thereafter, the cells were scraped of the plate, the lysate collected in an Eppendorf tube and centrifuged at 20000 x g and 4°C for 10 minutes. 20 µL of the supernatant were transferred into a well in a white 96 well microtiter plate and mixed with 45 µL LARII solution. The emitted Firefly luminescence was detected in a Microplate Luminometer LB 96V. After detection 45 µL of Stop & Glow reagent supplemented with Stop & Glow substrate were added to the well to stop the Firefly reaction and start Renilla luminescence emission, which was detected as above. The protein content of each lysate was

determined by Bradford assay (VI.5.2.1). Firefly luciferase activity was normalized to either protein content or Renilla luciferase activity, as indicated in the figure legend. Figures show mean ± SEM of at least three independent experiments.

4.2. β-Galactosidase reporter assay

20 µL of LacZ substrate (10 mg/ml Chlorophenolred-β-D-galactopyranosid in PBS) were mixed with 160 µL of LacZ buffer and added to 20 µL lysate in a transparent mikrotiter plate and incubated at 37°C for 1 – 4 h. Afterwards, absorption was detected at 570 nm (630 nm reference) in the BioTek Elisaeader.

5. Protein analytical methods

5.1. Lysis of cells with Triton X-100

Prior to lysis the cells were washed with twice cold PBS and then lysed for 3 minutes on ice in RIPA-buffer containing protease (Complete™ Protease Inhibitor Cocktail Tablets) and phosphatase (2 mM sodium orthovanadate, 10 mM sodium fluoride) inhibitors. After scraping the lysates were precleared by centrifugation at 20000 x g and 4°C for 10 min.

5.2. Determination of protein concentration

5.2.1. Bradford protein assay

Protein concentration measurement using the Bradford method (Bradford, 1976) is based on the absorbance shift of Coomassie Brilliant Blue G-250 from red to blue in proportion with protein binding (absorption maximum: 595 nm). The protein lysate of interest was mixed with 100 µL of Bradford solution and incubated for 5 minutes at room temperature. Then the absorption was measured at 595 nm in a BioTek Elisareader. The protein concentration was determined by comparison with a standard curve of BSA (1 - 10 µg).

5.2.2. BCA protein assay

Protein concentration measurement using the BCA protein (Smith *et al.*, 1985) assay is based on the reduction of copper ions from Cu^{2+} to Cu^{+} by peptides in a temperature-dependent reaction. Cu^{+} gets chelated by bicinchoninic acid (BCA), which causes a color change from light green to purple in proportion to the protein concentration (absorption maximum: 562 nm). The BCA assay was carried out with the Micro BCA Protein Assay Kit according to manufacturer's instructions. The absorption was measured at 570 nm in a BioTek Elisareader. The protein concentration was determined by comparison with a standard curve of BSA.

5.3. SDS-Polyacrylamid Gel Electrophoresis

SDS-Polyacrylamid Gel Electrophoresis (SDS-PAGE) was mainly carried out as described before (Laemmli, 1970). Samples were run on two-layered gels consisting of stacking and separating gel in a polyacrylamide gel electrophoresis system Vertical Elpho "B". The stacking gel contained 5% acrylamide solution in 127 mM Tris-HCl pH 6.8, 0.1% (w/v) SDS, 4.5% (v/v) glycerol and 0.1% (w/v) APS. The separating gel contained 7 – 15 % acrylamid solution (according to protein size) in 377 mM Tris-HCl pH 8.8, 0.1% (w/v) SDS and 0.1% (w/v) APS. To start the polymerization reaction 0.1 % (v/v) TEMED was added. Before SDS-PAGE all samples were mixed with the appropriate amount of Laemmli buffer and boiled at 95 °C for 2 minutes to remove all secondary, tertiary and quaternary structures. The Precision Plus Protein™ Dual Color Standard was used as molecular weight

standard. SDS-PAGE was performed at 80 – 140 V. After electrophoresis gels were either Coomassie stained (VI.5.4) or transferred to a PVDF membrane for western blotting (VI.5.5).

5.4. Coomassie staining of SDS-PAGE gels

For Coomassie staining gels were washed for 10 minutes in Coomassie R-250 solution followed by removal of unbound colour by incubation in Coomassie destaining solution for several hours in. For drying, gels were inserted air bubble-free between two wet layers of cellophane and left for 1- 2 h in a GelAir dryer.

5.5. Western blotting

For Western blotting SDS-PAGE was performed (VI.5.3) and afterwards proteins were transferred to a PVDF membrane. Therefore, the polyacrylamide gel was blotted air-bubble free in Tris-Glycin-SDS buffer in the Mini Trans-Blot Cell at 100 V for 1 h in the following order: anode, pad, 2 layers of Whatman paper, PVDF membrane, polyacrylamide gel, 2 layers of Whatman paper, pad and cathode.

5.6. Immunoblot detection

After blotting the proteins were transferred to the PVDF membrane and providing access for reaction with immunodetection reagents. To block unspecific binding sites the membrane was incubated in milk for at least 1 h at room temperature or 4°C over night. The membrane was then incubated with the first antibody in milk (VI.1.10.1) for at least 1 h at room temperature or 4°C over night, afterwards washed three times in TBST buffer for 5 minutes and incubated with the secondary horseradish peroxidase conjugated anti-IgG antibody diluted in milk (VI.1.10.2) for 1 – 2 h. Thereafter the membrane was washed again three times in TBST buffer for 5 minutes and luminescent bands were detected on Hyperfilm MP using the Western Lightning^{TM} Chemoluminescence Reagent Plus or ECL Plus Reagent according to manufacturer's instructions.

5.7. Stripping

To reincubate with a different set of antibodies the membrane was stripped to remove all bound antibodies. Therefore, the membrane was washed two times for 10 minutes in TBST buffer and then incubated at 50°C in a closed container in stripping buffer. Afterwards the membrane was washed three more times in TBST buffer for 5 minutes before it was ready to be incubated with another set of antibodies.

5.8. Densitometric analysis of western blots

Densiomatric analysis of western blots was done with AIDA software and normalized to total lysates or ratios.

5.9. Small G-protein pull-down assays

Preparation of GST-Rhotekin-RBD and GST-PAK-CRIB fusion protein was done using *E. coli Rosetta*^{TM} (DE). An overnight culture in LB medium supplemented with the corresponding antibiotics and 1% glucose was diluted 1/200 in fresh LB medium and incubated at 37°C while shaking (180 rpm) until the OD reached 0.6. Protein expression was induced by addition of 1 mM IPTG and cells were incubated at 30° for 90 min followed centrifugation at 1200 x g and 4°C for 30 minutes. The pelleted bacteria were lysed in ice-cold TPE lysis buffer containing protease inhibitors (1/20th of the original volume), tranferred to prechilled 50 mL Falcon tubes and sonicated on ice 6 times for 10 seconds at the strongest level in a sonicator Sonoplus HD70. Afterwards the lysate was centrifuged at 25000 x g and 4°C or 30 minutes and the supernatant snap-frozen in liquid nitrogen and stored at -80°C.
Optimized amounts of lysate were used for coupling to Glutathione Sepharose beads directly prior to GTPase pull-down assays. The pull-down assays were carried out as described before (Sander *et al.*,

1998; Ren and Schwartz, 2000). 1 x 10^7 MDCK cells were seeded in 10 cm dishes to form a confluent monolayer and cultured for 36 h. After medium exchange cells were lysed in 800 µL GTPase lysis buffer containing protease inhibitors and the lysates cleared by centrifugation. 50 µL of the supernatant were mixed with an appropriate amount of Laemmli buffer and kept as total lysate, the remaining 750 µL of supernatant were incubated with immobilized GST-Rhotekin-RBD or GST-PAK-CRIB on the rotating wheel at 4°C for 35 minutes. Thereafter the beads were washed three times in GTPase wash buffer, carefully aspirated and finally mixed with 20 µL Laemmli buffer. As controls, cell lysates were incubated either with uncoupled beads alone or preincubated with GTPγS (1 mM for 10 minutes) prior to precipitation. Bound proteins were detected by Western blotting.

5.10. Immunoprecipitation

For each immunoprecipitation 1 x 10^7 MDCK cells were electroporated with 10 µg of each Flag-actin and HA-MAL and seeded in a 10 cm ∅ plate to form a confluent monolayer. A medium exchange to fresh medium was performed 12 h later and another 24 h later the medium was replaced with either calcium reduced or normal medium as control. After the times desired the cells were lysed in 500 µL RIPA buffer containing protease and phosphatase inhibitors and the lysate was cleared by centrifugation at maximum speed at 4°C for 10 minutes. The resulting supernatant was combined with 20 µL TX-buffer washed Flag M2 agarose beads in 500 µL TX buffer and incubated on a rotating wheel at 4°C for 2 h. Afterwards the beads were pelleted at 3000 x g and 4°C for 5 minutes. To prepare the total lysate 50 µL of the supernatant were supplemented with 3x Laemmli buffer and frozen at -20°C. The rest of the supernatant was frozen at -80°C or discarded. The beads were washed three times in ice-cold TX-buffer and after the final aspiration resuspended in 20 µL 3 x Laemmli buffer. Afterwards they were, together with the total lysate, incubated at 95°C for 2 minutes, cooled on ice, spun down at 3000 x g for 5 minutes and analyzed by SDS-PAGE followed by western blotting.

5.11. Determination of the G- to F-actin ratio by ultracentrifugation

MDCK cell were seeded in a 6 cm plate to form a confluent monolayer. 24 h later the medium was exchanged to normal medium as control or reduced calcium medium. After the desired time cells were lysed in 750 µL UZ buffer on ice for 10 minutes. Thereafter the cells were scraped off, transferred into suitable polycarbonate tubes and centrifuged at 100,000 x g in a Beckman TL-100 Ultracentrifuge at 4°C for 1 h. 75 µL of the supernatant were transferred into Laemmli buffer giving the G-actin fraction. The rest of the supernatant was removed and the pellet resuspended in 750 µL UZ buffer, mixed with Laemmli buffer, sonicated for 10 seconds at maximum level in the sonicator Sonoplus HD70, giving the F-actin fraction. The G- to F-actin ratio was determined by Western blotting.

6. Immonufluorescence techniques

6.1. Immonofluorescence staining

Cells were seeded on uncoated glass coverslips (∅ = 12 mm) and the assay of interest was performed. Prior to fixation, the cells were washed twice in PBS on ice. This step was omitted when cells were stimulated and the wash would have influenced the result, e.g by washing out a drug or reversing a short lasting effect. Then, cells were fixed in 4% PFA for 10 – 15 minutes at RT and permeabilized for 10 minutes in 0.2% Triton X-100 in PBS. Alternatively, the cells were fixed and permeabilized by 2 minutes incubation in ice-cold methanol at -20°C followed by 3 rehydration washes in PBS. Unspecific epitopes were blocked by incubation for 30 minutes – 2 h in blocking solution. Then cells were incubated with the first antibody (VI.1.10.1) diluted as indicated in the Results section or according to manufacturer's instructions in blocking solution for 1 – 2 h. Afterwards cells were washed three times in PBS and incubated with the second antibody diluted as indicated in section VI.1.10.2 in blocking solution for 30 minutes – 1 h. If desired, labelled phalloidin or/and DAPI (2 µg/mL) or Hoechst 33258 (1 µg/mL) was/were incubated together with the second antibody. Thereafter cells were again washed 3 times in PBS followed by 1 short was in deionised water to

reduce salt effects and mounted with Mowiol (prepared according to Harlow and colleague (Harlow, 1999)) on a microscopic slide. Mowiol was allowed to harden prior to microscopic analysis for at least 1 hour.

6.2. Microscopy

6.2.1. Conventional immunofluorescence microscopy

Standard micrographs were taken using a Zeiss Axioplan 2 with MetaVue™ software. To allow direct comparability of different micrographs, all specimens within one experimental setup were stained in parallel and pictures were taken with the same exposure time without further computational calculations.

6.2.2. Confocal microscopy

Confocal microscopy was carried out on a Leica TCS SP2 AOBS confocal laser scanning microscope with SoftWoRx software. All specimens within one experimental setup were stained in parallel and pictures were taken with identical settings.

6.2.3. Life imaging

Life imaging was performed using a Zeiss Axiovert 200M microscope with MetaMorph™ software. The induction profile showing the time course of EGFP expression was calculated by subtracting the arbitrary fluorescence intensity at each time point in the *mock* experiment from the equivalent arbitrary fluorescence intensity upon calcium withdrawal.

VII. References

Abe, K., Rossman, K.L., Liu, B., Ritola, K.D., Chiang, D., Campbell, S.L., Burridge, K., and Der, C.J. (2000). Vav2 is an activator of Cdc42, Rac1, and RhoA. J Biol Chem *275*, 10141-10149.
Abe, K., and Takeichi, M. (2008). EPLIN mediates linkage of the cadherin catenin complex to F-actin and stabilizes the circumferential actin belt. Proc Natl Acad Sci U S A *105*, 13-19.
Adams, C.L., Chen, Y.T., Smith, S.J., and Nelson, W.J. (1998). Mechanisms of epithelial cell-cell adhesion and cell compaction revealed by high-resolution tracking of E-cadherin-green fluorescent protein. J Cell Biol *142*, 1105-1119.
Aguda, A.H., Burtnick, L.D., and Robinson, R.C. (2005). The state of the filament. EMBO Rep *6*, 220-226.
Amano, M., Ito, M., Kimura, K., Fukata, Y., Chihara, K., Nakano, T., Matsuura, Y., and Kaibuchi, K. (1996). Phosphorylation and activation of myosin by Rho-associated kinase (Rho-kinase). J Biol Chem *271*, 20246-20249.
Anderson, J.M., Van Itallie, C.M., and Fanning, A.S. (2004). Setting up a selective barrier at the apical junction complex. Curr Opin Cell Biol *16*, 140-145.
Arsenian, S., Weinhold, B., Oelgeschlager, M., Ruther, U., and Nordheim, A. (1998). Serum response factor is essential for mesoderm formation during mouse embryogenesis. Embo J *17*, 6289-6299.
Balcarova-Stander, J., Pfeiffer, S.E., Fuller, S.D., and Simons, K. (1984). Development of cell surface polarity in the epithelial Madin-Darby canine kidney (MDCK) cell line. Embo J *3*, 2687-2694.
Balda, M.S., Whitney, J.A., Flores, C., Gonzalez, S., Cereijido, M., and Matter, K. (1996). Functional dissociation of paracellular permeability and transepithelial electrical resistance and disruption of the apical-basolateral intramembrane diffusion barrier by expression of a mutant tight junction membrane protein. J Cell Biol *134*, 1031-1049.
Balzac, F., Avolio, M., Degani, S., Kaverina, I., Torti, M., Silengo, L., Small, J.V., and Retta, S.F. (2005). E-cadherin endocytosis regulates the activity of Rap1: a traffic light GTPase at the crossroads between cadherin and integrin function. J Cell Sci *118*, 4765-4783.
Bamburg, J.R. (1999). Proteins of the ADF/cofilin family: essential regulators of actin dynamics. Annu Rev Cell Dev Biol *15*, 185-230.
Barrios-Rodiles, M., Brown, K.R., Ozdamar, B., Bose, R., Liu, Z., Donovan, R.S., Shinjo, F., Liu, Y., Dembowy, J., Taylor, I.W., Luga, V., Przulj, N., Robinson, M., Suzuki, H., Hayashizaki, Y., Jurisica, I., and Wrana, J.L. (2005). High-throughput mapping of a dynamic signaling network in mammalian cells. Science *307*, 1621-1625.
Bear, J.E., Svitkina, T.M., Krause, M., Schafer, D.A., Loureiro, J.J., Strasser, G.A., Maly, I.V., Chaga, O.Y., Cooper, J.A., Borisy, G.G., and Gertler, F.B. (2002). Antagonism between Ena/VASP proteins and actin filament capping regulates fibroblast motility. Cell *109*, 509-521.
Beddington, R.S., and Smith, J.C. (1993). Control of vertebrate gastrulation: inducing signals and responding genes. Curr Opin Genet Dev *3*, 655-661.
Behrens, J., Vakaet, L., Friis, R., Winterhager, E., Van Roy, F., Mareel, M.M., and Birchmeier, W. (1993). Loss of epithelial differentiation and gain of invasiveness correlates with tyrosine phosphorylation of the E-cadherin/beta-catenin complex in cells transformed with a temperature-sensitive v-SRC gene. J Cell Biol *120*, 757-766.
Betson, M., Lozano, E., Zhang, J., and Braga, V.M. (2002). Rac activation upon cell-cell contact formation is dependent on signaling from the epidermal growth factor receptor. J Biol Chem *277*, 36962-36969.
Birchmeier, W., Brinkmann, V., Niemann, C., Meiners, S., DiCesare, S., Naundorf, H., and Sachs, M. (1997). Role of HGF/SF and c-Met in morphogenesis and metastasis of epithelial cells. Ciba Found Symp *212*, 230-240; discussion 240-236.
Blanchoin, L., Pollard, T.D., and Mullins, R.D. (2000). Interactions of ADF/cofilin, Arp2/3 complex, capping protein and profilin in remodeling of branched actin filament networks. Curr Biol *10*, 1273-1282.
Boggon, T.J., Murray, J., Chappuis-Flament, S., Wong, E., Gumbiner, B.M., and Shapiro, L. (2002). C-cadherin ectodomain structure and implications for cell adhesion mechanisms. Science *296*, 1308-1313.

Bolender, D.L., and Markwald, R.R. (1979). Epithelial-mesenchymal transformation in chick atrioventricular cushion morphogenesis. Scan Electron Microsc, 313-321.
Bos, J.L., Rehmann, H., and Wittinghofer, A. (2007). GEFs and GAPs: critical elements in the control of small G proteins. Cell *129*, 865-877.
Boyer, A.S., Ayerinskas, II, Vincent, E.B., McKinney, L.A., Weeks, D.L., and Runyan, R.B. (1999). TGFbeta2 and TGFbeta3 have separate and sequential activities during epithelial-mesenchymal cell transformation in the embryonic heart. Dev Biol *208*, 530-545.
Boyer, B., and Thiery, J.P. (1993). Epithelium-mesenchyme interconversion as example of epithelial plasticity. Apmis *101*, 257-268.
Bradford, M.M. (1976). A rapid and sensitive method for the quantitation of microgram quantities of protein utilizing the principle of protein-dye binding. Anal Biochem *72*, 248-254.
Braga, V.M. (2002). Cell-cell adhesion and signalling. Curr Opin Cell Biol *14*, 546-556.
Braga, V.M., Del Maschio, A., Machesky, L., and Dejana, E. (1999). Regulation of cadherin function by Rho and Rac: modulation by junction maturation and cellular context. Mol Biol Cell *10*, 9-22.
Braga, V.M., Machesky, L.M., Hall, A., and Hotchin, N.A. (1997). The small GTPases Rho and Rac are required for the establishment of cadherin-dependent cell-cell contacts. J Cell Biol *137*, 1421-1431.
Braga, V.M., and Yap, A.S. (2005). The challenges of abundance: epithelial junctions and small GTPase signalling. Curr Opin Cell Biol *17*, 466-474.
Brault, E., Gautreau, A., Lamarine, M., Callebaut, I., Thomas, G., and Goutebroze, L. (2001). Normal membrane localization and actin association of the NF2 tumor suppressor protein are dependent on folding of its N-terminal domain. J Cell Sci *114*, 1901-1912.
Brennan, J.K., Mansky, J., Roberts, G., and Lichtman, M.A. (1975). Improved methods for reducing calcium and magnesium concentrations in tissue culture medium: application to studies of lymphoblast proliferation in vitro. In Vitro *11*, 354-360.
Bubb, M.R., Senderowicz, A.M., Sausville, E.A., Duncan, K.L., and Korn, E.D. (1994). Jasplakinolide, a cytotoxic natural product, induces actin polymerization and competitively inhibits the binding of phalloidin to F-actin. J Biol Chem *269*, 14869-14871.
Burridge, K. (2006). Cell biology: a break in the chain? Nature *440*, 38-39.
Calautti, E., Grossi, M., Mammucari, C., Aoyama, Y., Pirro, M., Ono, Y., Li, J., and Dotto, G.P. (2002). Fyn tyrosine kinase is a downstream mediator of Rho/PRK2 function in keratinocyte cell-cell adhesion. J Cell Biol *156*, 137-148.
Capaldo, C.T., and Macara, I.G. (2007). Depletion of E-cadherin disrupts establishment but not maintenance of cell junctions in Madin-Darby canine kidney epithelial cells. Mol Biol Cell *18*, 189-200.
Carlier, M.F., Laurent, V., Santolini, J., Melki, R., Didry, D., Xia, G.X., Hong, Y., Chua, N.H., and Pantaloni, D. (1997). Actin depolymerizing factor (ADF/cofilin) enhances the rate of filament turnover: implication in actin-based motility. J Cell Biol *136*, 1307-1322.
Cavey, M., Rauzi, M., Lenne, P.F., and Lecuit, T. (2008). A two-tiered mechanism for stabilization and immobilization of E-cadherin. Nature *453*, 751-756.
Cereijido, M., Robbins, E., Sabatini, D.D., and Stefani, E. (1984). Cell-to-cell communication in monolayers of epithelioid cells (MDCK) as a function of the age of the monolayer. J Membr Biol *81*, 41-48.
Charrasse, S., Comunale, F., Fortier, M., Portales-Casamar, E., Debant, A., and Gauthier-Rouviere, C. (2007). M-cadherin activates Rac1 GTPase through the Rho-GEF trio during myoblast fusion. Mol Biol Cell *18*, 1734-1743.
Chen, C., Ware, S.M., Sato, A., Houston-Hawkins, D.E., Habas, R., Matzuk, M.M., Shen, M.M., and Brown, C.W. (2006). The Vg1-related protein Gdf3 acts in a Nodal signaling pathway in the pre-gastrulation mouse embryo. Development *133*, 319-329.
Chen, X., and Macara, I.G. (2005). Par-3 controls tight junction assembly through the Rac exchange factor Tiam1. Nat Cell Biol *7*, 262-269.
Chereau, D., Kerff, F., Graceffa, P., Grabarek, Z., Langsetmo, K., and Dominguez, R. (2005). Actin-bound structures of Wiskott-Aldrich syndrome protein (WASP)-homology domain 2 and the implications for filament assembly. Proc Natl Acad Sci U S A *102*, 16644-16649.
Chhabra, E.S., and Higgs, H.N. (2007). The many faces of actin: matching assembly factors with cellular structures. Nat Cell Biol *9*, 1110-1121.

Cooper, J.A. (1987). Effects of cytochalasin and phalloidin on actin. J Cell Biol *105*, 1473-1478.
Copeland, J.W., and Treisman, R. (2002). The diaphanous-related formin mDia1 controls serum response factor activity through its effects on actin polymerization. Mol Biol Cell *13*, 4088-4099.
Correia, A.C., Costa, M., Moraes, F., Bom, J., Novoa, A., and Mallo, M. (2007). Bmp2 is required for migration but not for induction of neural crest cells in the mouse. Dev Dyn *236*, 2493-2501.
Cox, R.T., Kirkpatrick, C., and Peifer, M. (1996). Armadillo is required for adherens junction assembly, cell polarity, and morphogenesis during Drosophila embryogenesis. J Cell Biol *134*, 133-148.
Cui, W., Fowlis, D.J., Bryson, S., Duffie, E., Ireland, H., Balmain, A., and Akhurst, R.J. (1996). TGFbeta1 inhibits the formation of benign skin tumors, but enhances progression to invasive spindle carcinomas in transgenic mice. Cell *86*, 531-542.
Dalton, S., and Treisman, R. (1992). Characterization of SAP-1, a protein recruited by serum response factor to the c-fos serum response element. Cell *68*, 597-612.
Davies, J.A. (1996). Mesenchyme to epithelium transition during development of the mammalian kidney tubule. Acta Anat (Basel) *156*, 187-201.
Dawes-Hoang, R.E., Parmar, K.M., Christiansen, A.E., Phelps, C.B., Brand, A.H., and Wieschaus, E.F. (2005). folded gastrulation, cell shape change and the control of myosin localization. Development *132*, 4165-4178.
de Rooij, J., Kerstens, A., Danuser, G., Schwartz, M.A., and Waterman-Storer, C.M. (2005). Integrin-dependent actomyosin contraction regulates epithelial cell scattering. J Cell Biol *171*, 153-164.
de Rooij, J., Zwartkruis, F.J., Verheijen, M.H., Cool, R.H., Nijman, S.M., Wittinghofer, A., and Bos, J.L. (1998). Epac is a Rap1 guanine-nucleotide-exchange factor directly activated by cyclic AMP. Nature *396*, 474-477.
Debant, A., Serra-Pages, C., Seipel, K., O'Brien, S., Tang, M., Park, S.H., and Streuli, M. (1996). The multidomain protein Trio binds the LAR transmembrane tyrosine phosphatase, contains a protein kinase domain, and has separate rac-specific and rho-specific guanine nucleotide exchange factor domains. Proc Natl Acad Sci U S A *93*, 5466-5471.
Diekmann, D., Brill, S., Garrett, M.D., Totty, N., Hsuan, J., Monfries, C., Hall, C., Lim, L., and Hall, A. (1991). Bcr encodes a GTPase-activating protein for p21rac. Nature *351*, 400-402.
Drees, F., Pokutta, S., Yamada, S., Nelson, W.J., and Weis, W.I. (2005). Alpha-catenin is a molecular switch that binds E-cadherin-beta-catenin and regulates actin-filament assembly. Cell *123*, 903-915.
Du, K.L., Chen, M., Li, J., Lepore, J.J., Mericko, P., and Parmacek, M.S. (2004). Megakaryoblastic leukemia factor-1 transduces cytoskeletal signals and induces smooth muscle cell differentiation from undifferentiated embryonic stem cells. J Biol Chem *279*, 17578-17586.
Duband, J.L., and Thiery, J.P. (1987). Distribution of laminin and collagens during avian neural crest development. Development *101*, 461-478.
Ebnet, K., Suzuki, A., Ohno, S., and Vestweber, D. (2004). Junctional adhesion molecules (JAMs): more molecules with dual functions? J Cell Sci *117*, 19-29.
Eden, S., Rohatgi, R., Podtelejnikov, A.V., Mann, M., and Kirschner, M.W. (2002). Mechanism of regulation of WAVE1-induced actin nucleation by Rac1 and Nck. Nature *418*, 790-793.
Edwards, D.C., Sanders, L.C., Bokoch, G.M., and Gill, G.N. (1999). Activation of LIM-kinase by Pak1 couples Rac/Cdc42 GTPase signalling to actin cytoskeletal dynamics. Nat Cell Biol *1*, 253-259.
Fan, L., Sebe, A., Peterfi, Z., Masszi, A., Thirone, A.C., Rotstein, O.D., Nakano, H., McCulloch, C.A., Szaszi, K., Mucsi, I., and Kapus, A. (2007). Cell contact-dependent regulation of epithelial-myofibroblast transition via the rho-rho kinase-phospho-myosin pathway. Mol Biol Cell *18*, 1083-1097.
Farquhar, M.G., and Palade, G.E. (1963). Junctional complexes in various epithelia. J Cell Biol *17*, 375-412.
Finck, H. (1968). On the discovery of actin. Science *160*, 332.
Fitchett, J.E., and Hay, E.D. (1989). Medial edge epithelium transforms to mesenchyme after embryonic palatal shelves fuse. Dev Biol *131*, 455-474.
Franco, C.A., Mericskay, M., Parlakian, A., Gary-Bobo, G., Gao-Li, J., Paulin, D., Gustafsson, E., and Li, Z. (2008). Serum response factor is required for sprouting angiogenesis and vascular integrity. Dev Cell *15*, 448-461.

Fukuhara, T., Shimizu, K., Kawakatsu, T., Fukuyama, T., Minami, Y., Honda, T., Hoshino, T., Yamada, T., Ogita, H., Okada, M., and Takai, Y. (2004). Activation of Cdc42 by trans interactions of the cell adhesion molecules nectins through c-Src and Cdc42-GEF FRG. J Cell Biol *166*, 393-405.
Fukuyama, T., Ogita, H., Kawakatsu, T., Fukuhara, T., Yamada, T., Sato, T., Shimizu, K., Nakamura, T., Matsuda, M., and Takai, Y. (2005). Involvement of the c-Src-Crk-C3G-Rap1 signaling in the nectin-induced activation of Cdc42 and formation of adherens junctions. J Biol Chem *280*, 815-825.
Fukuyama, T., Ogita, H., Kawakatsu, T., Inagaki, M., and Takai, Y. (2006). Activation of Rac by cadherin through the c-Src-Rap1-phosphatidylinositol 3-kinase-Vav2 pathway. Oncogene *25*, 8-19.
Furuse, M., and Tsukita, S. (2006). Claudins in occluding junctions of humans and flies. Trends Cell Biol *16*, 181-188.
Gates, J., and Peifer, M. (2005). Can 1000 reviews be wrong? Actin, alpha-Catenin, and adherens junctions. Cell *123*, 769-772.
Gaush, C.R., Hard, W.L., and Smith, T.F. (1966). Characterization of an established line of canine kidney cells (MDCK). Proc Soc Exp Biol Med *122*, 931-935.
Geneste, O., Copeland, J.W., and Treisman, R. (2002). LIM kinase and Diaphanous cooperate to regulate serum response factor and actin dynamics. J Cell Biol *157*, 831-838.
Genth, H., Dreger, S.C., Huelsenbeck, J., and Just, I. (2008). Clostridium difficile toxins: more than mere inhibitors of Rho proteins. Int J Biochem Cell Biol *40*, 592-597.
Gherardi, E., Gray, J., Stoker, M., Perryman, M., and Furlong, R. (1989). Purification of scatter factor, a fibroblast-derived basic protein that modulates epithelial interactions and movement. Proc Natl Acad Sci U S A *86*, 5844-5848.
Gilman, M.Z., Wilson, R.N., and Weinberg, R.A. (1986). Multiple protein-binding sites in the 5'-flanking region regulate c-fos expression. Mol Cell Biol *6*, 4305-4316.
Gineitis, D., and Treisman, R. (2001). Differential usage of signal transduction pathways defines two types of serum response factor target gene. J Biol Chem *276*, 24531-24539.
Goley, E.D., and Welch, M.D. (2006). The ARP2/3 complex: an actin nucleator comes of age. Nat Rev Mol Cell Biol *7*, 713-726.
Gonzalez-Mariscal, L., Chavez de Ramirez, B., and Cereijido, M. (1985). Tight junction formation in cultured epithelial cells (MDCK). J Membr Biol *86*, 113-125.
Gooding, J.M., Yap, K.L., and Ikura, M. (2004). The cadherin-catenin complex as a focal point of cell adhesion and signalling: new insights from three-dimensional structures. Bioessays *26*, 497-511.
Gotzmann, J., Huber, H., Thallinger, C., Wolschek, M., Jansen, B., Schulte-Hermann, R., Beug, H., and Mikulits, W. (2002). Hepatocytes convert to a fibroblastoid phenotype through the cooperation of TGF-beta1 and Ha-Ras: steps towards invasiveness. J Cell Sci *115*, 1189-1202.
Gould, K.L., Bretscher, A., Esch, F.S., and Hunter, T. (1989). cDNA cloning and sequencing of the protein-tyrosine kinase substrate, ezrin, reveals homology to band 4.1. Embo J *8*, 4133-4142.
Green, K.J., and Simpson, C.L. (2007). Desmosomes: new perspectives on a classic. J Invest Dermatol *127*, 2499-2515.
Gronholm, M., Sainio, M., Zhao, F., Heiska, L., Vaheri, A., and Carpen, O. (1999). Homotypic and heterotypic interaction of the neurofibromatosis 2 tumor suppressor protein merlin and the ERM protein ezrin. J Cell Sci *112 (Pt 6)*, 895-904.
Grosse, R., Copeland, J.W., Newsome, T.P., Way, M., and Treisman, R. (2003). A role for VASP in RhoA-Diaphanous signalling to actin dynamics and SRF activity. Embo J *22*, 3050-3061.
Grunert, S., Jechlinger, M., and Beug, H. (2003). Diverse cellular and molecular mechanisms contribute to epithelial plasticity and metastasis. Nat Rev Mol Cell Biol *4*, 657-665.
Guettler, S., Vartiainen, M.K., Miralles, F., Larijani, B., and Treisman, R. (2008). RPEL motifs link the serum response factor cofactor MAL but not myocardin to Rho signaling via actin binding. Mol Cell Biol *28*, 732-742.
Gumbiner, B., Stevenson, B., and Grimaldi, A. (1988). The role of the cell adhesion molecule uvomorulin in the formation and maintenance of the epithelial junctional complex. J Cell Biol *107*, 1575-1587.
Gumbiner, B.M. (2005). Regulation of cadherin-mediated adhesion in morphogenesis. Nat Rev Mol Cell Biol *6*, 622-634.
Halliburton, W.D. (1887). On Muscle-Plasma. J Physiol *8*, 133-202.
Hansson, G.C., Simons, K., and van Meer, G. (1986). Two strains of the Madin-Darby canine kidney (MDCK) cell line have distinct glycosphingolipid compositions. Embo J *5*, 483-489.

Harlow, E.L., D. (1999). Using Antibodies - A Laboratory Manual.
Hartsock, A., and Nelson, W.J. (2008). Adherens and tight junctions: structure, function and connections to the actin cytoskeleton. Biochim Biophys Acta *1778*, 660-669.
Haussinger, D., Ahrens, T., Aberle, T., Engel, J., Stetefeld, J., and Grzesiek, S. (2004). Proteolytic E-cadherin activation followed by solution NMR and X-ray crystallography. Embo J *23*, 1699-1708.
Hay, E.D. (1995). An overview of epithelio-mesenchymal transformation. Acta Anat (Basel) *154*, 8-20.
Helwani, F.M., Kovacs, E.M., Paterson, A.D., Verma, S., Ali, R.G., Fanning, A.S., Weed, S.A., and Yap, A.S. (2004). Cortactin is necessary for E-cadherin-mediated contact formation and actin reorganization. J Cell Biol *164*, 899-910.
Higashida, C., Miyoshi, T., Fujita, A., Oceguera-Yanez, F., Monypenny, J., Andou, Y., Narumiya, S., and Watanabe, N. (2004). Actin polymerization-driven molecular movement of mDia1 in living cells. Science *303*, 2007-2010.
Hill, C.S., and Treisman, R. (1995). Differential activation of c-fos promoter elements by serum, lysophosphatidic acid, G proteins and polypeptide growth factors. Embo J *14*, 5037-5047.
Hill, C.S., Wynne, J., and Treisman, R. (1995). The Rho family GTPases RhoA, Rac1, and CDC42Hs regulate transcriptional activation by SRF. Cell *81*, 1159-1170.
Hinck, L., Nathke, I.S., Papkoff, J., and Nelson, W.J. (1994). Dynamics of cadherin/catenin complex formation: novel protein interactions and pathways of complex assembly. J Cell Biol *125*, 1327-1340.
Hipskind, R.A., Rao, V.N., Mueller, C.G., Reddy, E.S., and Nordheim, A. (1991). Ets-related protein Elk-1 is homologous to the c-fos regulatory factor p62TCF. Nature *354*, 531-534.
Huelsenbeck, J., Dreger, S., Gerhard, R., Barth, H., Just, I., and Genth, H. (2007). Difference in the cytotoxic effects of toxin B from Clostridium difficile strain VPI 10463 and toxin B from variant Clostridium difficile strain 1470. Infect Immun *75*, 801-809.
Huttenlocher, A., Ginsberg, M.H., and Horwitz, A.F. (1996). Modulation of cell migration by integrin-mediated cytoskeletal linkages and ligand-binding affinity. J Cell Biol *134*, 1551-1562.
Ikeda, W., Nakanishi, H., Miyoshi, J., Mandai, K., Ishizaki, H., Tanaka, M., Togawa, A., Takahashi, K., Nishioka, H., Yoshida, H., Mizoguchi, A., Nishikawa, S., and Takai, Y. (1999). Afadin: A key molecule essential for structural organization of cell-cell junctions of polarized epithelia during embryogenesis. J Cell Biol *146*, 1117-1132.
Ikenouchi, J., Umeda, K., Tsukita, S., Furuse, M., and Tsukita, S. (2007). Requirement of ZO-1 for the formation of belt-like adherens junctions during epithelial cell polarization. J Cell Biol *176*, 779-786.
Imamura, Y., Itoh, M., Maeno, Y., Tsukita, S., and Nagafuchi, A. (1999). Functional domains of alpha-catenin required for the strong state of cadherin-based cell adhesion. J Cell Biol *144*, 1311-1322.
Innocenti, M., Zucconi, A., Disanza, A., Frittoli, E., Areces, L.B., Steffen, A., Stradal, T.E., Di Fiore, P.P., Carlier, M.F., and Scita, G. (2004). Abi1 is essential for the formation and activation of a WAVE2 signalling complex. Nat Cell Biol *6*, 319-327.
Ireton, R.C., Davis, M.A., van Hengel, J., Mariner, D.J., Barnes, K., Thoreson, M.A., Anastasiadis, P.Z., Matrisian, L., Bundy, L.M., Sealy, L., Gilbert, B., van Roy, F., and Reynolds, A.B. (2002). A novel role for p120 catenin in E-cadherin function. J Cell Biol *159*, 465-476.
Irie, K., Shimizu, K., Sakisaka, T., Ikeda, W., and Takai, Y. (2004). Roles and modes of action of nectins in cell-cell adhesion. Semin Cell Dev Biol *15*, 643-656.
Ishihara, H., Martin, B.L., Brautigan, D.L., Karaki, H., Ozaki, H., Kato, Y., Fusetani, N., Watabe, S., Hashimoto, K., Uemura, D., and et al. (1989). Calyculin A and okadaic acid: inhibitors of protein phosphatase activity. Biochem Biophys Res Commun *159*, 871-877.
Ishizaki, T., Maekawa, M., Fujisawa, K., Okawa, K., Iwamatsu, A., Fujita, A., Watanabe, N., Saito, Y., Kakizuka, A., Morii, N., and Narumiya, S. (1996). The small GTP-binding protein Rho binds to and activates a 160 kDa Ser/Thr protein kinase homologous to myotonic dystrophy kinase. Embo J *15*, 1885-1893.
Itoh, M., Nagafuchi, A., Moroi, S., and Tsukita, S. (1997). Involvement of ZO-1 in cadherin-based cell adhesion through its direct binding to alpha catenin and actin filaments. J Cell Biol *138*, 181-192.
Ivanov, A.I., McCall, I.C., Parkos, C.A., and Nusrat, A. (2004). Role for actin filament turnover and a myosin II motor in cytoskeleton-driven disassembly of the epithelial apical junctional complex. Mol Biol Cell *15*, 2639-2651.
Ivanov, A.I., Nusrat, A., and Parkos, C.A. (2004). Endocytosis of epithelial apical junctional proteins by a clathrin-mediated pathway into a unique storage compartment. Mol Biol Cell *15*, 176-188.

Izumi, G., Sakisaka, T., Baba, T., Tanaka, S., Morimoto, K., and Takai, Y. (2004). Endocytosis of E-cadherin regulated by Rac and Cdc42 small G proteins through IQGAP1 and actin filaments. J Cell Biol *166*, 237-248.
James, M.F., Manchanda, N., Gonzalez-Agosti, C., Hartwig, J.H., and Ramesh, V. (2001). The neurofibromatosis 2 protein product merlin selectively binds F-actin but not G-actin, and stabilizes the filaments through a lateral association. Biochem J *356*, 377-386.
Janda, E., Lehmann, K., Killisch, I., Jechlinger, M., Herzig, M., Downward, J., Beug, H., and Grunert, S. (2002). Ras and TGF[beta] cooperatively regulate epithelial cell plasticity and metastasis: dissection of Ras signaling pathways. J Cell Biol *156*, 299-313.
Jechlinger, M., Grunert, S., and Beug, H. (2002). Mechanisms in epithelial plasticity and metastasis: insights from 3D cultures and expression profiling. J Mammary Gland Biol Neoplasia *7*, 415-432.
Jou, T.S., and Nelson, W.J. (1998). Effects of regulated expression of mutant RhoA and Rac1 small GTPases on the development of epithelial (MDCK) cell polarity. J Cell Biol *142*, 85-100.
Just, I., Selzer, J., Wilm, M., von Eichel-Streiber, C., Mann, M., and Aktories, K. (1995). Glucosylation of Rho proteins by Clostridium difficile toxin B. Nature *375*, 500-503.
Just, I., Wilm, M., Selzer, J., Rex, G., von Eichel-Streiber, C., Mann, M., and Aktories, K. (1995). The enterotoxin from Clostridium difficile (ToxA) monoglucosylates the Rho proteins. J Biol Chem *270*, 13932-13936.
Kartenbeck, J., Schmid, E., Franke, W.W., and Geiger, B. (1982). Different modes of internalization of proteins associated with adhaerens junctions and desmosomes: experimental separation of lateral contacts induces endocytosis of desmosomal plaque material. Embo J *1*, 725-732.
Katoh, K., Kano, Y., Amano, M., Onishi, H., Kaibuchi, K., and Fujiwara, K. (2001). Rho-kinase--mediated contraction of isolated stress fibers. J Cell Biol *153*, 569-584.
Khosravi-Far, R., Solski, P.A., Clark, G.J., Kinch, M.S., and Der, C.J. (1995). Activation of Rac1, RhoA, and mitogen-activated protein kinases is required for Ras transformation. Mol Cell Biol *15*, 6443-6453.
Kim, S.H., Li, Z., and Sacks, D.B. (2000). E-cadherin-mediated cell-cell attachment activates Cdc42. J Biol Chem *275*, 36999-37005.
Kimelman, D. (2006). Mesoderm induction: from caps to chips. Nat Rev Genet *7*, 360-372.
Kimura, K., Ito, M., Amano, M., Chihara, K., Fukata, Y., Nakafuku, M., Yamamori, B., Feng, J., Nakano, T., Okawa, K., Iwamatsu, A., and Kaibuchi, K. (1996). Regulation of myosin phosphatase by Rho and Rho-associated kinase (Rho-kinase). Science *273*, 245-248.
Kinley, A.W., Weed, S.A., Weaver, A.M., Karginov, A.V., Bissonette, E., Cooper, J.A., and Parsons, J.T. (2003). Cortactin interacts with WIP in regulating Arp2/3 activation and membrane protrusion. Curr Biol *13*, 384-393.
Kissil, J.L., Wilker, E.W., Johnson, K.C., Eckman, M.S., Yaffe, M.B., and Jacks, T. (2003). Merlin, the product of the Nf2 tumor suppressor gene, is an inhibitor of the p21-activated kinase, Pak1. Mol Cell *12*, 841-849.
Kitazawa, T., Eto, M., Woodsome, T.P., and Brautigan, D.L. (2000). Agonists trigger G protein-mediated activation of the CPI-17 inhibitor phosphoprotein of myosin light chain phosphatase to enhance vascular smooth muscle contractility. J Biol Chem *275*, 9897-9900.
Kobielak, A., and Fuchs, E. (2004). Alpha-catenin: at the junction of intercellular adhesion and actin dynamics. Nat Rev Mol Cell Biol *5*, 614-625.
Kobielak, A., Pasolli, H.A., and Fuchs, E. (2004). Mammalian formin-1 participates in adherens junctions and polymerization of linear actin cables. Nat Cell Biol *6*, 21-30.
Kodama, A., Takaishi, K., Nakano, K., Nishioka, H., and Takai, Y. (1999). Involvement of Cdc42 small G protein in cell-cell adhesion, migration and morphology of MDCK cells. Oncogene *18*, 3996-4006.
Kooistra, M.R., Dube, N., and Bos, J.L. (2007). Rap1: a key regulator in cell-cell junction formation. J Cell Sci *120*, 17-22.
Kovacs, E.M., Ali, R.G., McCormack, A.J., and Yap, A.S. (2002). E-cadherin homophilic ligation directly signals through Rac and phosphatidylinositol 3-kinase to regulate adhesive contacts. J Biol Chem *277*, 6708-6718.
Kovacs, E.M., Goodwin, M., Ali, R.G., Paterson, A.D., and Yap, A.S. (2002). Cadherin-directed actin assembly: E-cadherin physically associates with the Arp2/3 complex to direct actin assembly in nascent adhesive contacts. Curr Biol *12*, 379-382.

Kovacs, M., Toth, J., Hetenyi, C., Malnasi-Csizmadia, A., and Sellers, J.R. (2004). Mechanism of blebbistatin inhibition of myosin II. J Biol Chem *279*, 35557-35563.
Kovar, D.R. (2006). Molecular details of formin-mediated actin assembly. Curr Opin Cell Biol *18*, 11-17.
Koyama, M., Ito, M., Feng, J., Seko, T., Shiraki, K., Takase, K., Hartshorne, D.J., and Nakano, T. (2000). Phosphorylation of CPI-17, an inhibitory phosphoprotein of smooth muscle myosin phosphatase, by Rho-kinase. FEBS Lett *475*, 197-200.
Laemmli, U.K. (1970). Cleavage of structural proteins during the assembly of the head of bacteriophage T4. Nature *227*, 680-685.
Lallemand, D., Curto, M., Saotome, I., Giovannini, M., and McClatchey, A.I. (2003). NF2 deficiency promotes tumorigenesis and metastasis by destabilizing adherens junctions. Genes Dev *17*, 1090-1100.
Lammers, M., Rose, R., Scrima, A., and Wittinghofer, A. (2005). The regulation of mDia1 by autoinhibition and its release by Rho*GTP. Embo J *24*, 4176-4187.
Lauffenburger, D.A., and Horwitz, A.F. (1996). Cell migration: a physically integrated molecular process. Cell *84*, 359-369.
Lazarides, E. (1975). Tropomyosin antibody: the specific localization of tropomyosin in nonmuscle cells. J Cell Biol *65*, 549-561.
Lazarides, E., and Burridge, K. (1975). Alpha-actinin: immunofluorescent localization of a muscle structural protein in nonmuscle cells. Cell *6*, 289-298.
Lee, J., and Jacobson, K. (1997). The composition and dynamics of cell-substratum adhesions in locomoting fish keratocytes. J Cell Sci *110 (Pt 22)*, 2833-2844.
Lehmann, K., Janda, E., Pierreux, C.E., Rytomaa, M., Schulze, A., McMahon, M., Hill, C.S., Beug, H., and Downward, J. (2000). Raf induces TGFbeta production while blocking its apoptotic but not invasive responses: a mechanism leading to increased malignancy in epithelial cells. Genes Dev *14*, 2610-2622.
Leung, T., Chen, X.Q., Manser, E., and Lim, L. (1996). The p160 RhoA-binding kinase ROK alpha is a member of a kinase family and is involved in the reorganization of the cytoskeleton. Mol Cell Biol *16*, 5313-5327.
Leung, T., Manser, E., Tan, L., and Lim, L. (1995). A novel serine/threonine kinase binding the Ras-related RhoA GTPase which translocates the kinase to peripheral membranes. J Biol Chem *270*, 29051-29054.
MacDonald, J.A., Borman, M.A., Muranyi, A., Somlyo, A.V., Hartshorne, D.J., and Haystead, T.A. (2001). Identification of the endogenous smooth muscle myosin phosphatase-associated kinase. Proc Natl Acad Sci U S A *98*, 2419-2424.
MacDonald, J.A., Eto, M., Borman, M.A., Brautigan, D.L., and Haystead, T.A. (2001). Dual Ser and Thr phosphorylation of CPI-17, an inhibitor of myosin phosphatase, by MYPT-associated kinase. FEBS Lett *493*, 91-94.
Machesky, L.M., Atkinson, S.J., Ampe, C., Vandekerckhove, J., and Pollard, T.D. (1994). Purification of a cortical complex containing two unconventional actins from Acanthamoeba by affinity chromatography on profilin-agarose. J Cell Biol *127*, 107-115.
Machesky, L.M., and Insall, R.H. (1998). Scar1 and the related Wiskott-Aldrich syndrome protein, WASP, regulate the actin cytoskeleton through the Arp2/3 complex. Curr Biol *8*, 1347-1356.
Maeda, M., Matsui, T., Imamura, M., Tsukita, S., and Tsukita, S. (1999). Expression level, subcellular distribution and rho-GDI binding affinity of merlin in comparison with Ezrin/Radixin/Moesin proteins. Oncogene *18*, 4788-4797.
Mallavarapu, A., and Mitchison, T. (1999). Regulated actin cytoskeleton assembly at filopodium tips controls their extension and retraction. J Cell Biol *146*, 1097-1106.
Malliri, A., van Es, S., Huveneers, S., and Collard, J.G. (2004). The Rac exchange factor Tiam1 is required for the establishment and maintenance of cadherin-based adhesions. J Biol Chem *279*, 30092-30098.
Manchanda, N., Lyubimova, A., Ho, H.Y., James, M.F., Gusella, J.F., Ramesh, N., Snapper, S.B., and Ramesh, V. (2005). The NF2 tumor suppressor Merlin and the ERM proteins interact with N-WASP and regulate its actin polymerization function. J Biol Chem *280*, 12517-12522.
Mandell, K.J., Babbin, B.A., Nusrat, A., and Parkos, C.A. (2005). Junctional adhesion molecule 1 regulates epithelial cell morphology through effects on beta1 integrins and Rap1 activity. J Biol Chem *280*, 11665-11674.

Manser, E., Leung, T., Salihuddin, H., Zhao, Z.S., and Lim, L. (1994). A brain serine/threonine protein kinase activated by Cdc42 and Rac1. Nature *367*, 40-46.
Markwald, R.R., Fitzharris, T.P., and Manasek, F.J. (1977). Structural development of endocardial cushions. Am J Anat *148*, 85-119.
Martinez-Palomo, A., Meza, I., Beaty, G., and Cereijido, M. (1980). Experimental modulation of occluding junctions in a cultured transporting epithelium. J Cell Biol *87*, 736-745.
Martins-Green, M., and Erickson, C.A. (1987). Basal lamina is not a barrier to neural crest cell emigration: documentation by TEM and by immunofluorescent and immunogold labelling. Development *101*, 517-533.
McDowell, N., and Gurdon, J.B. (1999). Activin as a morphogen in Xenopus mesoderm induction. Semin Cell Dev Biol *10*, 311-317.
McGough, A., Pope, B., Chiu, W., and Weeds, A. (1997). Cofilin changes the twist of F-actin: implications for actin filament dynamics and cellular function. J Cell Biol *138*, 771-781.
Mege, R.M., Gavard, J., and Lambert, M. (2006). Regulation of cell-cell junctions by the cytoskeleton. Curr Opin Cell Biol *18*, 541-548.
Minato, H., and Katayama, T. (1970). SStudies on the metabolites of Zygosporium masonii. II. Structures of zygosporins D, E, F, and G. J Chem Soc [Perkin 1] *1*, 45-47.
Miralles, F., Posern, G., Zaromytidou, A.I., and Treisman, R. (2003). Actin dynamics control SRF activity by regulation of its coactivator MAL. Cell *113*, 329-342.
Miyoshi, J., and Takai, Y. (2008). Structural and functional associations of apical junctions with cytoskeleton. Biochim Biophys Acta *1778*, 670-691.
Mockrin, S.C., and Korn, E.D. (1980). Acanthamoeba profilin interacts with G-actin to increase the rate of exchange of actin-bound adenosine 5'-triphosphate. Biochemistry *19*, 5359-5362.
Morita, T., Mayanagi, T., and Sobue, K. (2007). Dual roles of myocardin-related transcription factors in epithelial mesenchymal transition via slug induction and actin remodeling. J Cell Biol *179*, 1027-1042.
Mullis, K.B., and Faloona, F.A. (1987). Specific synthesis of DNA in vitro via a polymerase-catalyzed chain reaction. Methods Enzymol *155*, 335-350.
Munevar, S., Wang, Y.L., and Dembo, M. (2004). Regulation of mechanical interactions between fibroblasts and the substratum by stretch-activated Ca2+ entry. J Cell Sci *117*, 85-92.
Murata-Hori, M., Suizu, F., Iwasaki, T., Kikuchi, A., and Hosoya, H. (1999). ZIP kinase identified as a novel myosin regulatory light chain kinase in HeLa cells. FEBS Lett *451*, 81-84.
Nagafuchi, A., Ishihara, S., and Tsukita, S. (1994). The roles of catenins in the cadherin-mediated cell adhesion: functional analysis of E-cadherin-alpha catenin fusion molecules. J Cell Biol *127*, 235-245.
Nakagawa, M., Fukata, M., Yamaga, M., Itoh, N., and Kaibuchi, K. (2001). Recruitment and activation of Rac1 by the formation of E-cadherin-mediated cell-cell adhesion sites. J Cell Sci *114*, 1829-1838.
Nakas, M., Higashino, S., and Loewenstein, W.R. (1966). Uncoupling of an epithelial cell membrane junction by calcium-ion removal. Science *151*, 89-91.
Nathke, I.S., Hinck, L., Swedlow, J.R., Papkoff, J., and Nelson, W.J. (1994). Defining interactions and distributions of cadherin and catenin complexes in polarized epithelial cells. J Cell Biol *125*, 1341-1352.
Nichols, D.H. (1981). Neural crest formation in the head of the mouse embryo as observed using a new histological technique. J Embryol Exp Morphol *64*, 105-120.
Nishimura, T., Yamaguchi, T., Kato, K., Yoshizawa, M., Nabeshima, Y., Ohno, S., Hoshino, M., and Kaibuchi, K. (2005). PAR-6-PAR-3 mediates Cdc42-induced Rac activation through the Rac GEFs STEF/Tiam1. Nat Cell Biol *7*, 270-277.
Nobes, C.D., and Hall, A. (1995). Rho, rac, and cdc42 GTPases regulate the assembly of multimolecular focal complexes associated with actin stress fibers, lamellipodia, and filopodia. Cell *81*, 53-62.
Noren, N.K., Liu, B.P., Burridge, K., and Kreft, B. (2000). p120 catenin regulates the actin cytoskeleton via Rho family GTPases. J Cell Biol *150*, 567-580.
Noren, N.K., Niessen, C.M., Gumbiner, B.M., and Burridge, K. (2001). Cadherin engagement regulates Rho family GTPases. J Biol Chem *276*, 33305-33308.
Oft, M., Heider, K.H., and Beug, H. (1998). TGFbeta signaling is necessary for carcinoma cell invasiveness and metastasis. Curr Biol *8*, 1243-1252.

Oft, M., Peli, J., Rudaz, C., Schwarz, H., Beug, H., and Reichmann, E. (1996). TGF-beta1 and Ha-Ras collaborate in modulating the phenotypic plasticity and invasiveness of epithelial tumor cells. Genes Dev *10*, 2462-2477.
Ozdamar, B., Bose, R., Barrios-Rodiles, M., Wang, H.R., Zhang, Y., and Wrana, J.L. (2005). Regulation of the polarity protein Par6 by TGFbeta receptors controls epithelial cell plasticity. Science *307*, 1603-1609.
Patel, S.D., Ciatto, C., Chen, C.P., Bahna, F., Rajebhosale, M., Arkus, N., Schieren, I., Jessell, T.M., Honig, B., Price, S.R., and Shapiro, L. (2006). Type II cadherin ectodomain structures: implications for classical cadherin specificity. Cell *124*, 1255-1268.
Peifer, M. (1993). The product of the Drosophila segment polarity gene armadillo is part of a multi-protein complex resembling the vertebrate adherens junction. J Cell Sci *105 (Pt 4)*, 993-1000.
Pellegrin, S., and Mellor, H. (2007). Actin stress fibres. J Cell Sci *120*, 3491-3499.
Peng, J., Wallar, B.J., Flanders, A., Swiatek, P.J., and Alberts, A.S. (2003). Disruption of the Diaphanous-related formin Drf1 gene encoding mDia1 reveals a role for Drf3 as an effector for Cdc42. Curr Biol *13*, 534-545.
Peracchia, C., and Peracchia, L.L. (1980). Gap junction dynamics: reversible effects of divalent cations. J Cell Biol *87*, 708-718.
Perez-Moreno, M., Davis, M.A., Wong, E., Pasolli, H.A., Reynolds, A.B., and Fuchs, E. (2006). p120-catenin mediates inflammatory responses in the skin. Cell *124*, 631-644.
Perez-Moreno, M., and Fuchs, E. (2006). Catenins: keeping cells from getting their signals crossed. Dev Cell *11*, 601-612.
Pipes, G.C., Creemers, E.E., and Olson, E.N. (2006). The myocardin family of transcriptional coactivators: versatile regulators of cell growth, migration, and myogenesis. Genes Dev *20*, 1545-1556.
Pollard, T.D., and Borisy, G.G. (2003). Cellular motility driven by assembly and disassembly of actin filaments. Cell *112*, 453-465.
Posern, G., Miralles, F., Guettler, S., and Treisman, R. (2004). Mutant actins that stabilise F-actin use distinct mechanisms to activate the SRF coactivator MAL. Embo J *23*, 3973-3983.
Posern, G., Rapp, U.R., and Feller, S.M. (2000). The Crk signaling pathway contributes to the bombesin-induced activation of the small GTPase Rap1 in Swiss 3T3 cells. Oncogene *19*, 6361-6368.
Posern, G., Sotiropoulos, A., and Treisman, R. (2002). Mutant actins demonstrate a role for unpolymerized actin in control of transcription by serum response factor. Mol Biol Cell *13*, 4167-4178.
Posern, G., and Treisman, R. (2006). Actin' together: serum response factor, its cofactors and the link to signal transduction. Trends Cell Biol *16*, 588-596.
Potempa, S., and Ridley, A.J. (1998). Activation of both MAP kinase and phosphatidylinositide 3-kinase by Ras is required for hepatocyte growth factor/scatter factor-induced adherens junction disassembly. Mol Biol Cell *9*, 2185-2200.
Prehoda, K.E., Scott, J.A., Mullins, R.D., and Lim, W.A. (2000). Integration of multiple signals through cooperative regulation of the N-WASP-Arp2/3 complex. Science *290*, 801-806.
Price, M.A., Rogers, A.E., and Treisman, R. (1995). Comparative analysis of the ternary complex factors Elk-1, SAP-1a and SAP-2 (ERP/NET). Embo J *14*, 2589-2601.
Pruyne, D., Evangelista, M., Yang, C., Bi, E., Zigmond, S., Bretscher, A., and Boone, C. (2002). Role of formins in actin assembly: nucleation and barbed-end association. Science *297*, 612-615.
Prywes, R., and Roeder, R.G. (1986). Inducible binding of a factor to the c-fos enhancer. Cell *47*, 777-784.
Pujuguet, P., Del Maestro, L., Gautreau, A., Louvard, D., and Arpin, M. (2003). Ezrin regulates E-cadherin-dependent adherens junction assembly through Rac1 activation. Mol Biol Cell *14*, 2181-2191.
Qin, Y., Capaldo, C., Gumbiner, B.M., and Macara, I.G. (2005). The mammalian Scribble polarity protein regulates epithelial cell adhesion and migration through E-cadherin. J Cell Biol *171*, 1061-1071.
Quinlan, M.P., and Hyatt, J.L. (1999). Establishment of the circumferential actin filament network is a prerequisite for localization of the cadherin-catenin complex in epithelial cells. Cell Growth Differ *10*, 839-854.

Raible, D.W. (2006). Development of the neural crest: achieving specificity in regulatory pathways. Curr Opin Cell Biol *18*, 698-703.
Rampal, A.L., Pinkofsky, H.B., and Jung, C.Y. (1980). Structure of cytochalasins and cytochalasin B binding sites in human erythrocyte membranes. Biochemistry *19*, 679-683.
Ren, X.D., Kiosses, W.B., and Schwartz, M.A. (1999). Regulation of the small GTP-binding protein Rho by cell adhesion and the cytoskeleton. Embo J *18*, 578-585.
Ren, X.D., and Schwartz, M.A. (2000). Determination of GTP loading on Rho. Methods Enzymol *325*, 264-272.
Resjo, S., Oknianska, A., Zolnierowicz, S., Manganiello, V., and Degerman, E. (1999). Phosphorylation and activation of phosphodiesterase type 3B (PDE3B) in adipocytes in response to serine/threonine phosphatase inhibitors: deactivation of PDE3B in vitro by protein phosphatase type 2A. Biochem J *341 (Pt 3)*, 839-845.
Richardson, J.C., Scalera, V., and Simmons, N.L. (1981). Identification of two strains of MDCK cells which resemble separate nephron tubule segments. Biochim Biophys Acta *673*, 26-36.
Robertson, J.D. (1963). The Occurrence Of A Subunit Pattern In The Unit Membranes Of Club Endings In Mauthner Cell Synapses In Goldfish Brains. J Cell Biol *19*, 201-221.
Rohatgi, R., Ho, H.Y., and Kirschner, M.W. (2000). Mechanism of N-WASP activation by CDC42 and phosphatidylinositol 4, 5-bisphosphate. J Cell Biol *150*, 1299-1310.
Rose, R., Weyand, M., Lammers, M., Ishizaki, T., Ahmadian, M.R., and Wittinghofer, A. (2005). Structural and mechanistic insights into the interaction between Rho and mammalian Dia. Nature *435*, 513-518.
Rosenblatt, J., Peluso, P., and Mitchison, T.J. (1995). The bulk of unpolymerized actin in Xenopus egg extracts is ATP-bound. Mol Biol Cell *6*, 227-236.
Rothen-Rutishauser, B., Riesen, F.K., Braun, A., Gunthert, M., and Wunderli-Allenspach, H. (2002). Dynamics of tight and adherens junctions under EGTA treatment. J Membr Biol *188*, 151-162.
Rottner, K., Hall, A., and Small, J.V. (1999). Interplay between Rac and Rho in the control of substrate contact dynamics. Curr Biol *9*, 640-648.
Rouleau, G.A., Merel, P., Lutchman, M., Sanson, M., Zucman, J., Marineau, C., Hoang-Xuan, K., Demczuk, S., Desmaze, C., Plougastel, B., and et al. (1993). Alteration in a new gene encoding a putative membrane-organizing protein causes neuro-fibromatosis type 2. Nature *363*, 515-521.
Royal, I., and Park, M. (1995). Hepatocyte growth factor-induced scatter of Madin-Darby canine kidney cells requires phosphatidylinositol 3-kinase. J Biol Chem *270*, 27780-27787.
Sahai, E., Alberts, A.S., and Treisman, R. (1998). RhoA effector mutants reveal distinct effector pathways for cytoskeletal reorganization, SRF activation and transformation. Embo J *17*, 1350-1361.
Sahai, E., and Marshall, C.J. (2002). ROCK and Dia have opposing effects on adherens junctions downstream of Rho. Nat Cell Biol *4*, 408-415.
Sahai, E., and Olson, M.F. (2006). Purification of TAT-C3 exoenzyme. Methods Enzymol *406*, 128-140.
Saitou, M., Furuse, M., Sasaki, H., Schulzke, J.D., Fromm, M., Takano, H., Noda, T., and Tsukita, S. (2000). Complex phenotype of mice lacking occludin, a component of tight junction strands. Mol Biol Cell *11*, 4131-4142.
Sakisaka, T., Nakanishi, H., Takahashi, K., Mandai, K., Miyahara, M., Satoh, A., Takaishi, K., and Takai, Y. (1999). Different behavior of l-afadin and neurabin-II during the formation and destruction of cell-cell adherens junction. Oncogene *18*, 1609-1617.
Samarin, S.N., Ivanov, A.I., Flatau, G., Parkos, C.A., and Nusrat, A. (2007). Rho/Rho-associated kinase-II signaling mediates disassembly of epithelial apical junctions. Mol Biol Cell *18*, 3429-3439.
Sambrook, J., Fritsch, E. F., and Maniatis, M. (1989). Molecular Cloning: A laboratory manual. Cold Spring Habor Laboratory Press: Cold Spring Habor.
Sambrook, J., Russel, DW. (2001). Molecular Cloning: A laboratory manual. Third Edition. Cold Spring Habor Laboratory Press: Cold Spring Habor.
Sampath, P., and Pollard, T.D. (1991). Effects of cytochalasin, phalloidin, and pH on the elongation of actin filaments. Biochemistry *30*, 1973-1980.
Sander, E.E., van Delft, S., ten Klooster, J.P., Reid, T., van der Kammen, R.A., Michiels, F., and Collard, J.G. (1998). Matrix-dependent Tiam1/Rac signaling in epithelial cells promotes either cell-cell adhesion or cell migration and is regulated by phosphatidylinositol 3-kinase. J Cell Biol *143*, 1385-1398.

Sato, T., Fujita, N., Yamada, A., Ooshio, T., Okamoto, R., Irie, K., and Takai, Y. (2006). Regulation of the assembly and adhesion activity of E-cadherin by nectin and afadin for the formation of adherens junctions in Madin-Darby canine kidney cells. J Biol Chem *281*, 5288-5299.
Schächterle, C. (2008). Lokalisation, Interaktionspartner und Beteiligung des GTP-Austauschfaktors Trio im Serum Response Factor Signalweg in Epithelzellen. Diploma Thesis.
Schirenbeck, A., Arasada, R., Bretschneider, T., Stradal, T.E., Schleicher, M., and Faix, J. (2006). The bundling activity of vasodilator-stimulated phosphoprotein is required for filopodium formation. Proc Natl Acad Sci U S A *103*, 7694-7699.
Schirmer, J., and Aktories, K. (2004). Large clostridial cytotoxins: cellular biology of Rho/Ras-glucosylating toxins. Biochim Biophys Acta *1673*, 66-74.
Schneeberger, E.E., and Lynch, R.D. (2004). The tight junction: a multifunctional complex. Am J Physiol Cell Physiol *286*, C1213-1228.
Schratt, G., Philippar, U., Berger, J., Schwarz, H., Heidenreich, O., and Nordheim, A. (2002). Serum response factor is crucial for actin cytoskeletal organization and focal adhesion assembly in embryonic stem cells. J Cell Biol *156*, 737-750.
Schratt, G., Weinhold, B., Lundberg, A.S., Schuck, S., Berger, J., Schwarz, H., Weinberg, R.A., Ruther, U., and Nordheim, A. (2001). Serum response factor is required for immediate-early gene activation yet is dispensable for proliferation of embryonic stem cells. Mol Cell Biol *21*, 2933-2943.
Schuebel, K.E., Movilla, N., Rosa, J.L., and Bustelo, X.R. (1998). Phosphorylation-dependent and constitutive activation of Rho proteins by wild-type and oncogenic Vav-2. Embo J *17*, 6608-6621.
Scott, J.A., Shewan, A.M., den Elzen, N.R., Loureiro, J.J., Gertler, F.B., and Yap, A.S. (2006). Ena/VASP proteins can regulate distinct modes of actin organization at cadherin-adhesive contacts. Mol Biol Cell *17*, 1085-1095.
Scott, V.R., Boehme, R., and Matthews, T.R. (1988). New class of antifungal agents: jasplakinolide, a cyclodepsipeptide from the marine sponge, Jaspis species. Antimicrob Agents Chemother *32*, 1154-1157.
Sekine, A., Fujiwara, M., and Narumiya, S. (1989). Asparagine residue in the rho gene product is the modification site for botulinum ADP-ribosyltransferase. J Biol Chem *264*, 8602-8605.
Shewan, A.M., Maddugoda, M., Kraemer, A., Stehbens, S.J., Verma, S., Kovacs, E.M., and Yap, A.S. (2005). Myosin 2 is a key Rho kinase target necessary for the local concentration of E-cadherin at cell-cell contacts. Mol Biol Cell *16*, 4531-4542.
Shore, P., and Sharrocks, A.D. (1995). The MADS-box family of transcription factors. Eur J Biochem *229*, 1-13.
Siliciano, J.D., and Goodenough, D.A. (1988). Localization of the tight junction protein, ZO-1, is modulated by extracellular calcium and cell-cell contact in Madin-Darby canine kidney epithelial cells. J Cell Biol *107*, 2389-2399.
Skoble, J., Auerbuch, V., Goley, E.D., Welch, M.D., and Portnoy, D.A. (2001). Pivotal role of VASP in Arp2/3 complex-mediated actin nucleation, actin branch-formation, and Listeria monocytogenes motility. J Cell Biol *155*, 89-100.
Small, J.V., Anderson, K., and Rottner, K. (1996). Actin and the coordination of protrusion, attachment and retraction in cell crawling. Biosci Rep *16*, 351-368.
Smith, P.K., Krohn, R.I., Hermanson, G.T., Mallia, A.K., Gartner, F.H., Provenzano, M.D., Fujimoto, E.K., Goeke, N.M., Olson, B.J., and Klenk, D.C. (1985). Measurement of protein using bicinchoninic acid. Anal Biochem *150*, 76-85.
Somlyo, A.P., and Somlyo, A.V. (2003). Ca2+ sensitivity of smooth muscle and nonmuscle myosin II: modulated by G proteins, kinases, and myosin phosphatase. Physiol Rev *83*, 1325-1358.
Sotiropoulos, A., Gineitis, D., Copeland, J., and Treisman, R. (1999). Signal-regulated activation of serum response factor is mediated by changes in actin dynamics. Cell *98*, 159-169.
Spector, I., Braet, F., Shochet, N.R., and Bubb, M.R. (1999). New anti-actin drugs in the study of the organization and function of the actin cytoskeleton. Microsc Res Tech *47*, 18-37.
Spector, I., Shochet, N.R., Kashman, Y., and Groweiss, A. (1983). Latrunculins: novel marine toxins that disrupt microfilament organization in cultured cells. Science *219*, 493-495.
Stoker, M. (1989). Effect of scatter factor on motility of epithelial cells and fibroblasts. J Cell Physiol *139*, 565-569.

Straight, A.F., Cheung, A., Limouze, J., Chen, I., Westwood, N.J., Sellers, J.R., and Mitchison, T.J. (2003). Dissecting temporal and spatial control of cytokinesis with a myosin II Inhibitor. Science *299*, 1743-1747.
Sun, Q., Chen, G., Streb, J.W., Long, X., Yang, Y., Stoeckert, C.J., Jr., and Miano, J.M. (2006). Defining the mammalian CArGome. Genome Res *16*, 197-207.
Takaishi, K., Sasaki, T., Kotani, H., Nishioka, H., and Takai, Y. (1997). Regulation of cell-cell adhesion by rac and rho small G proteins in MDCK cells. J Cell Biol *139*, 1047-1059.
Tamada, M., Perez, T.D., Nelson, W.J., and Sheetz, M.P. (2007). Two distinct modes of myosin assembly and dynamics during epithelial wound closure. J Cell Biol *176*, 27-33.
Tanimura, S., Chatani, Y., Hoshino, R., Sato, M., Watanabe, S., Kataoka, T., Nakamura, T., and Kohno, M. (1998). Activation of the 41/43 kDa mitogen-activated protein kinase signaling pathway is required for hepatocyte growth factor-induced cell scattering. Oncogene *17*, 57-65.
Thiery, J.P. (2002). Epithelial-mesenchymal transitions in tumour progression. Nat Rev Cancer *2*, 442-454.
Thiery, J.P., and Sleeman, J.P. (2006). Complex networks orchestrate epithelial-mesenchymal transitions. Nat Rev Mol Cell Biol *7*, 131-142.
Treisman, R. (1986). Identification of a protein-binding site that mediates transcriptional response of the c-fos gene to serum factors. Cell *46*, 567-574.
Treisman, R. (1994). Ternary complex factors: growth factor regulated transcriptional activators. Curr Opin Genet Dev *4*, 96-101.
Trelstad, R.L., Hayashi, A., Hayashi, K., and Donahoe, P.K. (1982). The epithelial-mesenchymal interface of the male rate Mullerian duct: loss of basement membrane integrity and ductal regression. Dev Biol *92*, 27-40.
Trichet, L., Sykes, C., and Plastino, J. (2008). Relaxing the actin cytoskeleton for adhesion and movement with Ena/VASP. J Cell Biol *181*, 19-25.
Trofatter, J.A., MacCollin, M.M., Rutter, J.L., Murrell, J.R., Duyao, M.P., Parry, D.M., Eldridge, R., Kley, N., Menon, A.G., Pulaski, K., and et al. (1993). A novel moesin-, ezrin-, radixin-like gene is a candidate for the neurofibromatosis 2 tumor suppressor. Cell *72*, 791-800.
Tucker, G.C., Duband, J.L., Dufour, S., and Thiery, J.P. (1988). Cell-adhesion and substrate-adhesion molecules: their instructive roles in neural crest cell migration. Development *103 Suppl*, 81-94.
Uehata, M., Ishizaki, T., Satoh, H., Ono, T., Kawahara, T., Morishita, T., Tamakawa, H., Yamagami, K., Inui, J., Maekawa, M., and Narumiya, S. (1997). Calcium sensitization of smooth muscle mediated by a Rho-associated protein kinase in hypertension. Nature *389*, 990-994.
Umeda, K., Ikenouchi, J., Katahira-Tayama, S., Furuse, K., Sasaki, H., Nakayama, M., Matsui, T., Tsukita, S., Furuse, M., and Tsukita, S. (2006). ZO-1 and ZO-2 independently determine where claudins are polymerized in tight-junction strand formation. Cell *126*, 741-754.
Van Furden, D., Johnson, K., Segbert, C., and Bossinger, O. (2004). The C. elegans ezrin-radixin-moesin protein ERM-1 is necessary for apical junction remodelling and tubulogenesis in the intestine. Dev Biol *272*, 262-276.
Vartiainen, M.K., Guettler, S., Larijani, B., and Treisman, R. (2007). Nuclear actin regulates dynamic subcellular localization and activity of the SRF cofactor MAL. Science *316*, 1749-1752.
Vasioukhin, V., Bauer, C., Yin, M., and Fuchs, E. (2000). Directed actin polymerization is the driving force for epithelial cell-cell adhesion. Cell *100*, 209-219.
Viebahn, C. (1995). Epithelio-mesenchymal transformation during formation of the mesoderm in the mammalian embryo. Acta Anat (Basel) *154*, 79-97.
Vilozny, B., Amagata, T., Mooberry, S.L., and Crews, P. (2004). A new dimension to the biosynthetic products isolated from the sponge Negombata magnifica. J Nat Prod *67*, 1055-1057.
Vincent-Salomon, A., and Thiery, J.P. (2003). Host microenvironment in breast cancer development: epithelial-mesenchymal transition in breast cancer development. Breast Cancer Res *5*, 101-106.
Vinson, V.K., De La Cruz, E.M., Higgs, H.N., and Pollard, T.D. (1998). Interactions of Acanthamoeba profilin with actin and nucleotides bound to actin. Biochemistry *37*, 10871-10880.
Volberg, T., Geiger, B., Kartenbeck, J., and Franke, W.W. (1986). Changes in membrane-microfilament interaction in intercellular adherens junctions upon removal of extracellular Ca2+ ions. J Cell Biol *102*, 1832-1842.

Wang, A.Z., Ojakian, G.K., and Nelson, W.J. (1990). Steps in the morphogenesis of a polarized epithelium. I. Uncoupling the roles of cell-cell and cell-substratum contact in establishing plasma membrane polarity in multicellular epithelial (MDCK) cysts. J Cell Sci *95 (Pt 1)*, 137-151.
Wang, D., Chang, P.S., Wang, Z., Sutherland, L., Richardson, J.A., Small, E., Krieg, P.A., and Olson, E.N. (2001). Activation of cardiac gene expression by myocardin, a transcriptional cofactor for serum response factor. Cell *105*, 851-862.
Wang, Z., Wang, D.Z., Hockemeyer, D., McAnally, J., Nordheim, A., and Olson, E.N. (2004). Myocardin and ternary complex factors compete for SRF to control smooth muscle gene expression. Nature *428*, 185-189.
Watabe, M., Nagafuchi, A., Tsukita, S., and Takeichi, M. (1994). Induction of polarized cell-cell association and retardation of growth by activation of the E-cadherin-catenin adhesion system in a dispersed carcinoma line. J Cell Biol *127*, 247-256.
Weaver, A.M., Heuser, J.E., Karginov, A.V., Lee, W.L., Parsons, J.T., and Cooper, J.A. (2002). Interaction of cortactin and N-WASp with Arp2/3 complex. Curr Biol *12*, 1270-1278.
Weber, K., and Groeschel-Stewart, U. (1974). Antibody to myosin: the specific visualization of myosin-containing filaments in nonmuscle cells. Proc Natl Acad Sci U S A *71*, 4561-4564.
Weed, S.A., Karginov, A.V., Schafer, D.A., Weaver, A.M., Kinley, A.W., Cooper, J.A., and Parsons, J.T. (2000). Cortactin localization to sites of actin assembly in lamellipodia requires interactions with F-actin and the Arp2/3 complex. J Cell Biol *151*, 29-40.
Wells, C.M., Walmsley, M., Ooi, S., Tybulewicz, V., and Ridley, A.J. (2004). Rac1-deficient macrophages exhibit defects in cell spreading and membrane ruffling but not migration. J Cell Sci *117*, 1259-1268.
Wennerberg, K., Rossman, K.L., and Der, C.J. (2005). The Ras superfamily at a glance. J Cell Sci *118*, 843-846.
Whitesell, L., Edwardson, J.M., and Cuthbert, A.W. (1981). Adhesive properties of MDCK cell membranes possible role in epithelial histogenesis. J Cell Sci *51*, 255-271.
Wilde, C., and Aktories, K. (2001). The Rho-ADP-ribosylating C3 exoenzyme from Clostridium botulinum and related C3-like transferases. Toxicon *39*, 1647-1660.
Winer, J., Jung, C.K., Shackel, I., and Williams, P.M. (1999). Development and validation of real-time quantitative reverse transcriptase-polymerase chain reaction for monitoring gene expression in cardiac myocytes in vitro. Anal Biochem *270*, 41-49.
Yamada, S., and Nelson, W.J. (2007). Localized zones of Rho and Rac activities drive initiation and expansion of epithelial cell-cell adhesion. J Cell Biol *178*, 517-527.
Yamada, S., Pokutta, S., Drees, F., Weis, W.I., and Nelson, W.J. (2005). Deconstructing the cadherin-catenin-actin complex. Cell *123*, 889-901.
Yang, J., and Weinberg, R.A. (2008). Epithelial-mesenchymal transition: at the crossroads of development and tumor metastasis. Dev Cell *14*, 818-829.
Yap, A.S., and Kovacs, E.M. (2003). Direct cadherin-activated cell signaling: a view from the plasma membrane. J Cell Biol *160*, 11-16.
Yap, A.S., Niessen, C.M., and Gumbiner, B.M. (1998). The juxtamembrane region of the cadherin cytoplasmic tail supports lateral clustering, adhesive strengthening, and interaction with p120ctn. J Cell Biol *141*, 779-789.
Zaidel-Bar, R., Ballestrem, C., Kam, Z., and Geiger, B. (2003). Early molecular events in the assembly of matrix adhesions at the leading edge of migrating cells. J Cell Sci *116*, 4605-4613.
Zampella, A., Giannini, C., Debitus, C., Roussakis, C., and D'Auria, M.V. (1999). New jaspamide derivatives from the marine sponge Jaspis splendans collected in Vanuatu. J Nat Prod *62*, 332-334.
Zaromytidou, A.I., Miralles, F., and Treisman, R. (2006). MAL and ternary complex factor use different mechanisms to contact a common surface on the serum response factor DNA-binding domain. Mol Cell Biol *26*, 4134-4148.
Ziegler, W.H., Liddington, R.C., and Critchley, D.R. (2006). The structure and regulation of vinculin. Trends Cell Biol *16*, 453-460.

VIII. Abbreviations

Within this thesis the abbreviations showed in the following list were used. For additional abbreviations of chemical substances and reagents see section VI.1.2.

Abi1	abl interactor 1
AC	α-catenin
acta-2	*smooth-muscle α-actin* gene
ADF	actin-depolymerizing factor
ADP	adenosine diphosphate
AJ	Adherens junction
AJC	apical junctional complex
AlF_4^-	aluminium fluoride ion
Amp	ampecilline
AMP	adenosine monophosphate
Arp2/3 complex	actin-related protein-2/3 complex
as	antisense strand
ATP	adenosine triphosphate
ATPase	adenosine triphosphate phosphatase
B domain	basic domain
Blebb.	blebbistatin
C3	C3 exoenzyme derived from *C. botulinum*
Cal.A	calyculin A
Cam	chloramphenicol
cAMP	cyclic adenosine monophosphate
C. botulinum	*Clostridium botulinum*
CD	cytochalasin D
cDNA	complementary DNA
C. difficile	*Clostridium difficile*
CHO	chinese hamster ovary
CMV	cytomegalovirus
CPI-17	protein kinase C-potentiated protein phosphatase 1 inhibitory protein of 17 kDa
CRIP	Cdc42- and Rac-interacting domain
CRUK	Cancer Research United Kingdom
CSF-1	colony-stimulating factor-1
Cy3	carbocyanin 3
DMEM	Dulbecco's Modified Eagle Medium
DNA	deoxyribonucleic acid
E.coli	*Escherichia coli*
EC domain	extracellular cadherin domain
ECM	extracellular matrix
EGF	epidermal-growth factor
EGFP	enhanced green fluorescent protein
EGFR	epidermal-growth factor-receptor
EGR-1	early growth response protein-1
EMT	epithelail-mesenchymal transition
Ena/VASP	enabled/vasodilator stimulated phosphoprotein
EPLIN	epithelial protein lost in neoplasm
ERM	ezrin-radixin-moesin
EtOH	ethanol
F-actin	filamentous actin
FCS	fetal calf serum
FERM	four-point one, ERM
FGFR	fibroblast-growth factor-receptor

FH domain	forkhead domain
FITC	fluorescein isothiocyanate
fl	full length
FSP-1	fibroblast-specific protein 1
G-actin	globular actin
GAP	GTPase-activating protein
GBD	G protein binding
GDP	guanosine diphosphate
GEF	guanine nucleotide exchange factor
GST	glutathione S-transferase
GTP	guanosine triphosphate
GTPase	small guanosine triphosphatase
HA	hemagglutinin
HGF	hepatocyte growth factor
HIV	human immunodeficiency virus
HRP	horseraddish peroxidase
IF	immunofluorescence
IgG	immunoglobulin G
JAM	junctional adhesion molecules
Jasp	jasplakinolide
JMD	juxtamembrane domain
Kan	kanamycine
kDa	kilo Dalton
LatB	latrunculin B
LB broth	Luria-Bertani broth
LIMK	LIM kinase
LPA	lysophosphatidic acid
LZ	leucine zipper
MADS	MCM1, Agamous, Deficiens, SRF
MAL	Megakaryoblastic leukemia protein
MAPK	mitogen-activated protein kinase
MD	adhesion modulation domain
MDCK	Madin-Darby Canine Kidney
mDia	murine diaphanous
MeOH	methanol
MET	mesenchymal-epithelial transition
MLC	myosin light chain
MLCPP	myosin light chain phosphatase
MPI	Max Planck Institute
MRTF	myocardin related transcription factor
N-WASP	neuronal Wiskott-Aldrich syndrome protein
Nap1	NCK-associated protein 1
NF-2	*neurofibromatosis type-2* gene
NPF	nucleation promoting factor
P_i	γ-phosphate
PAGE	polyacrylamid gel electrophoresis
PAK	p21-activated kinase
PCR	polymerase chain reaction
PDGF	platelet-derived growth factor
PDGFR	platelet-derived growth factor-receptor
PDZ domain	post synaptic density protein, *Drosophila* disc large tumor suppressor, and zonula occludens-1 protein domain
PI3K	phosphatidylinositol-3 kinase
$PI(4,5)P_2$	phosphatidylinosditol-4,5-bisphosphat
PP	protein phosphatase
RBD	Rho-binding domain

RNA	ribonucleic acid
RIPA	radioimmunoprecipitation assay
ROCK	RhoA activated coiled-coil kinase
RS	restriction site
RT	reverse transcription
s.e.m.	standard error of the mean
SAP-1	sphingolipid activator protein-1
SAP domain	SAF-A/B, Acinus and PIAS domain
SCAR	suppressor of cyclic AMP repressor
shRNA	small hairpin RNA
SRF	serum response factor
ss	sense strand
TAT	trans-activator of transcription
TcdB	toxin B derived from *C. difficile* reference strain VPI 10463
TcdBF	toxin B derived from *C. difficile* serotype F strain 1470
TCF	ternary complex factor
tEC	truncated E-cadherin
TESK	testicular protein kinase
TGF-β	transforming growth factor-β
TJ	Tight junction
TPA	phorbol myristate acetate
TRITC	tetramethylrhodamine isothiocyanate
TUM	Technische Universität München
UDP	uracil diphosphate
VASP	vasodilator stimulated phosphoprotein
vcl	*vinculin* gene
VH domain	vinculin homology domain
WASP	Wiskott-Aldrich syndrome protein
WAVE	WASP-family verprolin-homolougous protein
wt	wild type
ZIPK	zipper-interacting protein kinase
ZO	zonula occludens protein

Amino acids were described by their one or three letter code.

IX. Publications

Parts of this thesis are published in:

Busche, S., Descot, A., Julien, S., Genth, H., and Posern, G. (2008). Epithelial cell-cell contacts regulate SRF-mediated transcription via Rac-actin-MAL signalling. J Cell Sci *121* (Pt 7), 1025-1035.

X. Acknowledgements

Many people have contributed to the accomplishment of this thesis. It was instructive, exciting and fun to work with you all in such a great environment. Thanks!!!

In particular, I am very grateful to

Prof. Dr. Johannes Buchner for supervising and promoting my thesis at the Technical University of Munich.

Dr. Guido Posern for giving me the chance to work on this exciting project, the supervision, valuable discussions and suggestions, and for supporting my ideas.

Prof. Dr. Axel Ullrich for supporting me with the excellent infrastructure in the Department of Molecular Biology at the Max Planck Institute of Biochemistry.

my PhD advisory committee members Dr. Hendrik Daub, Dr. Cord Brakebusch and especially Dr. Michael Sixt for productive discussions, guidance and advice.

my current and former lab members, particularly Laura Leitner, Monika Rex-Haffner and Arnaud Descot for all their help, discussions, the relaxed lab atmosphere, the distraction in stressful times…, and my student Carolin, it was fun to supervise your diploma thesis.

my current and former office colleagues, especially my neighbour Dr. Wolfgang Reindl, but not to forget Martin Gräber, Dr. Robert Torka, Dr. Hüseyin Cavga, Dr. Anke Kiessling and all the others for interesting discussions and distraction when needed.

all members of the Department of Molecular Biology for their help and the great time in and beyond the lab. Thanks Michaela, Nina S., Simone, Susanne, Ute, Jacqueline, Andreas R., Claus, Christoph, Felix, Markus, Martin, Mathias B., Matthias S., Philipp M., Phillip V. and Nils H., my most favourite Hermeking. Further I want to thank the departmental soccer team for all the fun we had playing and for giving me the opportunity to win the MPI tournament twice. And Christopher, my former fellow student, for a great time in SF.

Abschließend möchte ich ganz besonders meiner Familie und Vladia für die andauernde Unterstützung und die erholsamen Aufenthalte zu Hause während der Zeit dieser Doktorarbeit danken.